372

VOLTAGE DIP EVALUATION AND PREDICTION TOOLS

Task Force
C4.102

February 2009

TF C4.102

VOLTAGE DIP EVALUATION AND PREDICTION TOOLS

Members:

Juan A. Martínez-Velasco – Spain (Convenor)
Nick Abi-Samra – USA
MyoT. Aung – United Kingdom
Math Bollen – Sweden
Saša Ž. Djokić – United Kingdom
Nikos Hatziargyriou – Greece
Roberto C. Leborgne – Sweden
Jovica V. Milanović – United Kingdom
Gabriel Olguin – Sweden
Melanie Schilder – South Africa

ISBN :978-2-85873-059-9

TABLE OF CONTENTS

1. Introduction

1.1 Power quality

Electric power systems are designed to generate electric energy economically and with the minimum ecological disturbance and to transfer this energy over transmission lines and distribution networks with the maximum efficiency and reliability for delivery to customers at virtually fixed voltage and frequency. The optimal level of investment in designing such a system is to be achieved by means of a trade-off between reliability and costs. Some of the recent developments in electrical energy sector have led the change in design and operation of power systems, i.e.:

- Due to the re-regulation of the electricity industry, there is no longer a single vertically structured system but a number of independent companies linking electricity generation with end users and competing among themselves for customer. Distribution companies are under considerable pressure to improve the quality of the service they provide. Achieving these improvements requires very large investments. If, after having made these investments, they succeed in providing a better quality of service than their peers can achieve, the Regulator will reward them with a higher rate of return. On the other hand, a failure to deliver on promises of better quality of service is likely to result in severe financial penalties. It is thus essential to the future of these companies to target investments towards the network improvements that will be most effective. This can only be achieved through a careful quantification of the effects of faults on service reliability and power quality and the inclusion of these results in network design. Enhancing network designs to optimise service quality may therefore involve tradeoffs between reliability and power quality. Faults in the transmission network can also cause power quality problems that affect many customers and should therefore be taken into account in any comprehensive assessment.
- Electricity generation is shifting away from large power stations connected to the transmission system towards smaller units connected at lower voltage levels (e.g., combined-heat-and-power and renewable generation connected to distribution , low voltage, network).
- In addition to the re-regulation of electrical power industry customer expectations regarding the quality and reliability of their electricity supply are high and steadily rising. Outages, interruptions and voltage sags shut down industrial processes and computer systems, often causing enormous losses in productivity and materials. These disturbances also annoy and inconvenience residential customers who own an increasing array of electronic devices and find such problems less acceptable in an electricity supply industry that is privately owned and operates in a competitive environment. Customers with important and sensitive loads may soon demand from their distribution companies detailed data showing the number of outages, interruptions and voltage sags that should be expected at various locations in the network. Given the probability of sags of different types, magnitudes and shape, customers may also want to know how many of these sags will cause their variable speed drives, programmable logic controllers and computers to trip or fail. Combining these two types of data would indeed allow them to calculate the expected cost of failures and sags. This information could then be used to negotiate appropriate connection rates with the distribution companies. It could also guide the choice of location for new plants, the selection of manufacturing equipment or suggest the purchase of Custom Power devices.

Several definitions related to the “power quality” concept have been proposed in the past [1],

[2]:

- *Voltage quality* is concerned with deviations of the voltage from the ideal single-frequency sine wave of constant amplitude and frequency.
- *Current quality* is the complementary term to voltage quality concerned with the deviation of the current from the ideal single-frequency sine wave of constant amplitude and frequency, with the additional requirement that the current sine wave is in phase with the voltage sine wave.
- *Power quality,* in light of the above, could be considered as the combination of voltage and current quality.
- *Quality of supply* is a broader term and represents a combination of voltage quality and the non-technical aspects of the interaction between the electrical power network and its customers.

One of the most descriptive and probably the most inclusive definitions of power quality would be that the power quality is a multidisciplinary area of electrical engineering, related to the assessment, analysis, characterisation and quantification of all ranges of mutual interactions between the utilities and customers, expressed firstly as a measure of conformance to either declared or accepted basic specifications, and then against the sets of individual customer requirements, formulated in addition to basic specifications.

Additionally, the term *electromagnetic compatibility* (*EMC*) is often used to describe the interaction between equipment and its electromagnetic environment (e.g. the power system). Even though the EMC concept is more narrow (limited) than the power quality concept, the latter is often treated as a subset of the former (e.g., in IEC standards).

Power quality disturbances can be generally divided in two categories: variations and events [1], [2].

- *Variation* usually denotes small deviation of some voltage and/or current characteristic from its nominal or declared value/waveform. All characteristics of voltage and current are never exactly equal to their nominal or ideal values, since they change during the normal operation within relatively small ranges, depending on system/load interactions. These disturbances include: voltage and current magnitude/phase/ frequency variations (i.e., unbalances), harmonic and interharmonic distortions, flicker, notching, and presence of high frequency signals and noise. Variations are continuous phenomena that often have steady-state or periodical character, which can be measured and quantified at any moment in time. Generally, good design practice and selection of equipment with certain operating characteristics significantly reduce occurrence of variations. Once their presence is identified, they can be effectively controlled and mitigated with appropriate power conditioning equipment. Thus, variations are generally assumed to have less detrimental effects than events.
- *Events* are power quality disturbances related to usually large deviations of some voltage or current characteristics from their nominal or declared values/waveforms. They happen suddenly, representing brief or temporary occurrence of some phenomena that have notoriously stochastic nature (e.g., system faults, changes in load structure, etc.). This type of disturbances includes: voltage sags, voltage swells, undervoltages, overcurrents, overvoltages, voltage and current transients, and (short) interruptions. These events are related to the presence of excessively high or low voltages and/or currents which regardless of their short duration have much more detrimental effects on system/load operation than in the case of variations.

The difference between variations and events is not always obvious, and depends to a large extent on the way in which the disturbance is measured. Variations can be measured at any moment in time while events require prolonged monitoring periods and "waiting" for a voltage or current characteristic to exceed a pre-defined threshold.

1.2 Voltage dips

A voltage dip is a sudden reduction of the rms value of the ac voltage below a specified dip threshold followed by its recovery after a brief interval [3]. From the early 1970's, results of several extensive power quality surveys have identified voltage dips as one of the most common power quality disturbances, accounting for approximately 65% of the total number of all recorded events. They cause two serious power quality problems, responsible for frequent malfunctions of electrical equipment in industrial and commercial installations (e.g., adjustable-speed drives, process-control equipment, relays, contactors and computers). The economic impact of dips is often expressed in millions (or even billions) of funds per year.

Voltage dips are in general a three-phase phenomenon, in which all three phase voltages are involved (and sometimes even the neutral-to-ground voltage). Figure 1(a) shows a three-phase voltage dip due to a phase-to-phase fault in an underground cable that develops into a three-phase fault within two cycles. A more common way of presenting a voltage dip is through the rms voltages as a function of time; Figure 1(b) shows the rms voltage for the dip in Figure 1(a).

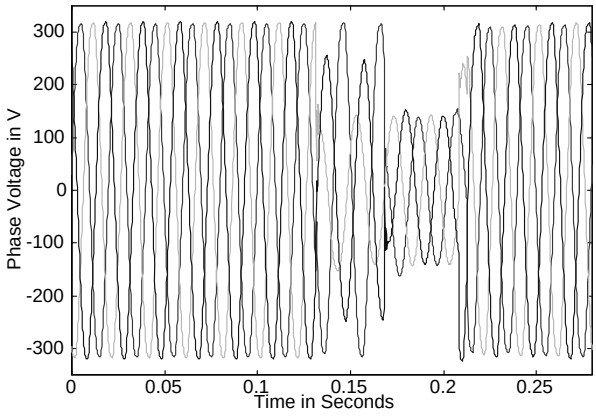

a) Measured voltages

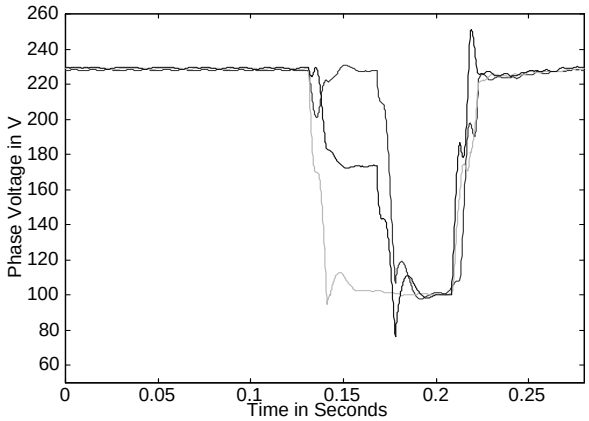

b) RMS voltages

Figure 1. Example of a three-phase voltage dip.

1.2.1 Causes of voltage dips

Without any doubt, the major cause of voltage dips are short-circuit faults in power supply system and inside the customer's installation. Excessive and adverse weather conditions such as lightning, wind and ice are often directly correlated with the occurrence of dips. Electrical degradation due to the ageing and contamination of insulators, animal and tree branch contacts, as well as accidents related to construction and transportation activities also cause short-circuit faults that result in voltage dips. Additionally, voltage dips are often caused by induction motor starting, transformer energizing or load switching. Even though a voltage dip may not be as damaging to industry as an interruption, there are far more voltage dips than interruptions so the total damage caused by dips can be sometimes larger then one caused by interruptions .

Examples of voltage dips obtained by computer simulations are shown in Figures 2 to 4. Note that the rms voltages shown in these figures are calculated over a one-cycle sliding window.

Figure 2 shows a voltage dip due to motor starting: a rather small sudden drop in voltage, followed by a gradual recovery. As electrical motors are three-phase balanced loads, the voltage drops are the same in the three phases.

The voltage dip depicted in Figure 3 also shows a sudden drop followed by a slow recovery. However, the drops are different in the three phases. This event is due to the energizing of a large transformer. The inrush current is different in the three phases and associated with large second and fourth harmonic distortion.

The voltage dip shown in Figure 4 is due to a fault: the voltage drops sharp in two phases, and recovers sharply a few cycles later. Drop and recovery are associated with fault initiation and fault clearing, respectively. The event in Figure 4 is associated with different voltage drops in two phases whereas the rms voltage in the third phase is not affected by the event. A noticeable characteristic of the event shown in Figure 4 are the sharp drop and recovery of the voltage associated with fault initiation and fault clearing, respectively. As mentioned previously, power system faults are the most important cause of voltage dips; they lead to the most severe drops in voltage and to the majority of equipment trips.

In the above example the voltage during the event is constant and the voltage recovers immediately. However, some events show multiple dip stages due to developing faults, (change in fault type over the tie) or due to the operation of protective devices. An example of a multi-stage voltage dip is shown in Figure 5.

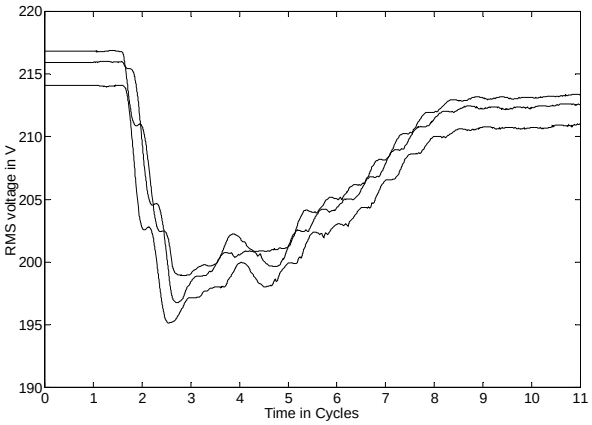

Figure 2. Voltage dip due to motor starting.

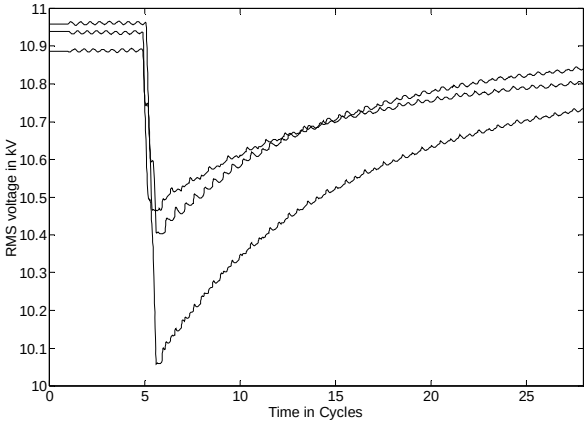

Figure 3. Voltage dip due to transformer energizing.

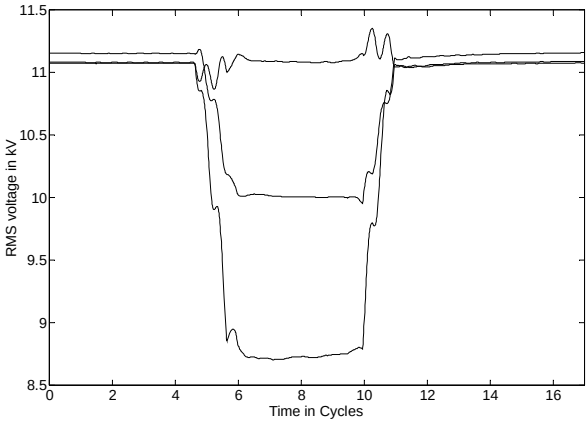

Figure 4. Voltage dip due to a fault.

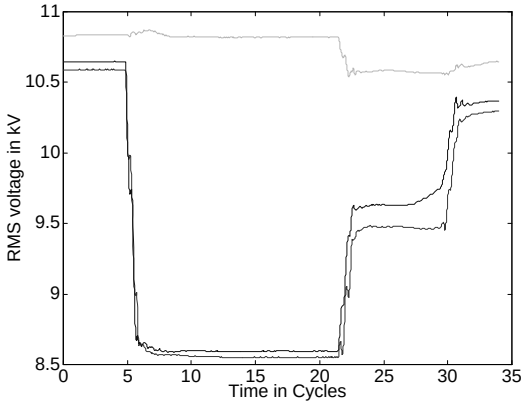

Figure 5. Multi-stage voltage dip due to a fault.

1.2.2 Consequences of voltage dips

The reduction in voltage caused during a voltage dip leads to a reduction in energy-transfer capability of the system, limits the fault-clearing time in transmission systems or results in disconnection of distributed generation from the grid. Many modern devices (power-electronic devices in particular) like computers, process-controllers, and adjustable-speed drives experience operational problems when the voltage drops below 85% for more than 40 ms. The common feature of power electronics based devices is that they are connected to the power system through a rectifier that converts ac to dc voltage. A voltage dip on the ac side of the rectifier leads to a drop in dc voltage, which in turn causes problems with the application voltages. An additional problem is the large inrush current following the voltage recovery after the dip (i.e., after fault clearing) which may lead to a damage of the rectifier components. In the case of three-phase rectifiers the unbalance of the currents through the rectifier and the ripple in the dc voltage are also potential causes of equipment failure.

1.2.3 Characteristics of voltage dips

Adequate post processing of the sampled/measured voltage waveforms is the essential requirement for characterisation of voltage dips. This is detailed in IEC 61000-4-30 [4], where the remaining voltage and the duration are defined as the two main characteristics to quantify a voltage dip. Both are obtained from the rms voltage as a function of time. The characterisation of three-phase measurements remains a point of discussion, and the current practice based on dip characterisation using worst affected phase (minimum magnitude maximum duration approach) is not entirely satisfactory. (Note: Two-dimensional dip definition, advocated in all existing standards, usually involves characterisation of a dip in terms of the minimum of all reduced phase rms voltages during the event and the total duration of the event, again regarding the durations of the individual dips in all affected phases.) Having identified and agreed on the relevant characteristics of a voltage dip it is possible to describe the voltage dip performance of a site or the whole network [5]. Approaches for identifying voltage dip characteristics and developing site- and system-indices have been proposed in the past. The system voltage dip performance is summarized in a form of magnitude duration tables in e.g., UNIPEDE Disdip table [6], IEC 61000-2-8 [3], IEEE Std.493 [7] and IEEE Std.1346 [8] or in the form of system performance indices like, SARFI (System Average RMS Variation Frequency) [5], [9].

1.2.4 Voltage dip mitigation

The ongoing discussion on voltage-dip mitigation concerns the responsibility sharing between the customer and the network. In some cases the costs of mitigation equipment are shared or the specific power-quality contracts define the responsibilities. In general, an agreement has to be reached between parties involved with respect to what are the “normal dips” and what are the “abnormal dips”. End-user equipment would then be expected to be immune to normal dips, whereas abnormal dips should have a small frequency of occurrence [1]. Various alternative methods can be considered to reduce the number of trips of equipment due to voltage dips. A list of the most effective methods would include reducing the number of faults, improving the performance of the protection system (e.g., faster fault clearing), improving the network design and operation, installing dedicated mitigation equipment at the point of interface, or improving voltage dip ride-through capabilities of end-user equipment.

1.3 Scope and content of the report

1.3.1 Scope of the Working Group

For many years, computer simulations have been recognised as the efficient and time saving tool in solving various problems. When applied in appropriate software environment, they offer the following advantages:

- Simple design of a fully controllable "environment" in which particular information of interest can be easily extracted, without the need for expensive measuring instruments, test beds and other laboratory equipment.
- Evaluation of the effects of various elements and components on simulated system, including fast assessment of improvements/degradations of the system performance and thorough "sensitivity" analysis in order to determine various thresholds, tolerances and areas of applicability.
- Easy implementation of various mathematical, numerical, optimisation, solution-search and any other analytical techniques, either inside one "off-the-shelf" program, or by using appropriate interfaces to other programs.
- Fast processing of large amount of information and efficient data storage, sharing and handling in related databases.
- Transparent and comprehensive application in training and education purposes.

In the power quality area, computer simulations may provide a convenient means to characterise, study and evaluate possible solutions to power quality problems, as well as to estimate or predict various power quality disturbance and their characteristics. Computer simulations in power quality also can be used as a complementary tool to the (permanent) monitoring, as a several years are usually necessary before the significant statistical data and information can be gathered. Adequate simulations can shorten monitoring time substantially, and provide an "instant" information if, for example, changes are introduced to the simulated network or if there are no monitoring data available. As a decision tool, simulations can help in choosing between the different system designs, equipment configurations or operating strategies, in order to find the best possible solution.

Several simulation tools have been developed and used in the past to predict voltage dip characteristics and describe voltage dip performance of the power networks. It has been proven that computer simulations can be useful for characterising the voltage dips and estimating voltage dip performance at the point of connection of sensitive equipment.

This report is aimed at providing

- a discussion on modelling guidelines for calculation of voltage dips using different solution methods;
- a review of the calculation/simulation techniques for dip prediction;
- a summary of capabilities of existing simulation tools;
- an overview of approaches used for calculation of voltage dip characteristics.

1.3.2 Content of the report

The report has been organised into two parts:

- The first part is aimed at introducing the subject of voltage dips and includes Chapters 2, 3 and 4, which cover voltage dip characterisation, equipment behaviour during voltage dips and mitigation techniques.
- The second part reviews the different techniques and simulation tools used for assessment of voltage dip and index calculations. Chapter 5 introduces the different simulation tools and techniques that can be applied to voltage dip studies. Chapter 6 proposes modelling guidelines for the representation of different power components in voltage dip calculations. Finally, Chapters 7 and 8 are dedicated respectively to the stochastic prediction of voltage dips and the calculation of voltage dip indices.

Although the techniques and tools reviewed in this brochure can be applied to the analysis of voltage dips due to any of the causes mentioned in the previous sections, the emphasis of this brochure is on voltage dips caused by faults (short-circuits) at any voltage level of a power system.

2. Voltage Dip Characterisation

2.1 Introduction

The aim of voltage-dip characterisation is two-fold: it allows for a kind of data compression, so as to describe the event with a limited number of parameters; it also allows a comparison between different events, classification of events based on severity: presentation of performance statistics; comparison with equipment performance; etc. A number of characteristics have been proposed in the literature, but the main ones in use are the residual voltage (or "magnitude") and duration.

In this chapter a brief description of a number of voltage-dip characteristics is given, the description is neither complete, not mathematically exact. For more details on voltage dip characterisation see, among others [1] and [5].

2.2 Residual voltage and duration

The only voltage-dip characteristics defined in an international standard are "residual voltage" and "duration". According to IEC 61000-4-30 [4] the residual voltage is the lowest one-cycle rms voltage measured in any of the voltage channels during the event. The duration is the time during which the one-cycle rms voltage for at least one voltage channel is below a voltage-dip threshold. The standard document does not prescribe a value for the threshold but a value equal to 90% of nominal voltage is commonly used. In North-American standards the term "magnitude" is used as a synonym for residual voltage. Before the publication of IEC 61000-4-30 the terms magnitude and duration were already in common use, e.g. in IEEE 493 [7] and IEEE 1159 [10], but without a strict measurement definition.

The "voltage channels" referred to in the IEC standard document may be one, two or three phase-to-phase, phase-to-ground or phase-to-neutral voltages. In most applications three channels are used, with either phase-to-phase or phase-to-neutral voltages.

An example is shown in Figure 6. The left-hand figure shows the voltage waveforms for the three channels. The right-hand figure shown the one-cycle rms voltage calculated every half-cycle as prescribed in IEC 61000-4-30. The solid line in the right-hand figure indicates the

voltage-dip threshold. In this case at least one of the rms voltages is below the threshold for five consecutive values, resulting in a voltage-dip duration equal to 2.5 cycles. The lowest rms voltage is equal to 4.81 kV or 79.4% of the nominal voltage.

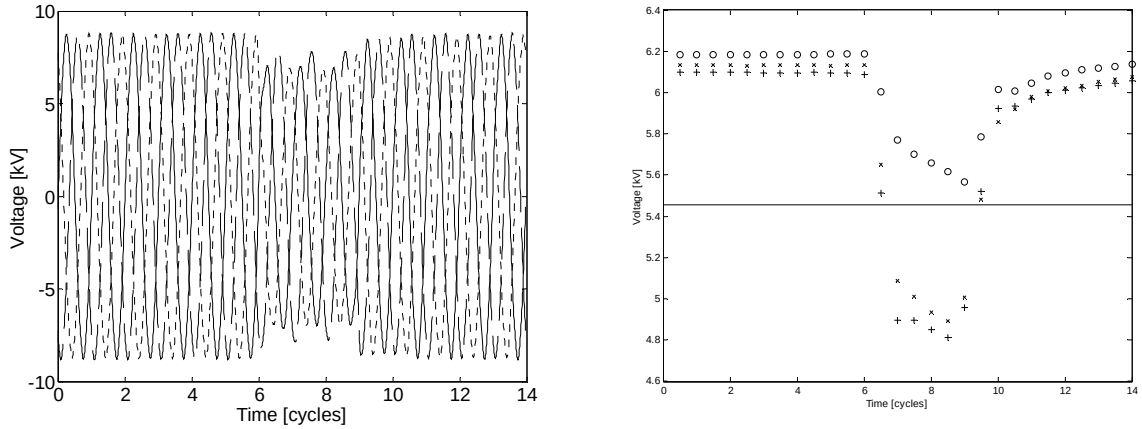

Figure 6. Example of voltage dip: voltage waveforms (left) and one-cycle rms voltages with voltage-dip threshold (right).

For voltage dips due to faults, the residual voltage of a voltage dip is related to the location of the fault; the duration is closely related to the fault-clearing time. Voltage dips due to faults at distribution level have on average a longer duration than those due to faults at transmission level. The majority of dips due to faults, at all voltage levels, have a duration less than 200 milliseconds. Longer-duration dips are more common among dips due to faults at distribution level than among those due to transmission-level faults.

For voltage dips due to motor starting and transformer energizing, the residual voltage is determined by the ratio between the motor or transformer size and the local fault level. The duration of dips due to motor starting is determined by the starting time of the motor. Non-loaded transformers give longer dip duration than loaded transformers.

2.3 Phase-angle jump

It was mentioned in the previous sections that short-circuits cause a drop in voltage magnitude at the terminals of equipment connected elsewhere in the system. This drop in voltage magnitude is in many cases associated with a change in the phase angle of the voltage. Two different causes of this phase-angle jump should be distinguished: the difference in X/R ratio between the source and the faulted feeder; and the difference in voltage drop in the different phases. For dips due to three-phase faults only the first cause is present, resulting in a relation between the phase-angle jump in any of the three phases and the X/R ratio of source and feeder impedance. For dips due to single-phase and two-phase faults, those relations are rather complex (see also Section 2.4).

To obtain the phase angle jump for a measured voltage dip, the phase angle of the voltage during the dip must be compared with the phase angle of the voltage before the dip. The phase angle of the voltage can be obtained from the voltage zero crossing or from the phase of the fundamental component of the voltage. In the latter case, care must be taken to prevent unrealistic values occurring at the beginning and end of the dip. An example of a voltage waveform and its phase angle versus time are shown in Figure 7. No general method exists for extracting one value of the phase-angle jump for a voltage dip in the same way as the definition of the residual voltage referred to in Section 2.2.

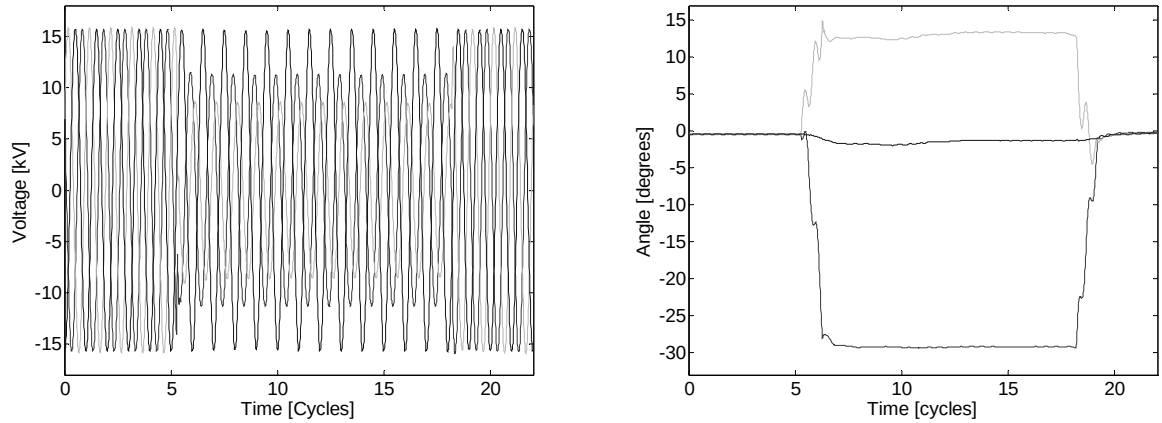

Figure 7. Voltage waveforms (left) and phase-angle versus time (right).

2.4 Other characteristics

In some publications the phase angle at which the voltage dip starts and the phase angle at which the voltage recovers are used as additional characteristics. These angles are referred to as "point-on-wave of dip initiation" and "point-on-wave of voltage recovery"; they give a more accurate picture of the start and end of the fault than using the one-cycle rms voltage.

The point-on-wave of voltage recovery is determined by the X/R ratio of the source impedance at the location of the circuit breaker that clears the fault. For two-phase-to-ground and three-phase faults the voltage recovers in two or three stages when the different poles of the breaker clear the fault. It should be noted that the point-on-wave of voltage recovery cannot be defined for dips due to motor starting and due to transformer energizing.

Instead of using two characteristics to characterize a voltage dip, residual voltage and duration, in some cases a voltage dip is characterized through one value only. This is advantageous in some cases as a first step in quantifying the performance of the supply through voltage-dip indices [5]. Two examples of single-value characteristics are given in [5]: the voltage-dip energy being the integral of the square of the voltage drop over time; and the voltage-dip severity obtained by comparing residual voltage and duration with a reference curve.

When interpreting voltage-dip characteristics it should further be noticed that a certain fraction of voltage dips is of more complex character than the examples shown here. Examples of more complex dips are:

- Dips due to developing faults, e.g. a single-phase fault that develops into a two-phase fault.
- Dips due to faults in meshed parts of the system where there is a clear difference in fault-clearing time for the breakers on different side of the faulted line.
- Dips with a heavy motor-load influence where the voltage drops slowly during the fault.
- Dips where the voltage recovers slowly due to the reacceleration of motor load and /or the saturation of power transformers after voltage recovery.

2.5 Three-phase voltage dips

Most voltage-dip recordings contain three voltage channels so that non-symmetrical faults can cause a different rms voltage in different channels. The standard way of characterisation, see Section 2.2, is to take the lowest of the three rms voltages. This approach has a number of disadvantages: single-phase faults in non-solidly-grounded systems give a very low residual voltage whereas the impact on end-user equipment is small; phase-to-phase connected monitors give a different residual voltage than phase-to-neutral connected monitors; the residual voltages may change significantly when the dip propagates through a transformer.

An alternative classification of voltage dips, more suitable for three-phase systems, is proposed in [11] and described in detail in, among others, [1], [12], [13] and [14]. A number of alternative descriptions of the classification method are available in the literature, with different levels of mathematical detail. The method classifies dips into a number of different types, where the types A, C and D are the most important ones, corresponding to an equal drop in amplitude in three voltages, a drop in two voltages and a drop in one voltage, respectively. Instead of the lowest rms voltage, the so-called "characteristic voltage" is used to quantify the severity of the dip. The characteristic voltage is a complex value being any of the three complex voltages for type A events, the difference between the complex voltages in the two affected channels for a type C event, and the complex voltage in the main affected channel for a type D event.

The (complex) characteristic voltage has an absolute value (or magnitude) and an argument (or phase). The absolute value corresponds to the residual voltage; the argument corresponds to the phase-angle jump.

Voltage dips of the three main types (A, C and D) are shown in Figure 8 and Figure 9. The upper figures present the phasor diagrams where the dashed lines are the pre-fault voltage phasors forming a balanced three-phase system. The bottom figures show the rms voltage as a function of time. Note that these are synthetic dips where the phasors are kept constant during the event; for real measured dips the phasors often vary somewhat as a function of time, but their general character is in most cases similar to the synthetic events shown in the figures.

For the dips shown in Figure 8, the argument (phase angle) of the complex characteristic voltage is zero (zero "characteristic phase-angle jump"). This corresponds to the situation where there is no difference in X/R ratio between the source impedance and the impedance to the fault. For the dips in Figure 9 a non-zero characteristic phase-angle jump is assumed. For dips of type C and type D this introduces an additional asymmetry resulting in all three rms voltages being different.

3. Equipment Behaviour

3.1 Introduction

Generally speaking electrical equipment prefers a constant rms voltage. The other extreme is no voltage for a longer period of time. In that case the equipment will simply completely stop operating. Some equipment will stop within 1 s, other equipment can withstand a supply interruption much longer. For each piece of equipment it is possible to determine how long it will continue to operate after the supply becomes interrupted. A rather simple test would give

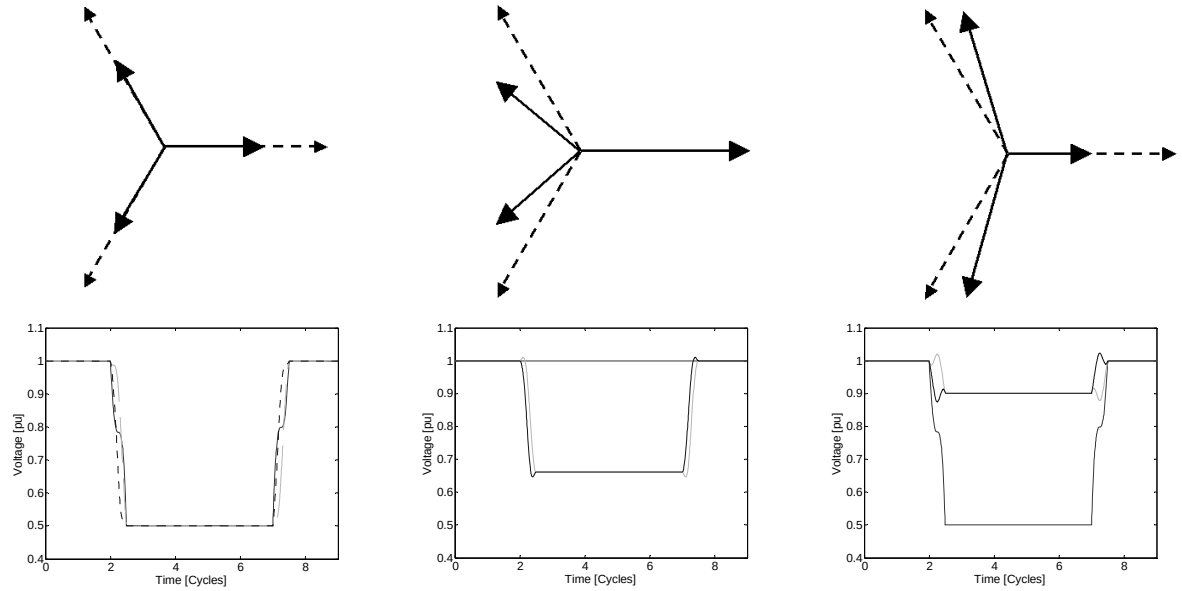

Figure 8. Voltage dips of type A (left), type C (centre) and type D (right) with zero characteristic phase-angle jump; phasor diagrams (top) and rms voltage versus time (bottom).

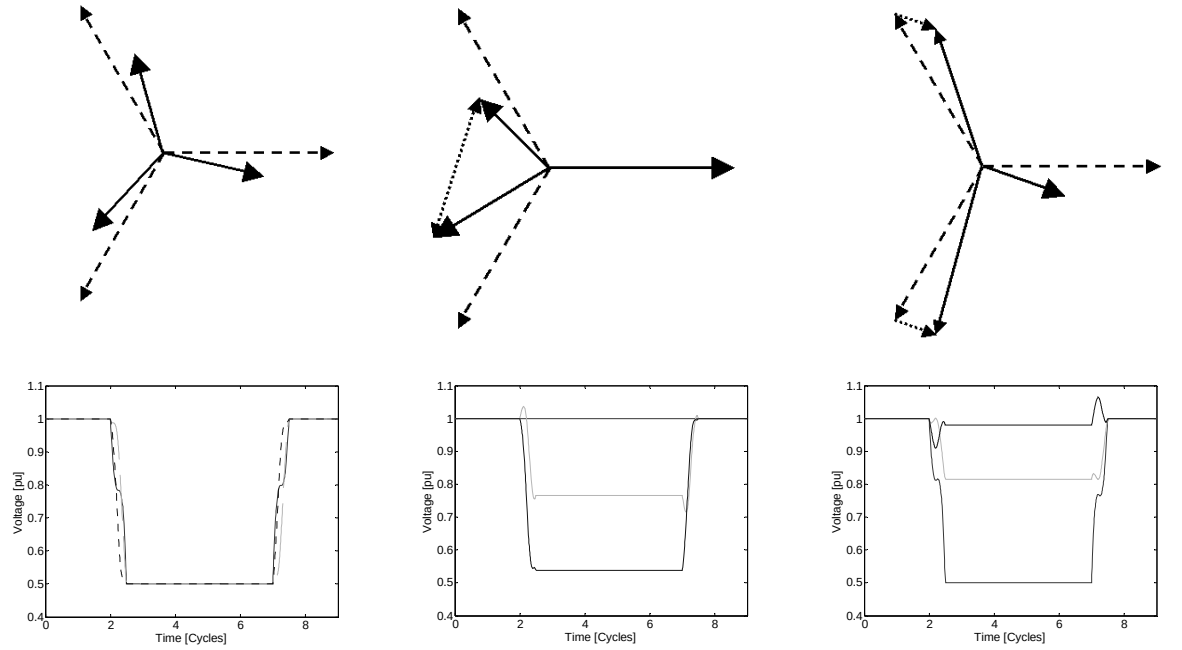

Figure 9. Voltage dips of type A (left), type C (centre) and type D (right) with non-zero characteristic phase-angle jump; phasor diagrams (top) and rms voltage versus time (bottom).

the answer. The same test can be done for a voltage of 10% (of nominal), for a voltage of 20%, etc. If the voltage becomes high enough, the equipment will be able to operate on it indefinitely. Connecting the points obtained by performing these tests, results in the so-called "*voltage-tolerance curve*".

Testing is probably the simplest and the most efficient way for the assessment of equipment sensitivity to power quality disturbances. Monitoring and computer simulations are two alternative approaches, but they have some significant drawbacks. Although most closely related to the actual conditions of the equipment utilisation and operation, monitoring is extremely time-consuming, as it relies on the recording of the disturbances, which are random and infrequent events. Computer simulations may provide fast and convenient means to

characterise and study various power quality disturbances and their influence on equipment operation. However, simulations are only as precise and reliable as are the used models of the equipment and system components. Even the most complex and realistic models cannot include all factors of influence. From the equipment sensitivity point of view, the results obtained in both, monitoring and simulations should always be validated against the results obtained in testing.

3.2 Voltage tolerance

The concept of voltage-tolerance curve was introduced in 1978 by Thomas Key [15]; he developed a voltage-tolerance curve known as the CBEMA (Computer Business Equipment Manufacturers Association) curve. This curve was redesigned in 1996 and renamed for its supporting organization, the Information Technology Industry Council (ITIC). Like the CBEMA curve, the ITIC curve is recommended as a design target for manufacturers of computer equipment [16].

IEC 61000-4-11 describes how to obtain voltage tolerance of equipment [17]. The standard does, however, not mention the term voltage-tolerance curve; instead it defines a number of preferred magnitudes and durations of dips for which the equipment has to be tested. The equipment does not need to be tested for all these values, but one or more of the magnitudes and durations may be chosen. Table I gives an overview of the voltage tolerance of currently available equipment. The values should be read as follows: A voltage tolerance of (α ms, β%) implies that the equipment can tolerate a zero voltage of α ms and a voltage of β% of nominal indefinitely. Any dip longer than α ms and deeper than β% will lead to trip-ping or malfunction of the equipment. In other words: the equipment voltage-tolerance curve is rectangular with a "knee" at (α ms, β%). These values not necessarily apply to a specific piece of equipment, they are only meant to illustrate equipment sensitivity to voltage dips. It is in all cases assumed that a dip with longer duration and lower residual voltage will have a more severe impact on equipment. This is confirmed, with some minor exceptions, by practical experience, by laboratory tests and by simulations.

Table I – Voltage-tolerance ranges of various equipment presently in use [8].

Equipment	Voltage tolerance		
	Upper range	Average	Lower range
PLC	20 ms, 75%	260 ms, 60%	620 ms, 45%
PLC input card	20 ms, 80%	40 ms, 55%	40 ms, 30%
5 h.p. ac drive	30 ms, 80%	50 ms, 75%	80 ms, 60%
Ac control relay	10 ms, 75%	20 ms, 65%	30 ms, 60%
motor starter	20 ms, 60%	50 ms, 50%	80 ms, 40%
personal computer	30 ms, 80%	50 ms, 60%	70 ms, 50%

3.3 Computers and consumer electronics

The power supply of a computer and of most consumer-electronics equipment normally consists of a diode rectifier followed by some kind of electronic voltage regulator. The power supply of all these low-power electronic devices is similar and so is their sensitivity to voltage dips. A simplified configuration of the power supply of a computer is shown in Figure 10.

The capacitor connected to the non-regulated dc bus reduces the voltage ripple at the input of the voltage regulator. The voltage regulator transforms a non-regulated dc voltage of a few hundred volts into a regulated dc voltage of the order of 10 V. If the ac voltage drops, the voltage on the dc side of the rectifier drops. The voltage regulator is able to keep its output voltage constant over a certain range of input voltage. If the voltage at the dc bus becomes too low, the regulated dc voltage will also start to drop and ultimately errors will occur in the digital electronics.

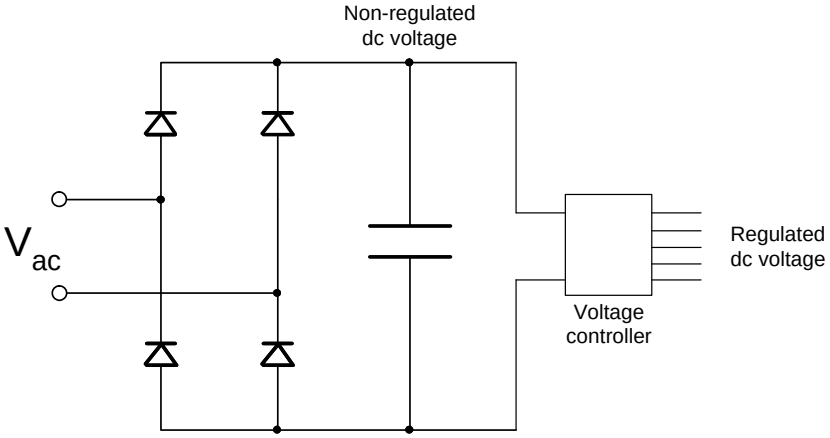

Figure 10. Computer power supply.

Figure 11 shows what happens with the dc voltage during a dip. When the rms voltage drops suddenly, the maximum ac voltage remains less than the dc voltage for the whole cycle. Thus the capacitor continues to discharge. This discharging goes on for a number of cycles, until the capacitor voltage drops below the maximum of the ac voltage. After that a new equilibrium will be reached. It is important to realise that the discharging of the capacitor is only determined by the load connected to the dc bus, not by the ac voltage. Thus all dips will cause the same initial decay in dc voltage. But the duration of the decay is determined by the magnitude of the dip. The deeper the dip the longer it takes before the capacitor has discharged enough to enable charging from the supply.

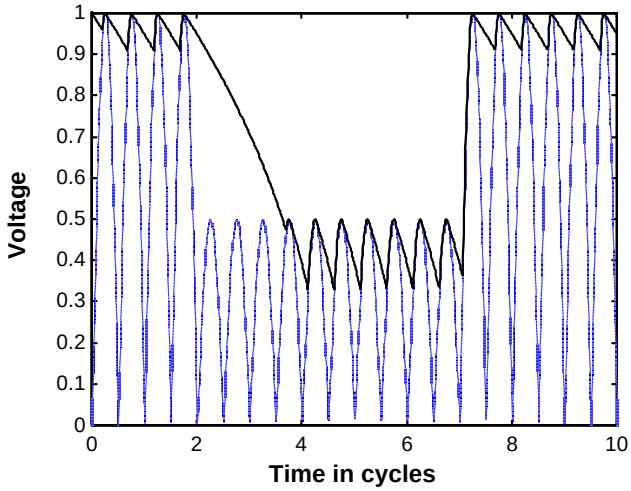

Figure 11. Effect of a voltage dip on dc bus voltage for a single-phase rectifier: absolute value of the ac voltage (dashed line) and dc bus voltage (solid line) (Adapted from [1]).

Table II gives some values of voltage tolerance. This results in what is called a “rectangular voltage tolerance curve”, shown in Figure 12.

Table II – Voltage tolerance of computers and consumer-electronics equipment.

Minimal dc bus voltage	5% dc ripple	1% dc ripple
0	5 cycles	25 cycles
50%	4 cycles	19 cycles
70%	2.5 cycles	13 cycles
90%	1 cycle	5 cycles

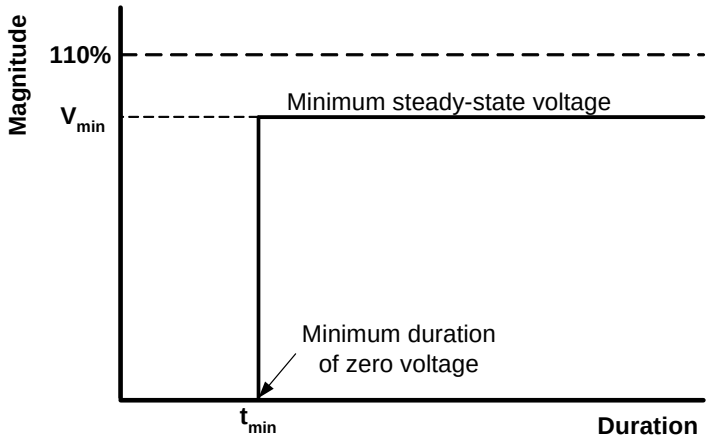

Figure 12. Voltage-tolerance curve of a computer: an example of a rectangular voltage-tolerance curve.

3.4 Sensitive loads

3.4.1 Adjustable speed ac drives

Figure 13 shows an usual configuration of an ac drive. The three ac voltages are fed to a three-phase diode rectifier. The output voltage of the rectifier is smoothened by means of a dc capacitor. The inductance present in some drives aims at smoothening the dc link current and so reducing the harmonic distortion in the current taken from the supply. The dc voltage is inverted to an ac voltage of variable frequency and magnitude. The motor speed is controlled through the magnitude and frequency of the output voltage of the voltage source converter (VSC). For ac motors, the rotational speed is mainly determined by the frequency of the stator voltages. Thus by changing the frequency an easy method of speed control is obtained.

Adjustable-speed drives are often very sensitive to voltage dips. Tripping of adjustable-speed drives occurs due to several phenomena:

- The drive controller or protection will detect the sudden change in operating conditions and trip the drive to prevent damage to the power electronic components. Tripping of the drive is mainly on dc bus undervoltage, sometimes on ac bus undervoltage, on dc voltage ripple, or on missing pulses through the rectifier diodes.
- The increased ac currents during the dip or the post-dip overcurrents charging the dc capacitor will cause an overcurrent trip or blowing of fuses protecting the power electronics components. This effect is normally considered in the drive design by setting the dc bus undervoltage protection such that the drive will trip before a dangerous overcurrent can occur.

- The process driven by the motor could not be able to tolerate the drop in speed or the torque variations due to the dip.
- During an unbalanced dip, the currents through the rectifier diodes become unbalanced. A small unbalance in voltage can lead to a large unbalance in current, with one current twice as large as number and another current zero. The large current may lead to component damage and tripping of the overcurrent protection.

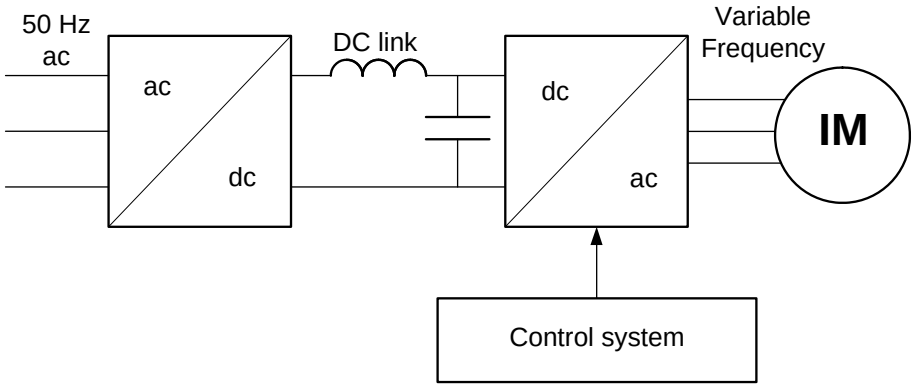

Figure 13. Typical ac drive configuration.

Many of the existing drives still trip on dc bus undervoltage. Some of the more modern drives restart immediately when the voltage comes back; others restart after a certain delay time or only after a manual restart. The various automatic restart options are only relevant when the process tolerates a certain level of speed and torque variations.

Several solutions have been developed to mitigate voltage dip effects on AC drives. They include: disabling the operation of the inverter, followed by automatic restart; installing additional energy storage; improving the rectifier or improving the inverter.

3.4.2 Adjustable-speed dc drives

DC drives have traditionally been much better suited for adjustable-speed operation than ac drives. The speed of ac motors is, in first approximation, proportional to the frequency of the voltage. The speed of dc motors is proportional to the magnitude of the voltage. Magnitude has been much easier to vary than frequency. Modern dc drives consist of a three-phase controlled rectifier powering the armature winding, and the single-phase controlled or non-controlled rectifier for the field winding. The armature circuit seldom contains any capacitance, as the inductance of the armature is high enough to keep the current constant. The field circuit is more resistive and thus needs some capacitance to prevent excessive current and torque ripples. The most sensitive part of the dc drive is the three-phase controlled rectifier. Most dips are unbalanced and thus associated with a phase-angle jump in at least one of the phases. The firing-angle control of the rectifier will be affected by this, and might even notice it as a missing pulse. The most likely reaction of the rectifier is to simply trip the drive. If the rectifier does not trip, the drop in armature voltage will cause a fast drop in armature current and thus in torque. Even a small drop in armature voltage can bring the torque down to zero, leading to a reduction in speed. As dc drives are often used for speed-sensitive processes, this will in most cases not be tolerated. During three-phase unbalanced dips, the drop in armature voltage will differ from the drop in field voltage. This can lead to strange drive behaviour, including overspeed.

3.4.3 Directly fed induction motors

A directly-fed induction motor is normally rather insensitive to voltage dips, but there are a few phenomena that could lead to process interruption due to a dip. Deep dips lead to severe torque oscillations at dip commencement and when the voltage recovers. These could damage the motor or interrupt the process. The recovery torque gets more severe when the internal flux is out of phase with the supply voltage, thus when the dip is associated with a phase-angle jump. For unbalanced dips the motor is subjected to both positive and negative sequence voltages at the terminals. The negative sequence voltage causes a torque ripple and a large negative sequence current. The phase currents are however still smaller than the starting currents, thus should not lead to process interruption. Many induction motors are protected by contactors, being motor trips actually due to tripping of the contactor. Using dc contactors will solve this problem.

3.4.4 Directly fed synchronous motors

Synchronous motor problems are similar to those of induction motors: overcurrents, torque oscillations and drop in speed. However, a synchronous motor can loose synchronism with the supply: an induction motor is very likely able to reaccelerate again after the fault, when a synchronous motor loses synchronism it has to be stopped and the load has to be removed before it can be brought back to nominal speed again.

3.4.5 Lighting

Most lamps just flicker when a voltage dips occur; users will probably notice it, but it cannot be considered as something serious. It is different when the lamp completely extinguishes and takes several minutes to recover. In industrial environments, where a large number of people are gathered, or with street lighting, this can lead to dangerous situations.

3.5 Equipment testing and sensitivity

Standards related to testing of electrical equipment to voltage dips are almost exclusively concerned with only two parameters: root mean square (rms) value of voltage magnitude, and duration. Existing standards consider such a “two-dimensional” characterisation as sufficient, and seldom mention any other dip/interruption characteristic. Testing of electrical equipment is always related to a reproduction of a simple rectangular voltage dip. Practical instructions about quantification and characterisation of non-rectangular dips are not given, nor how to assess their effects on equipment operation. In actual power systems, however, voltage dips are seldom rectangular one-stage events.

Other important aspect of existing standard for testing of electrical equipment is that they completely neglect the presence and possible influence of non-ideal voltage supply characteristics. Current standards recommend that voltage waveforms used in test should be ideal sine waves at nominal frequency and they do not consider the influence of the simultaneous occurrence of several disturbances. Sensitivity of the equipment cannot be fully and precisely assessed if any of the influential factors is excluded from the analysis, or not included in tests. Therefore, it can be generally concluded that standards and recommendations for testing of electrical equipment to voltage dips are inadequate, and should be improved, extended and reformulated in order to include additional characteristics, parameters and conditions of influence.

Factors that may have an influence on the equipment response to voltage disturbances can be divided into three following general categories [18]:

1. Voltage supply related electrical characteristics. The sensitivity of the equipment may be influenced by both, voltage supply characteristics present before the occurrence of the disturbance, and voltage supply characteristics after the end of the disturbance. Therefore, voltage supply related characteristics could be further divided into three sub-categories: pre-disturbance voltage supply characteristics (usually are related to the voltage magnitude and frequency variations, as well as to the presence of the harmonics and unbalance), during-disturbance voltage supply characteristics (magnitude and duration, phase shift during the dip, points on wave of initiation and ending, shape, type), and post-disturbance voltage supply characteristics (the individual dip characteristics and separate phenomena that may occur after the initial disturbance was cleared).
2. Equipment specific electrical characteristics: Equipment can be strongly influenced by some equipment specific factors. These factors can be divided in two general categories: *Equipment operating/loading conditions, as* trivial as the position in which equipment operates, and *Equipment malfunction criteria*, that is any condition that represents degradation/loss of some of equipment functions may be selected as equipment malfunction criterion.
3. Other, non-electrical characteristics: Usually related to environmental conditions encompassing both, voltage supply and the equipment itself. The most common factors from this category are characteristics of the ambient in which both equipment and power supply system should operate: temperature, humidity, air pressure, altitude, the presence of vibrations, etc.

All types of equipment are neither influenced by the factors from all three categories, nor by all factors from the same category. Depending on the equipment type, the effects of some factors might be so small that they can be neglected during the assessment of equipment sensitivity. The most reliable approach in deciding what factors can be neglected and what cannot is the direct testing of equipment. Examples of the voltage dip tolerance of different sensitive equipment were presented in [19], [20] and [21].

4. Voltage Dip Mitigation

4.1 Introduction

Equipment trip is the main voltage quality problem related to voltage dips. The underlying event of the equipment trip is a short-circuit fault, which will always cause a voltage dip for some customers. If the fault takes place in a radial part of the system, the protection system can also lead to an interruption. Short-duration, shallow dips can be mitigated by improving equipment tolerance characteristics. Long-duration, deep dips and interruptions can be avoided by changing structure and/or operation of the power system. For industrial customers, who do not normally have access to system or equipment improvement, the installation of additional mitigation equipment is often the only option left to achieve the desired quality of supply at the system-load interface. Traditional devices include motor-generator sets and constant voltage or ferroresonant transformers.

Mitigation methods, which include solution such as reducing the number of short-circuit faults or the fault-clearing time, changing the system to obtain less severe events at equipment terminals, connecting mitigation equipment between sensitive equipment and the supply or improving the immunity of the equipment [1], have been classified into three groups whose main advantages and limitations are discussed in the following subsections.

4.2 Improving the system

4.2.1 Reducing the number of faults

Reducing the number of short-circuit faults in a system, not only reduces the dip frequency but also the frequency of sustained interruptions. It is thus a very effective way of improving the quality of supply. The solution is unfortunately most of the time not that obvious. A short-circuit not only leads to a voltage dip or interruption at the customer interface but also causes damage to utility equipment and plant. Therefore most utilities will already have reduced the fault frequency as far as economically feasible. Some examples of fault mitigation are: replacement of overhead lines by underground cables; use of special wires for overhead lines; implementation of a strict policy of tree trimming; installation of additional shielding wires; increase of the insulation level; increase of the maintenance and inspection frequencies.

4.2.2 Reducing the fault-clearing time

A reduction of fault-clearing time is achieved by using current-limiting fuses or static circuit breakers, which are able to clear a fault within one half-cycle. Additionally several types of fault-current limiters have been proposed which not so much clear the fault, but significantly reduce the fault current magnitude within one or two cycles. At transmission levels the fault-clearing time is often limited by transient-stability constraints and is already short, so further reduction is much more difficult. Some remaining options are the use of faster circuit breakers, a certain reduction in grading margin and faster back-up protection, such as the use of inter-tripping for distance protection and breaker-failure protection.

4.2.3 Changing the power system

The severity of an event can be reduced by implementing changes in the supply system. Some examples are:

- Installation of a generator near the sensitive load. The generators will keep up the voltage during a remote dip. The reduction in voltage drop is equal to the percentage contribution of the generator station to the fault current.
- Splitting busses or substations in the supply path to limit the number of feeders in the exposed area.
- Installation of current-limiting coils at strategic places in the system to increase the “electrical distance” to the fault. This can make the dip worse for other customers.
- Feeding sensitive equipment from two or more substations. A voltage dip in one substation will be mitigated by the infeed from the other substations. The more independent the substations are the more the mitigation effect. The best mitigation effect is by feeding from two different transmission substations. Introducing the second infeed increases the number of dips, but reduces their severity.

The number of short interruptions can be prevented by connecting less customers to one recloser (thus by installing more reclosers), or by getting rid of the recloser scheme altogether. Short as well as long interruptions are considerably reduced in frequency by installing additional redundancy in the system. The costs for this are only justified for large industrial and commercial customers. Intermediate solutions reduce the duration of (long) interruptions by having a level of redundancy available within a certain time.

4.3 Installing mitigation equipment

A standard solution for low-power equipment is the UPS (Uninterruptible Power Supply), which consists of a diode rectifier followed by an inverter. The energy storage device is usually a battery block connected to the dc link. Low cost, simple operation and control have made the UPS the standard solution for low-power equipment like computers. For higher-power loads, UPS costs associated with conversion losses and maintenance of the batteries become too high and this solution is not economically feasible.

Custom power devices are a more modern solution based on power electronics [22]. The most common devices are the static series compensator (SSC) [23] and the static transfer switch (STS) [24]. A static series compensator is a voltage source converter connected in series on the distribution feeder, which provides a controllable source, whose voltage adds to the source voltage to obtain the desired load voltage. Depending on the control strategy, it is possible to use the additional voltage source to correct supply voltage unbalance, perform load voltage regulation, compensate for voltage dips and cancel low-order supply voltage harmonics. A static transfer switch consists of two three-phase static switches, each constituted by two anti-parallel thyristors per phase. The switch on the primary source is fired regularly, while the other one is off. In the event of a voltage disturbance, the STS is used to transfer the load from the preferred source to an alternative healthy source. The load will see a disturbance during the interval in which the transfer takes place; therefore, it must be completed so quickly that the duration of the resulting disturbance at the load terminals is short enough not to cause equipment trips. Other custom power devices, such as the Static Voltage Regulator (SVR) [25] or a series combination of a STS and a SSC have been used to mitigate voltage dips.

4.4 Improving equipment immunity

It is probably the most effective solution, but as a short-time solution it is often not suitable. Equipment immunity is very hard to achieve for short interruptions; but it is impossible for long interruptions. Apart from improving large equipment (drives, process control computers) a thorough inspection of the immunity of all contactors, relays, sensors, etc. can also significantly improve the process ride-through. When new equipment is installed, information about its immunity should be obtained from the manufacturer beforehand. Where possible, immunity requirements should be included in the equipment specification. Most adjustable-speed drives have become off-the-shelf equipment where the customer has no influence on the specifications. Only large industrial equipment is custom-made for a certain application, which enables the incorporation of voltage-tolerance requirements.

5. Simulation Tools

5.1 Introduction

Voltage dip calculations and studies can be performed by means of several types of simulation tools. The selection of an adequate tool depends on several factors; e.g. goals of the study, users experience or the accuracy required in calculations. Basically, three groups of simulation tools can be distinguish:

- custom-made tools, whose development is generally based on commercially available software packages;
- specialized simulation tools, e.g. a program for short-circuit calculations;
- general purpose simulation packages; e.g. EMTP-like tools.

However, to date no one tool can be used to perform all tasks that can be required in voltage dip studies; for instance stochastic prediction and voltage dip index calculations. At the end, users will have to use more than one commercial software package or develop their own custom-made tool.

The following sections present

- an overview of the capabilities required to obtain the characteristics of a single voltage dip or to perform voltage dip studies;
- a summary of the main solution techniques implemented in simulation tools that can be used in the calculation of voltage dip characteristics;
- a comparison of simulation tools that can be used in voltage dip studies.

5.2 Calculation of event characteristics

The different methods used to obtain voltage dip characteristics by means of digital simulation can be classified into the following three groups:

5.2.1 Fault current calculations

This is the simplest method: it results only in the during-fault voltage. Most power system analysis packages contain a module for such calculations. The retained voltage is obtained directly from this method (no further calculations are needed). The duration is equal to the fault-clearing time. The protection does not need to be modelled, and a fault-clearing time can be allocated to each fault position.

5.2.2 Time-varying phasors

It is a step further. The generator and load impedances are still represented as a complex number (a phasor) but are calculated as a function of time. The fault-current calculation from the previous method is in fact repeated every time step. To obtain the dip duration, protective devices must be included into the model. The calculation of the residual voltage and the duration of the dip require some additional steps. The standard methods for calculations of dip characteristics apply to (measured) waveforms; but it seems reasonable to consider the

magnitude and the argument of the complex voltage to be equal to the rms voltage and phase angle, as would be obtained from measurements.

5.2.3 Time-domain calculations

This is the most complex method, since it solves differential equations that characterize the transient performance of the system. Simulations performed with time-domain tools can capture all voltage dip characteristics (magnitude, duration, phase angle jump, point of wave) with a high accuracy. Since models in most time-domain software packages, e.g. EMTP-like tools, can be improved as much as required, the accuracy of calculations will depend on the accuracy of the models implemented or selected by users.

Table III shows a summary of modelling guidelines and capabilities of simulation tools required to perform each type of calculation.

Table III – Required capabilities for voltage dip calculations.

Calculation method	Voltage dip characteristics	Modelling guidelines	Software tool capabilities
Fault-current calculations	Retained voltage	Steady-state models	Three-phase phasor calculations. Models adequate for steady state calculations.
Time-varying phasors	Retained voltage Duration	Steady-state models	Three-phase phasor calculations. Models to reproduce the dynamic behaviour and the control systems of generators. Protective device models.
Time-domain calculations	All	Time-domain low-frequency transient models	Three-phase calculations. Models to reproduce the transient behaviour of power components, protective devices and generators. Options to capture voltage dip characteristics. Load modelling options.

5.3 Voltage dip studies

The studies in which voltage dip calculations are involved can be classified as follows:

5.3.1 Single-event simulations

The simulation is aimed at determining characteristics of voltage dips caused at the power system buses of concern during a transient phenomenon.

5.3.2 Statistical simulations

The goal is to obtain the probability density function of voltage dips and the number of trips at load buses. A Monte Carlo simulation is the natural approach for stochastic prediction of

voltage dips when dip causes are of random nature (e.g., short-circuits at either transmission or distribution levels); however, other approaches can be successfully used when the number of random variables is not too high. A Monte Carlo simulation is a numerical procedure applied to problems involving random variables. The goal of this method is to derive the performance of a system as a function of some stochastic input variables. Sampling is repeated until convergence is achieved; the solution converges as the number of samples $n \rightarrow \infty$, being zero the rate of the statistical error convergence. A Monte Carlo method has a convergence which is independent of the phase space dimension; however, the solution has a slower convergence that a numerical solution.

5.3.3 Sensitivity studies

A sensitivity analysis is performed to evaluate the variation of a variable caused by changes of one parameter. This type of analysis is especially useful when one or more parameters cannot be accurately specified. A sensitivity analysis will determine for which range of values a parameter is of concern.

5.3.4 Calculation of voltage dip indices

Voltage dip indices can be used to indicate the different performance experienced at the different voltage levels of a power system. They can be used to characterise a single event, a site or a system. System indices can be used as a basis for system improvement.

Table IV shows a summary of the simulation tool capabilities required to obtain the goals detailed above.

Table IV – Required capabilities for voltage dip studies.

Study	Goals	Capabilities
Single-event calculations	Obtain some or all characteristics of voltage dips at buses of a power system.	See Table III.
Stochastic predictions	Obtain the probability density function of some or all characteristics of voltage dips at buses of a power system. Obtain the rate of occurrence of different voltage dip characteristics.	Capabilities shown in Table III plus a multiple run option (this should include all options required to perform a Monte Carlo solution) and post-processing capabilities (i.e. those capabilities needed to determine probability density functions and rates of occurrence).
Sensitivity analyses	Deduce the effect that some system and fault parameter can have on the voltage dip performance; e.g. the number of trips at a given load bus.	Capabilities shown in Table III plus a multiple run option and post-processing capabilities. If the analysis is used to obtain the sensitivity of a stochastic assessment, then options to perform a Monte Carlo method are also required.
Voltage dip index calculations	Obtain index values for either sites or the entire system.	Similar to those required for stochastic predictions.

5.4 Solution techniques

Two basic techniques are generally applied in voltage dip calculations, using any of the simulation tools mentioned above: frequency-domain and time-domain solution technique. Their main characteristics are summarized in the following paragraphs.

5.4.1 Time-domain solution

Although several approaches have been developed for time-domain simulations, the most common one, implemented in many time-domain simulation tools, is the scheme developed by H.W. Dommel; it combines the trapezoidal rule and the Bergeron's method [26], [27]. The differential equations of network components are converted into algebraic equations involving voltages, currents and past values. These algebraic equations are assembled using a nodal approach

$$[G][v(t)] = [i(t)][I] \quad (1)$$

where[**G**] is the nodal conductance matrix, [**v**(t)] is the vector of bus voltages, [**i**(t)] is the vector of current sources, and [**I**] is the vector of "history" terms.

Two methods are generally used to solve nonlinear networks: pseudo-nonlinear representation of power components and compensation. Using the first approach, the conductance matrix is changed and re-triangularized whenever the solution moves from one straight-line segment to another. Using compensation, nonlinear elements are represented as current injections that are superimposed to the solution of the linear network after this solution has been computed.

5.4.2 Frequency-domain solution

Although frequency-domain techniques can be used to obtain time-domain solutions, they are mostly applied to obtain the ac steady state solution of linear networks. At least, two approaches can be used in voltage dip calculations

- Bus admittance matrix

  The solution for a single frequency is obtained from the following set of equations

  $$[Y][V] = [I] \quad (2)$$

  where elements of [**Y**], [**V**] and [**I**] are complex phasor values. Elements of the matrix [**Y**] are calculated at the frequency of concern.

- Bus impedance matrix

  The solution for a single frequency is obtained from the following set of equations

  $$[Z][I] = [V] \quad (3)$$

  where [**Z**] is the impedance matrix calculated at the frequency of concern. As with the admittance equations, elements of [**Z**], [**V**] and [**I**] are phasor values.

  The impedance matrix is a suitable means for calculating fault currents and voltages. It is also a very efficient tool for voltage dip studies when the goal is to obtain dip magnitudes and to analyse the propagation of voltage dips.

An important disadvantage of these solution methods is that they cannot be applied in the presence of nonlinear components or variable topology circuits, which can produce steady-state harmonics.

Hybrid techniques have already been used, mainly in steady state solutions of systems with non-linearities and variable-topology converters. In fact, both frequency- and time-domain solution methods are available in many EMTP-like programs. And even hybrid techniques have been implemented in some of these tools to obtain steady state solution in power systems with some specific non-linearities.

5.5 Comparison of simulation tools

Although many simulation tools have been used to date for simulation and analysis of voltage dips, they can be classified into two main groups whose main characteristics, advantages and disadvantages are summarized in Table V. In the introduction of this chapter, a third group of simulation tools has been mentioned; however, software packages for a single task; e.g. short-circuit calculations, are presently very rare since these tasks are included in most general purpose simulation tools.

Table V – Comparison of simulation tools for voltage dip studies.

Type of tool	Main characteristics	Advantages	Disadvantages
Custom-made simulation tool	They are based on either a high level language, e.g. C++, or on a equation-oriented simulation tool, e.g. MATLAB.	Since these tools are developed for a very specific purpose, they can be very efficient and fast, mainly if they are only based on capabilities of high level languages.	The development of these tools can be a very difficult or even a non-affordable task if the goal is too ambitious and too many sophisticated capabilities have to be developed.
General purpose simulation tool	They are generally circuit oriented tools with capabilities that allow users to expand the scope of applications. Several commercial and non-commercial packages are presently used for voltage dip studies; they are usually integrated power system simulation tools or EMTP-like tools. Their solution techniques are based or either a frequency-domain or on a time-domain method, or even on a combination of both methods.	These simulation tools have many built-in power component models, needed for voltage dip studies and capabilities for adapting the tool to this type of studies; e.g. a multiple run option or capabilities for the development of custom-made power component models.	Since the scope of application of these tools is too broad and the built-in models and capabilities are too many, simulations can be significantly slow, mainly for some sophisticated studies, e.g. stochastic prediction of voltage dips in large transmission and distribution networks.

6. Modelling for Voltage Dip Calculations

6.1 Introduction

The representation of the equipment involved in a transient process is usually chosen taking into account the range of frequencies that are associated to the simulated phenomenon [28], [29]. In general, transients associated to voltage dip causes can be classified as low frequency and slow front transients. If only voltage dips caused by faults are simulated, the frequency range of transients is in general below 5 kHz; therefore, models to be implemented should be capable of reproducing very accurately transients below that frequency.

As discussed in the previous chapter, simulation tools for voltage dip calculation are selected taking into account the voltage dip characteristics to be predicted: if only the retained voltage is of concern, a frequency-domain tool and steady -state models can be used; however, if other characteristics must be estimated, e.g. the voltage dip duration, a more detailed model of the study zone will be developed and calculations will be usually performed with a time-domain simulation tool.

Built-in capabilities available in most time-domain simulation tools, e.g. EMTP-like tools, can be used to reproduce very accurately most transients in power systems. However, an accurate representation of some components is not easy; e.g. a transformer model may require the representation of its nonlinear and frequency-dependent behaviour. In addition, the user can be forced to choose between an accurate model and a feasible model. For instance, a detailed model of a dynamic voltage restorer (DVR) requires a very small time step size (about 1 μs) in time-domain simulations and would be time consuming in probabilistic studies; in those cases a different approach should be considered, e.g. an average steady-state model based on a voltage-controlled source.

The list of models to be used in voltage dip calculations using a time-domain simulation tool can be classified as follows:

- conventional (bulk power) and distributed generators,
- power components (transformers, lines, cables, voltage regulators, capacitor banks),
- protective devices (breakers, protective relays, reclosers, fuses),
- mitigation devices (DVR, STATCOM, STS),
- loads.

Monitoring devices, aimed at measuring or estimating voltage dip characteristics, can be also part of the model, since many time-domain software tools allow users to develop their own modules to process voltage characteristics during simulation time.

Load modelling is an important and complex issue [30]; although most calculations are performed by assuming a constant impedance representation or without including any load model, a representation of the load is crucial in many voltage dip studies; e.g. studies aimed at estimating voltage dip indices or at analyzing the performance of sensitive equipment, for which a detailed representation can be made.

Two different approaches can be considered for representing some components: deterministic or probabilistic; their selection depends on the type of study to be performed. Table VI shows a summary of modelling guidelines to be used by default for voltage dip simulation when using a tool based on a time-domain solution. When a stochastic prediction is to be performed and the test system must be simulated several thousand times, a maximum time-step size is recommendable, e.g. 100 μs, and some simplified models should be used. Note that the table includes guidelines for network equivalents, which can be needed when the system model represents only a distribution network.

The following sections summarize modelling guidelines to be considered for the most important components of a power system. Although the guidelines can be considered when using any type of simulation tool, they are mainly addressed to users of time-domain simulation tools.

Table VI – Modelling guidelines for voltage dip studies.

Component	Modelling guidelines
Conventional and distributed generators	The representation of any generator will depend on the area of vulnerability of the voltage dip. If the generator is connected to an affected bus then a detailed model, suitable for simulation of slow transients (incorporating control units and nonlinear effects) can be needed; otherwise a constant voltage source behind its transient reactance can suffice.
Network equivalents	The most accurate representation should be deduced from the frequency response of the transmission system that is feeding the distribution network; however, a three-phase Thevenin equivalent model deduced from the short-circuit capacity will be good enough when simulating low frequency transients, e.g. voltage dip transients.
Lines and cables	Distributed-parameter models should be used to obtain very accurate simulation results; however, lumped-parameter models are usually acceptable and they should be used in probabilistic studies.
Transformers	Saturable models are needed when transformer energization is the voltage dip cause; however, when the event is caused by a short-circuit, linear models will produce accurate enough results.
Protection systems	Circuit breakers, reclosers and any type of disconnectors can be represented as ideal switches in low-frequency transients. A non-linear resistance is needed to represent fuses. Protective relay models should only incorporate delays and reclosing times. A more accurate model should also incorporate instrument transformers.
Power electronics equipment	A switching model with semiconductor devices represented as ideal switches will generally suffice, although averaged or steady-state models can be also considered. Very rarely more advanced and detailed models will be needed.
Loads	A constant impedance (i.e. a parallel R-L) model can be good enough in many dip studies; a more accurate load model could also show voltage dependence, dynamic behaviour and voltage dip sensitivity. In probabilistic studies, the load model could incorporate a daily variation and a random nature.

6.2 Lines and cables

Most EMTP-like tools have supporting routines for the calculation of line and cable parameters [27]. These routines can provide the following models: lumped-parameter equivalent or nominal pi-circuits, at the specified frequency; a constant distributed-parameter model, at the specified frequency; frequency-dependent distributed parameter model, fitted for a given frequency range. A frequency-dependent distributed parameter is the best representation for a single simulation if the goal is to capture very accurately voltage dip characteristics. The frequency response of the model should be fitted in a given range, e.g. below 5 kHz. However, a constant distributed parameter model will suffice for most cases.

If models are to be used in probabilistic studies, distributed-parameter models have two important drawbacks: they are time consuming and can require a very small time step size

when the fault that causes the voltage dip is produced not far from a line/cable terminal. A lumped parameter model is then recommended. If the goal is to obtain approximated values of voltage dip characteristics (magnitude, duration, phase jump), then a symmetrical-component model will suffice.

6.3 Transformers

Transformer modelling is an important issue in voltage dip simulations. Some aspects to be considered when developing a transformer model are: core and winding configuration, saturation, eddy current effects [31], [32]. Saturation, as well as core configuration, can be critical if the voltage dip is caused by a transformer energization. Besides, a very small step size (less than 10 μs) is usually required for simulation of nonlinear transformer models. If a nonlinear model is required, voltage dip assessment using a stochastic prediction and a time-domain simulation technique will be time consuming [33]. An advantage to be considered for transformer representation when only dips caused by faults are simulated is that in most cases transformers do not saturate during the event, so a linear model can be used. An important drawback when using nonlinear topology-based models for representing three-phase core transformers is the lack of standards for determination of parameters [32]. If a linear model is accurate enough, both a linear matrix representation and a saturable model can be used, but only the first approach is reliable enough for representing all transformer cores.

Voltage dip characteristics obtained from transformer models with and without including saturation will be very similar during a fault condition. The later is an important consequence since linear models can be used to obtain accurate enough voltage dip characteristics. However, this does not mean that all simulation results will be always the same, irrespectively of the transformer model, since an inrush transient is always produced when voltage is recovered; only a nonlinear model can accurately reproduce such transient.

6.4 Modelling of protection systems

The most severe voltage dips in transmission and distribution networks are caused by faults. Since a fault usually implies the operation of protective devices, voltage dip characteristics caused by faults depend on the performance of the protection system. Therefore, an accurate computer model for voltage dip studies must include a good enough representation of protective devices.

The main principles of present protection systems are very different at transmission and distribution levels. While overcurrent protection is the most commonly used scheme at distribution level, several other protection schemes are used at transmission levels.

The following subsections discuss modelling guidelines to be used when representing main protective devices in voltage dip studies at both transmission and distribution levels. Although instrument transformers are a very important part of a protection system, their models are not discussed here. It is assumed, by default, that voltages and currents inputted to protective relays are not modified by instrument transformers, whose models are assumed to have an ideal performance. This can be untrue, and the protective relay response, as well as that of the circuit breaker, can be seriously affected by the behaviour of instrument transformers. For a discussion about modelling of instrument transformers and their effect on the transient behaviour of protection systems see reference [29].

6.4.1 Modelling of transmission level protective devices

In general, circuit breakers, protective relays and instrument transformers need to be represented in the model of a protection system at transmission levels. Modelling guidelines of circuit breakers and protective relays are summarized below. The subject is too wide, mainly for relays; for more details readers are referred to Chapter 7 of reference [29].

A. Circuit breakers

The separation of the contacts of a circuit breaker causes the generation of an electric arc. Several levels of model complexity can be considered in transient simulations during opening operations. If the aim is to represent a device which is controlled by a protective relay and its model is incorporated to estimate voltage dip durations, the breaker can be represented as an ideal controlled-switch that opens at first current-zero crossing after the tripping signal is given. The model may include a current margin parameter for approximate modelling of possible current chopping.

A breaker operation is not always successful. The way in which this feature is incorporated into the breaker model depends on the approach used to represent the breaker behaviour during a transient phenomenon. For instance, unsuccessful operation can be included in an ideal switch model by means of a random variable whose value will determine if the circuit breaker opens or remain closed.

B. Protective relays

There are at least two approaches for developing a computer model of a protective relay:

- The first approach consists of including every relay component (electro-mechanical, electronic or software) into the model. If the model is intended to accurately represent all aspects of a physical relay, then it may be very complex and would require long simulation times.
- The second approach is to develop more abstract models, which behave in a similar manner to the relay within certain bounds. A macro-model can be the best choice in voltage dip studies.

However, several limitations have to be accounted for when developing a relay model, since accurate models can be difficult to develop and verify, and manufacturers do not divulge sensitive information about inner workings of their product. Although some simplifications can lead to erroneous conclusions, a relay model does not have to represent all performance specifications. Obviously, the lack of detailed information can be a serious drawback when attempting to develop a very accurate model.

Relay modelling may be based on phasor models of the power system faults and relay operating characteristics. Phasor methods lead to the symmetrical component representation of faulted power systems. This also may lead to relay modelling using only phasor representation of the relay operating characteristic. Modelling relay using only phasor methods is generally not sufficient, especially for predicting relay time-of-operation within 1 ms. Only more accurate time-domain models should be used. Figure 14 shows the several submodels into which a digital or microprocessor-based relay model can be divided into:

- the first submodel consists of the input auxiliary transformers (if any) and the anti-alising low-pass filter,
- next is the analog-to-digital conversor process,
- the third submodel is the detector that estimates fundamental frequency information,
- the relay measuring principles are next,
- finally, a submodel that represents the trip logic.

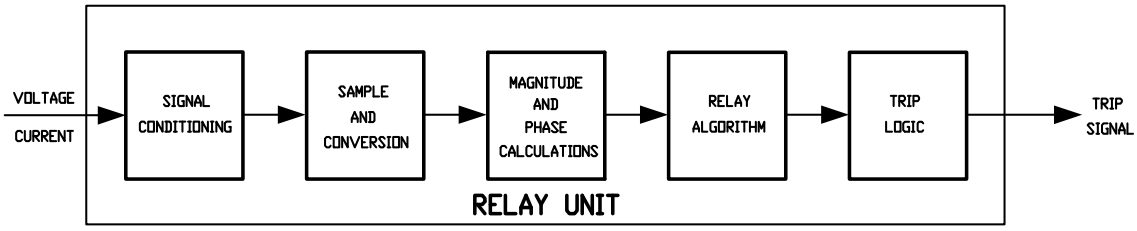

Figure 14. Schematic diagram of a microprocessor-based relay.

Although several types of relays (electromechanical, electronic, microprocessor-based) may need to be represented, computational capabilities are usually available in present time-domain simulation tools.

6.4.2 Modelling of distribution level protection systems

Modelling guidelines for the most common types of protective devices used in distribution systems (circuit breakers, reclosers and fuses) are provided. The main characteristics of each device that must be included in time-domain models are discussed. As with any other component several modelling levels can be considered; if models have to be used in statistical studies (i.e., stochastic prediction of voltage dips) then they should fulfil some conditions, e.g. provide accurate enough results with time-step sizes of about 100 μs [34].

A. Fuses

Fuse modelling, irrespectively of the type to be represented, has to duplicate the following stages [35]: current sensing, arc initiation, arc interruption, current interruption. The melting period, during which temperature rises, begins with the fault and finishes when the fuse melts; during this stage the current flows without limitation. The melting mechanism of a fuse depends on the magnitude and the duration of the current, as well as on the electrical properties of the fuse. This characteristic is shown in the so-called time-current curve provided by manufacturers. The performance of a fuse is depicted by means of the minimum melting and the total clearing curves: a fuse has an arcing time, which is the time needed to interrupt the current after the fuse melts, so the total clearing time curve is deduced by adding the arcing time to the melting time, see Figure 15.

An expulsion fuse interrupts a fault current at current zero, a current limiting fuse interrupts a fault current by forcing a current zero. Upon interruption, the operation of a current limiting fuse results in the insertion of additional impedance and the development of an arc voltage, when this voltage exceeds the system voltage, the arc is extinguished and the action accomplished. An expulsion fuse heats to its melting point when the fault occurs; the current continues to flow in the form of an arc, at zero current the arc is extinguished, being the fuse subjected to a transient recovery voltage (TRV), whose frequency and magnitude depend on the operating conditions. One or several arc reignitions can be caused by the TRV; the process stops only when the dielectric strength build up is faster than that caused by the TRV.

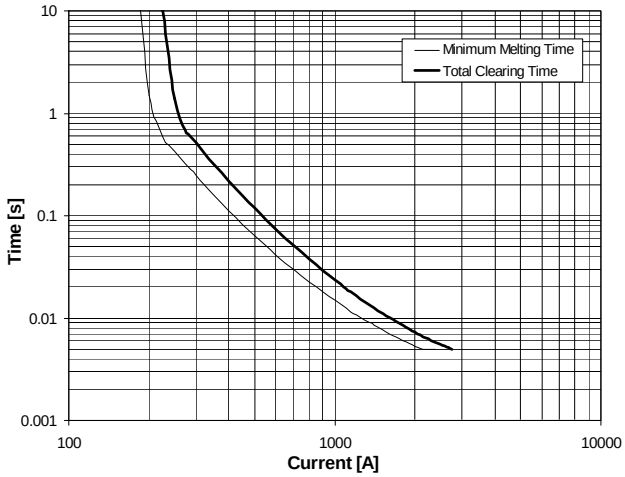

Figure 15. Extreme time-current characteristics of a fuse.

Although minimum melting curves are similar for all fuses, the approach chosen for representing every type should be different. Since the action of a current limiting fuse results in the sudden insertion of a high value resistance, this type of fuse can be modelled as a variable resistance, whose value can be assumes to vary according to the following expression:

$$R(t) = \begin{cases} t < T_m & \Rightarrow \quad R_s \\ t \geq T_m & \Rightarrow \quad R_s + K \cdot \left(1 - e^{-P \cdot (t - T_m)}\right) \end{cases} \tag{4}$$

where R_s is the fuse resistance prior to any fault condition, T_m is the melting time, deduced from the time-current curve, K and P are two factors used to adjust the fuse resistance value in the post-melting period.

An expulsion fuse can be represented as a switch that opens at the first zero-current. For more details on modelling of both types of fuses see references [36] - [39].

B. Circuit breakers

The performance of a distribution-level breaker during an opening operation is governed by the characteristics of the overcurrent relay. There are two types of relays: instantaneous and time-delay. The time-current characteristic of an overcurrent relay can consist of two sections, the first one is independent of the current, the second one has an operating time that varies inversely with current, see Figure 16. Depending on the rate with which the relay operating time and current are related, the time-overcurrent characteristic can be classified as inverse, very inverse and extremely inverse.

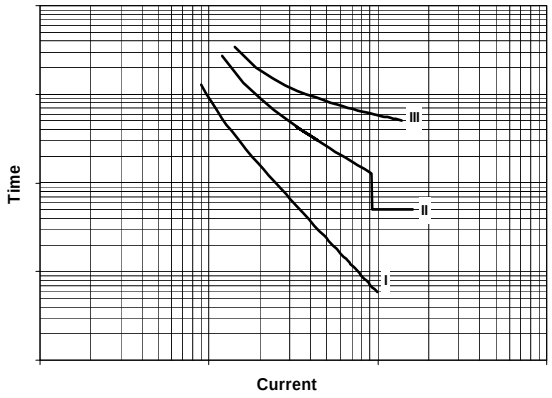

Figure 16. Time-current characteristics of overcurrent relays.

The time-current characteristic can be represented by the following expression [40], [41]

$$t(I) = \frac{K}{(I / I_a)^n - 1} \tag{5}$$

where n is a factor that characterizes each type of relay, K is a factor to distinguish each member of a family, and I_a is the pickup current; i.e. the smallest value of the current that will trigger the breaker to operate.

Circuit breaker models can be based on a controlled switch, whose time-current curve is altered by specifying the parameters mentioned above.

C. Reclosers

A recloser is an overcurrent protective device that can sense and interrupt fault currents as well as reclose automatically a predefined number of times a feeder. Its operation is similar to that of a breaker with a reclosing relay. In general, reclosers have less interrupting capability and cost less than breakers [35]. Recloser operation uses two time-current curves. The first curve, known as fast or instantaneous, is mainly used to save lateral fuses under temporary fault conditions. The second curve is known as slow or time-delay, and its main purpose is to delay recloser tripping, and allow fuses to blow under permanent fault conditions. A recloser can be set for a number of different operations, although a very common reclosing sequence has two fast operations followed by two time-delay trips. A recloser model can be based on a controlled-switch module that should allow users to include two tripping curves (fast and slow), select the type of time-current characteristic (inverse, very inverse, extremely inverse), and specify the number of reclosing operations for each characteristic and the duration of each reclosing interval.

6.5 Modelling of power electronics equipment

Models of power electronics converters in voltage dip studies can be needed to represent some components of the power delivery system, e.g. FACTS and custom power devices, or parts of end-use installations, e.g. adjustable-speed drives [42], [43]. In addition, they can be also part of the interface of distributed generators and storage devices. Figure 17 shows a scheme of the different units that can be included in the model of a power converter, which performs as an interface between two systems.

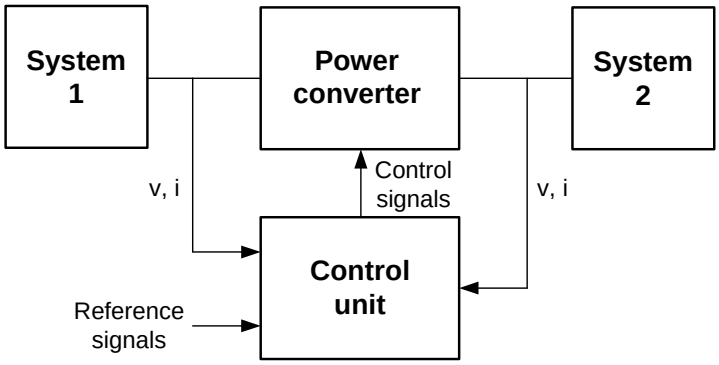

Figure 17. Scheme of a power converter interface.

The representation of power converters and their control units in transient simulations may be made using different modelling levels, i.e. from a detailed representation of each semiconductor device to an average representation of the converter without explicitly

modelling semiconductor devices at all. In many applications, an approximate converter model can be used without losing too much accuracy. Although detailed modelling of the power semiconductor devices can be required to accurately assess switching transients, device stresses and losses, in many cases "ideal" switch models can be used for modelling the power semiconductor devices [44], [45]. A summary of the different levels of models for power converters and their semiconductor devices, taken from reference [45], is presented in the following paragraphs.

6.5.1 Non-switching model

For many studies, averaged or steady-state models of the converters can be used. The power semiconductor devices are not modelled explicitly, although the internal device characteristics can be incorporated into the converter model. Instead, an averaged behavioural model for the converter, based on terminal characteristics, is developed. The converter is often represented as either a dependent current source or a dependent voltage source. In some cases, the converter will be viewed as a current source when seen from one side and a voltage source when seen from the other direction. These models are typically used for steady state operation and to study the response of slower converter control schemes for power system dynamic studies where large simulation time steps are often preferred.

6.5.2 Switching models

The degree of detail in the converter model often depends on the relationship between the frequency of interest in the simulation results and the switching frequencies in the converter. Switching models are needed when the frequencies of interest are within an order of magnitude of the switching frequencies. The control model must now include the gating circuits and the synchronization scheme. In some cases, a model of the snubber circuits has to be incorporated; in other cases, the snubber circuit can be ignored, although a numerical snubber may be needed as part of the switch model when using some transients programs.

The degree of detail depends on the relationship between the time periods of the frequencies of interest and the switch transition times of the power semiconductor devices. The latter are usually much shorter than the intervals between converter switching operations. There will be transients associated with these turn-on/turn-off transitions. If these transients (or transients with similar frequencies) are of interest, then more detailed device models will be required. In addition, when the slowest transition time of the power semiconductor device (which is often at turn-off) approaches the period between switch operations, more detailed device turn-on and turn-off models are required. Use of these models also requires more detail in modelling the parasitic inductances and capacitances in the converter.

The converter terminal characteristics are often sufficient for many simulations involving power converters. In such cases, simpler or aggregate device models can be used for which the converter can be reduced to a simpler equivalent. In addition, it is sometimes sufficient to represent a converter made up of many converter modules as a simpler converter. If the converter is connected to a system where the time scales of the dynamic response of interest are very long compared to the device turn-on and turn-off times, ideal switch models can be used. In this case, the power electronic device is assumed to open or close in one time step, as the simulation progresses (essentially instantaneously as far as the external system is concerned).

The behaviour of an ideal switch device models can be summarized as follows:

- when the device is off, it behaves as an open circuit
- when the device is on, it behaves as a short-circuit
- the device turns on at the next time step after a firing command
- the device turns off at next time step after firing command, or for diodes and thyristors at the next time step after next current zero crossing
- switch transition time is equal to one simulation time step.

These models can be applied when frequencies of interest are much slower than switch turn-on and turn-off times, or when converter losses, device voltage stresses and device current stresses are not important. They are accurate enough when representing power converters in voltage dip studies.

More detailed device models are required in other circumstances, usually of more interest to the converter designer. As voltage source converters move to more Custom Power and distributed generation applications it could become necessary to perform insulation coordination studies for these applications, especially for stresses experienced by transformers. These models must include device turn-on/turn-off behaviour and conduction behaviour while the device is on or off. More detail in other aspects of the switching circuit, e.g. parasitic inductances and capacitances, wire and lead resistance, snubber circuit characteristics, and accurate gate circuit models, can be needed.

6.6 Load modelling

Load modelling for dynamic performance analysis has been the subject of a significant effort during the last years [46] – [51]. Load modelling can be important in voltage dip studies since the model chosen to represent the demand can have a strong influence on some dip characteristics. Although not much effort has been dedicated to the representation of the load in voltage dip studies, some interesting works have been performed and some experience is already available [52] – [54]. In fact, load models to be used in voltage dip studies can be very similar to those proposed for transient stability studies, since in both cases slow transients are to be analyzed. The retained voltage is hardly affected by load conditions if the dip is caused by a fault. However, other voltage dip characteristics can be strongly influenced by the approach chosen for representing the load. Important aspects to be considered are listed below.

- Field measurements have shown that power demand is voltage dependent [55].
- Induction motors constitute a significant percentage of the load in a power system, so the load model has to incorporate a dynamic behaviour and a frequency dependency.
- The impact of a voltage dip will depend on the percentage of the sensitive equipment that is connected to the system affected by the disturbance; therefore, acceptability curves must be also incorporated into the load model [56].
- If the goal is to predict the characteristic of voltage dips (i.e. density functions of magnitude and duration), the study must be based on a probabilistic approach [30]; therefore the daily variation and the random nature of the load must be also included.

Table VII shows a summary of load models for voltage dip calculations based on the goal of the study [30].

Table VII – Load models for voltage dip studies.

Goal		Solution technique	Load model
Calculation of voltage dip characteristics	Voltage drop	Steady state / Time domain	It is generally unimportant, a constant impedance representation will suffice
	Dip duration	Time domain	
	Phase jump	Steady state / Time domain	
Calculation of the undelivered energy		Time domain	The model has to incorporate voltage and frequency dependency, dynamic behaviour and sensitivity to voltage dips (acceptability curves)
Stochastic prediction of voltage dip characteristics (dips per year)	Voltage drop	Steady state / Time domain	It is generally unimportant, a constant impedance representation will suffice
	Dip duration	Time domain	
	Phase jump	Steady state / Time domain	
Stochastic prediction of the undelivered energy		Time domain	The model has to incorporate voltage and frequency dependency, dynamic behaviour, daily variation (including random variation) and sensitivity to voltage dips (acceptability curves)

Models for load representation can be divided into two main groups: deterministic and probabilistic, whose main characteristics are detailed below.

6.6.1 Deterministic models

A complete load model should include voltage and frequency dependency, dynamic behaviour and tolerance to voltage dips. Different models incorporating one or several of these features can be considered.

1. Static model. A power demand that incorporates voltage dependence can be expressed as follows:

$$S = P_0 \sum_{k=0}^{n_p} a_k V^k + jQ_0 \sum_{k=0}^{n_q} b_k V^k \qquad \left(\sum_{k=0}^{n_p} a_k = 1 \quad ; \quad \sum_{k=0}^{n_q} b_k = 1 \right) \tag{6}$$

where P_0 and Q_0 are respectively the rated real and reactive power at nominal voltage, and V is the p.u. voltage.

Expression (6) assumes that there could be a part of a power demand that is voltage-independent. In fact, this is the approach implemented in the majority of load flow programs. By using this approach, the power demand remains the same irrespectively of the values of bus voltages. This is not a realistic model for voltage dip calculation, as it would mean that even for very low retained voltages, the demand will be the same as that prior to the dip. A V^1 dependence means that the load behaves as a constant current source, while a V^2 dependence means that a load behaves as a constant impedance.

2. Dynamic model. Since a significant percentage of the electric consumption is constituted by induction motors, the load model has to include a dynamic performance. Although models for representation of induction motors based on a block diagram have been developed [46],

other dynamic loads have to be considered. Figure 18 shows the diagram of a dynamic load model that can be applied to both real and reactive powers with different parameters [50].

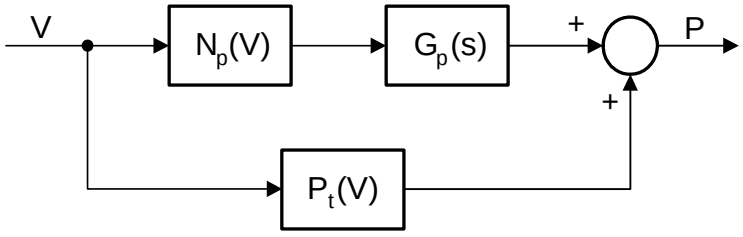

Figure 18. Diagram of a dynamic model for active power.

Several levels of sophistication have been proposed for the model depicted in the figure; in this work the block $G(s)$ is represented as a first order model. Time-domain equations of this model can be written as follows:

$$\begin{aligned}
&\tau_p \frac{dP_r(V)}{dt} + P_r(V) = N_p(V) \quad ; \quad \tau_q \frac{dQ_r(V)}{dt} + Q_r(V) = N_q(V) \\
&N_p(V) = P_0 \sum_{k=0}^{n_p} a_{sk} V^k - P_t(V) \quad ; \quad N_q(V) = Q_0 \sum_{k=0}^{n_q} b_{sk} V^k - Q_t(V) \\
&P_t(V) = P_0 \sum_{k=0}^{n_p} a_{tk} V^k \quad ; \quad Q_t(V) = Q_0 \sum_{k=0}^{n_q} b_{tk} V^k \\
&P = P_r(V) + P_t(V) \quad ; \quad Q = Q_r(V) + Q_t(V)
\end{aligned} \tag{7}$$

where τ_p and τ_q are recovery time constants, $P_r(V)$ and $Q_r(V)$ are respectively the active and reactive power recoveries, while $P_t(V)$ and $Q_t(V)$ are the active and reactive powers of the dynamic part. $P_r(V)$, $Q_r(V)$, $P_t(V)$ and $Q_t(V)$ are represented by a polynomial expression such as that shown in expression (6), but coefficients for each power component are different.

The model described by the above equations is known as *exponential recovery model*; since not all dynamic loads can be represented by this model, see for instance [54], other approaches can be needed.

3. Hybrid model. It is the model that results from a combination of any of the above models, to which an induction motor load can be also incorporated.

4. Load tripping. Sensitivity or tolerance of equipment to voltage dips can be represented by acceptability or voltage-tolerance curves. The incorporation of this curve is straightforward: since either the above approach requires a voltage measurement, this value is used to decide whether the magnitude and duration of the voltage dip will force a trip or not. Another aspect to be considered is the tolerance of the equipment to phase jump; if this must be incorporated, then a phase jump measurement is also required.

6.6.2 Probabilistic models

The daily demand variation will be based on two curves for the active and reactive power, respectively, and a normal probability density function for each power. The determination of the real and reactive power at a given bus for every period will be therefore based on the random generation of three values: the first one will be the fault instant, which is necessary to obtain the mean value of both active and reactive powers, and two additional random values, which are necessary to obtain the final values of both powers, considering the standard deviation for each one. One of the above deterministic models will be used after the values of

active and reactive powers have been determined. This approach can be extremely complex if all parameters to be specified in a deterministic model are assumed variable and random.

Other works on load modelling using an electromagnetic transients program has been previously reported, see for instance [57] - [60]. Other important issues are the estimation of load parameters [50], [51], or the effect that load conditions can have on voltage dip characteristics [60].

6.7 Models for bulk-power and distributed generators

In voltage dip studies a generator connected to a transmission network is usually represented as an ideal constant-voltage source. This model is acceptable if the generator is not inside the area of vulnerability (see Section 7.2 of this document). However, if the generator terminals are inside the area of vulnerability, then the control of the excitation will react and a more detailed generator model should be used. In voltage dip studies of distribution networks the electrical distance between faults and generators will be rather short, so detailed models of distributed energy sources are generally required.

The synchronous generator has been the main generation component for decades; although this is still the situation in all bulk power systems, many large wind energy farms, where the induction generator is often used, have been already connected to transmission networks. In addition, the effect that voltage dips can have on wind energy farms is a very important issue in modern power systems. The following subsections provide modelling guidelines of the most common generation technologies; the first one summarizes the main features of a synchronous generator model when it has to be included in voltage dip calculations; the second subsection discusses models to be used for distributed generation.

6.7.1 Bulk-power generators

Figure 19 shows the main components of a synchronous generator. In voltage dip studies a complete representation of both the electrical and the mechanical part of the machine, as well as the model of voltage control unit, will be generally required. Saturation effects may be also included in the model of the electrical part; although they do not affect the machine performance during a fault, they can have a strong influence during the post-fault period, especially with low retained voltage dip cases.

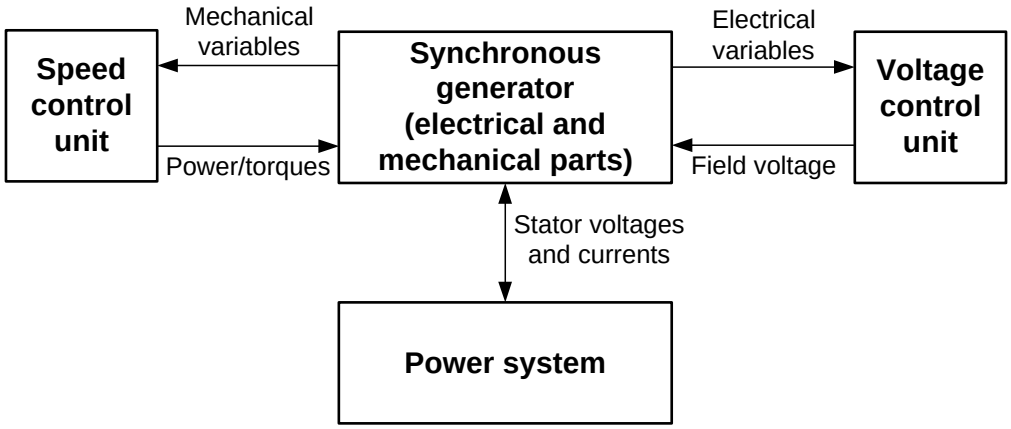

Figure 19. Schematic diagram of a synchronous generator and its control units.

The response of protective relays in transmission networks is usually very short (i.e. faults are generally cleared in less than two cycles of the operation frequency), and the model of the speed governor is not required. Very rarely breaker operations are delayed more than 10 cycles; only in those situations, and especially when turbines are equipped with fast controllers, speed governor models should be included. Detailed models of synchronous generator and the associated control units during low frequency transients have been presented in many references, see for instance [27], [61] – [64].

6.7.2 Distributed generation

The production of electrical energy from renewables and other distributed power sources often requires interfacing of the primary source to the grid or the local load via a power electronics converter. Typical examples in the field of the renewable energy sources are the variable speed wind turbines, whose aerodynamic power is first converted to AC power of varying magnitude and frequency, through a rotating electrical generator (induction or synchronous), then it is rectified to DC and subsequently inverted to the AC frequency of the grid. Similar is the situation in the case of photovoltaics, where their DC output power has again to be inverted to AC for grid-connected operation. Figure 20 shows a schematic representation of a dispersed generator: a generator model is used for the calculation of the power injected to the power electronics interface; a static converter model and its control system are used to calculate the power injected to the grid, as well as the voltage and frequency applied to the energy source and the common coupling point, respectively.

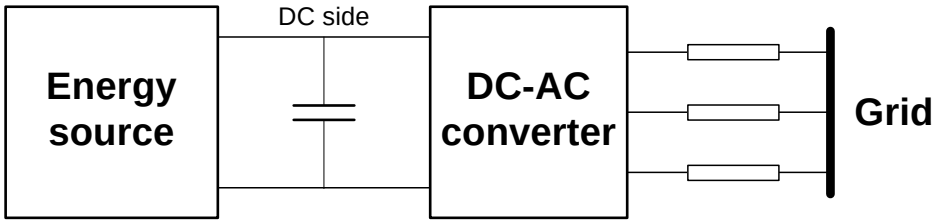

Figure 20. Dispersed generator configuration interfaced to the grid via power electronics.

Model requirements strongly depend on the application, i.e. on the time scale and nature of the phenomena to be reproduced. On the other hand, modelling of the energy source is case-specific and depends on the type of source under consideration (wind turbines, photovoltaics, fuel cells, etc.). In any case, the developed model is connected and solved together with the model of the output DC/AC converter, to represent the dynamics of the whole system [65].

A. Generation models

i. Wind energy conversion systems: They comprise several subsystems that are independently modelled: the aerodynamic, the generator, the mechanical system and the power converters, in case of variable speed wind turbines. The mechanical subsystem can be represented by means of three to six elastically connected masses. The use of at least two masses is necessary for the representation of the low-speed shaft torsional mode. As for the generator, it can be based on either a induction or a synchronous machine.

Induction machines can be represented by a fourth order model expressed in the arbitrary reference frame, while the controller can use either a scalar or a vector control strategy. Figure 21 shows the principle of a vector controller. Using the coordinate transformation to the rotating flux reference frame, the decoupled control of the machine torque and flux levels can be achieved. The control system consists of two major loops, one for the

rotating speed of blades and the other for the rotor flux linkage. Indirect field-oriented voltage control is applied to the generators. The wind speed input signal is led to the wind speed – blades optimal rotating speed characteristic, which produces the input signal to a low-pass filter. The output of the low-pass filter is used as input to the torque controller. For low wind speed, maximum energy efficiency is achieved by tracking the optimal rotating speed. At high wind speeds the control scheme imposes a constant rotating speed. The q-axis current component in the field-oriented frame can be obtained from the electromagnetic torque, while the d-axis current component can be obtained from the rotor flux. The desired voltage components in the field-oriented frame are obtained from the model of the induction machine. The main drawback of this control scheme is that it requires accurate knowledge of the machine parameters. It is commonly used with on-line parameter adaptive techniques for tuning the value of the parameters used in the indirect field controller, ensuring in this way successful operation.

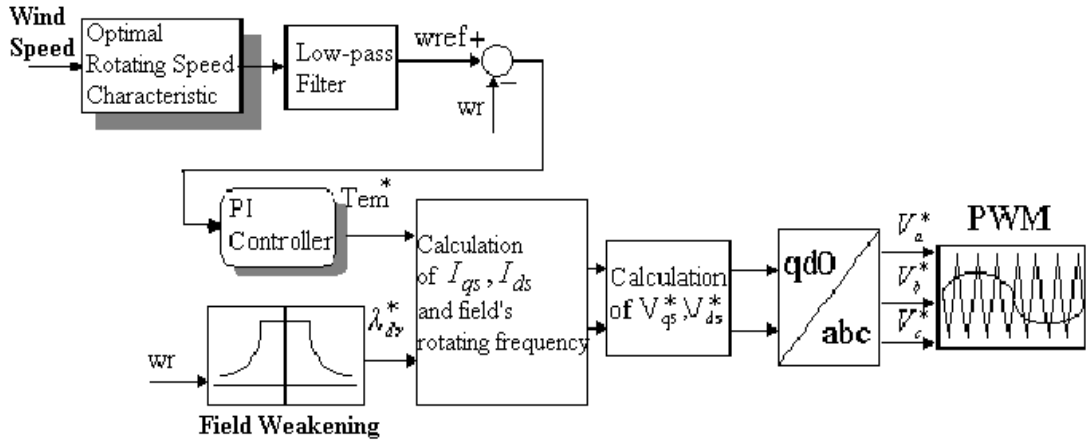

Figure 21. Indirect field-oriented voltage controller.

Figure 22 shows a variable speed wind turbine equipped with a synchronous generator. The variable frequency AC output of the generator is converted to DC by an uncontrolled diode-rectifier. A boost DC-DC converter interfaces the rectifier to the DC/AC grid-side converter. The generator rotor is electrically excited. Damper windings can be neglected, because they hardly affect the grid interaction in power system dynamics simulation, due to the decoupling effect of the power electronic converter. The generator torque control is performed by the DC chopper, which regulates the rectifier (and hence the generator) current through a simple current control loop. The DC current reference is the output of the speed control loop. Alternatively, it may be determined directly from a torque reference value, if the turbine operates in the torque control mode.

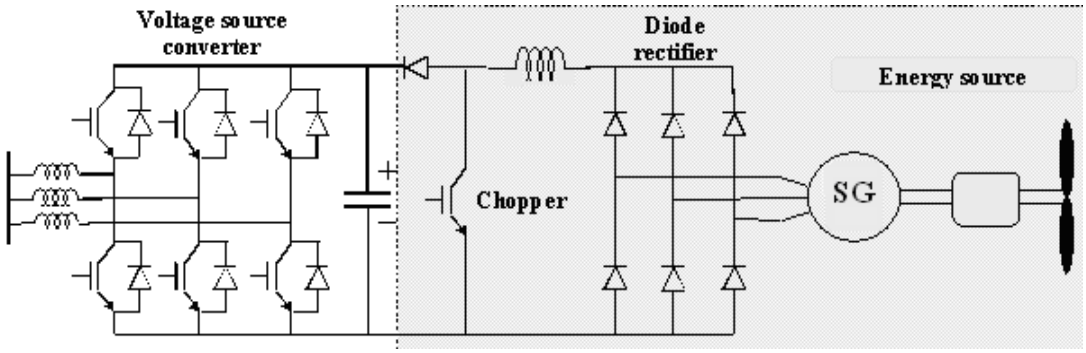

Figure 22. Wind turbine equipped with synchronous generator.

ii. Photovoltaic systems: Models of varying complexity can be used to describe the behaviour of a PV array. To choose an appropriate model, the most important factor is accuracy; there is always a trade-off between accuracy and simplicity.

1. Simplified single-diode model

The model inputs are the ambient temperature, solar irradiance; array voltage while the output of the model is the array current. Voltage will be an input from the MPPT control scheme embedded in the inverter. When using this model, it is assumed that:

- All the cells are identical and they work with the same irradiance and temperature. Also, voltage drops in the conductors that interconnect the cells are negligible.
- Short-circuit current is affected only by the irradiance and temperature of the cells.
- Open circuit voltage of the cells depends exclusively on the temperature of the cells.
- Temperature of the solar cells depends exclusively on the irradiance and ambient temperature.
- Series resistance and diode quality factor of the cells are considered constant for all operating temperature and irradiance range.

2. Integrated MPPT (Maximum Power Point Track) model

It considers that the PV array is working always at its maximum power point for given temperature and irradiance conditions. This model is based on the linear variation of a PV module power with its temperature; its inputs are the ambient temperature and the solar irradiance, while its output is the maximum array power. When using this model, it is assumed that:

- All the cells are identical and they work with the same irradiance and temperature.
- There are no lo losses in the array.
- The PV array is always working on its maximum power point for given irradiance and ambient temperature conditions, but if these conditions change, the model instantaneously changes its maximum operation point.
- Temperature of the solar cells depends exclusively on the irradiance and ambient temperature.

iii. Fuel cells: A power generation fuel cell model has to represent three main parts: the *fuel processor*, which converts fuels such as natural gas to hydrogen and by product gases; the *power section*, which generates the electricity; the *power conditioner*, which converts *dc* power to ac power output and includes current, voltage and frequency control. All the reactions that occur in the fuel cell have an associated time delay. The chemical response in the fuel processor is usually slow, as it is associated with the time needed to change the chemical reaction parameters after a change in the flow of reactants. This dynamic response function is modelled as a first-order transfer function with a time delay constant, which is generally short and associated with the speed at which the chemical reaction is capable of restoring the charge drained by the load. The dynamic response function of the flow is also modelled as a first-order transfer function with the time delay constant of the respective element. The outputs of this model provide the potential difference between anode and cathode and the reaction current. A conventional battery can be connected to the dc output of the fuel cell to provide fast response to load step increases. The interface

with the grid is made through an inverter that may include a power frequency control loop for stand-alone operation.

B. DC/AC interface

The control of the active and reactive power flow to the grid is performed by a DC/AC converter. In the case of a voltage source inverter, the controlled variables are the frequency ω_i and the magnitude V_i of the fundamental component of its AC voltage, which is synthesized by properly switching on and off its semiconductive elements. A decoupled regulation of P and Q permits the implementation of the control principle illustrated in Figure 23. The active and reactive power regulation loops are independent but not fully decoupled. P^* and Q^* are the set points for the output active and reactive powers, P and Q, whereas the actual P and Q, along with the power angle δ, are calculated from measurements of the phase voltages and currents. The determination of the P^* and Q^* reference values depends on the specific application and installation considered. A usual practice is to utilize the Q^* input in order to maintain constant output power factor (often unity, hence $Q^* = 0$). Alternatively, Q^* may be varied in order to regulate -or simply support- the bus voltage at (or near to) the output of the converter, provided that the current rating of the converter permits it.

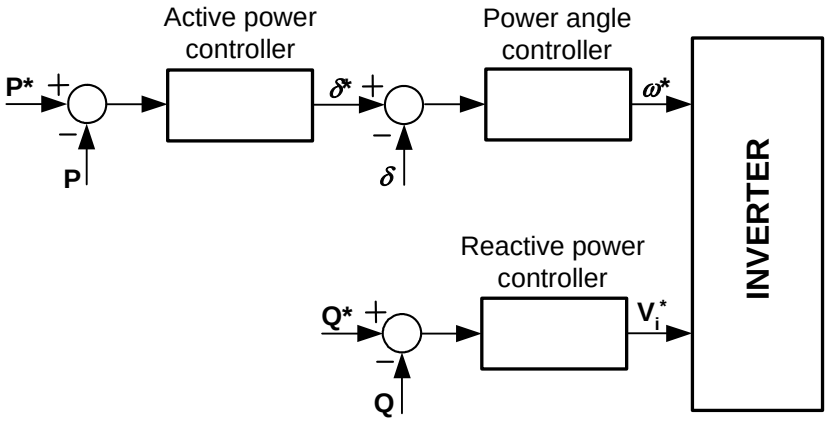

Figure 23. Active and reactive output power control principle.

If the DC/AC converter is current controlled (which requires a relatively high switching frequency and is not yet common at high power levels), decoupling of the active and reactive power regulation loops can be achieved by means of the vector control principle. For the fundamental frequency modelling of the converter system shown in Figure 20, the differential equations of the DC capacitor and the output inductances are used, along with the power balance equation of the DC/AC converter.

7. Voltage Dip Evaluation

7.1 Introduction

The stochastic approach is the most suitable way to predict the number and characteristics of voltage dips in a network [66] – [75]. Though one cannot predict the exact time when the dip will occur, it is possible to estimate the probability of occurrence of the dip of particular characteristics at a given location. Stochastic prediction methods are as accurate as the model and the data used. While the accuracy of the models can easily be influenced and improved if necessary, the accuracy of the data is often outside of our control. The data involved in

voltage dip assessment are power system and component reliability data. Component reliability data can only be obtained through observing the behaviour of the system component over long period of time and hence they have the same uncertainties as the outcome of power quality monitoring. Many utilities have records of component failures over several decades.

Faults can be categorised as self-clearing, temporary and permanent. A self-clearing fault extinguishes itself without any external intervention. A temporary fault is a short-circuit that is cleared after the faulted component is de-energized and reenergized. A permanent fault is a short-circuit that persists until repaired. Faults can be observed at the customer's premises as long interruptions, short interruptions, dips and swells. Outages occur when permanent faults take place in the direct path feeding the customer. Short interruptions are the result of temporary faults cleared by the successful operation of a breaker or recloser. Dips and swells occur during faults that are not in the direct path supplying the load.

A distinction should be made between fault (a condition that causes a device or a component to fail; e.g., relay maloperation) and short-circuit (an abnormal connection of low impedance between two points of different potential). By default, it is assumed that all faults causing voltage dips are short-circuits. Therefore, fault statistics used in this publication are in fact short-circuit statistics.

Several random factors are involved in the analysis of voltage dips:

- Fault type. Three phase faults are more severe than single-phase faults, but the later are much more frequent.
- Fault location. Faults originated in transmission systems cause dips that can be seen tens of kilometres away, while faults at radial distribution systems have a more local effect.
- Fault initiation angle or point on wave. This uncertainty has an important effect on the ability of some equipment to tolerate the dip. It affects the transient behaviour of the fault current, but it does not have much relevance for the counting of events.
- Fault impedance. Solid faults cause more severe dips than impedance faults.
- Fault clearing time. Dips last for the time short-circuit current is allowed to flow throughout the system. Protection devices allow different settings causing dips of different duration. A post-fault dip may occur due to motor and transformer recovery.
- Reclosing time. It is common practice to set one or two reclosing attempts in radial distribution feeder protections. This practice is known as fuse saving and has an important impact on frequency of dips originated at distribution levels.
- Fault duration. Self-cleared faults cause dips which duration depends on the fault itself, not on the protection setting.
- Power system modifications. The impedance between the point of observation and the fault point affects the magnitude of a fault caused dip. However the system is not static and changes that affect this impedance are continuous.
- Severe weather. The occurrence of faults and dips is notoriously bigger during severe weather, which can take many forms such as wind, rain, ice or snow.

In stochastic prediction of voltage dips two methods are generally used:

- The method of fault positions calculates the characteristics of voltage dips (magnitude, duration and phase shift) at the equipment terminals for a number of faults spread throughout the system. Each fault position represents faults in a certain part of the system. By increasing the number of fault positions, the accuracy of the results can be increased. The expected number of fault occurrences per year is deduced from the monitored (historical) data for each fault position. The first step in applying the method is the selection of the actual fault positions. A random choice of new fault positions may not necessarily increase the accuracy of the result; it may only increase the computational effort. Fault positions and the type of fault in particular system can vary depending on weather conditions and utility maintenance. The main criterion in choosing the fault positions should be that each fault position represents a number of faults leading to voltage dips with a similar magnitude and duration at the location of interest.
- The method of critical distances calculates the fault position for a given voltage. By using some simple analytical expressions (strictly correct for radial systems only) it is possible to find out in which part of the system a fault would lead to a dip of given characteristics at desired location. Each fault closer to the load would cause deeper dip. Thus, the number of dips below a given threshold will be equal to the number of faults closer to the load than the indicated position.

The method of fault positions and the concept of the area of vulnerability are generally used to assess and understand the system voltage dip performance. The concept of the area of vulnerability enables to identify fault locations which will lead to dips deeper than a given voltage threshold. Voltage dip performance is assessed by performing system fault analysis in order to determine voltages at a particular bus as a function of fault locations throughout the system. The identification will yield an area that contains exposed buses and lines and associated area boundary crossing lines.

Voltage dips can be studied from different perspectives and the model used to describe the disturbance needs to satisfy the study objectives. To obtain statistics on magnitude of fault originated voltage dips modelling based on phasors has been considered suitable. It should be noted that the use of phasors restricts the model to the context of steady state alternating linear systems. The modelling used in this chapter is intended to obtain the during-fault voltage or the retained voltage during the fault but not its evolution as function of time. Figure 24 shows a three-phase unbalanced voltage dip in an 11 kV distribution network and the approximation considered in this chapter. Depending on the fault type the shape of the rms voltage evolution will show different behaviours [76].

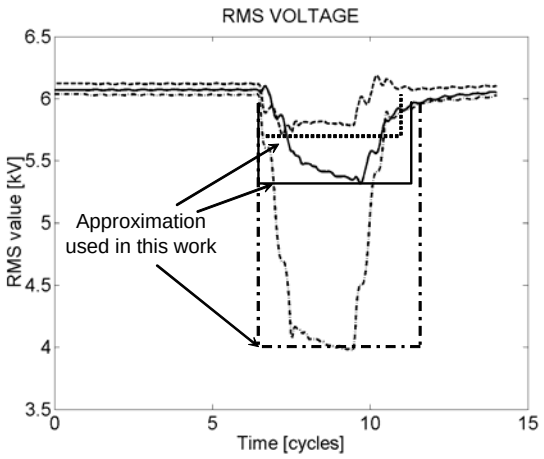

Figure 24. Three-phase voltage dip: Rms voltage vs. time.

The following sections present the main principles of voltage dip calculations using the method of fault positions and a frequency-domain technique, as well as its application to the stochastic prediction of voltage dips in transmission networks. The application of a time-domain technique to the stochastic prediction of voltage dips in distribution networks will be presented in the following chapter; that example will be also used to illustrate the calculation of voltage dip indices.

7.2 Voltage dip calculation

7.2.1 The impedance matrix

An electrical network under short-circuit fault conditions can be considered as a network supplied by generators with a single load connected at the faulted bus. The pre-fault load currents can usually be ignored since they are small compared to the fault current. Usually they are considered by means of the superposition theorem if needed.

The use of the impedance matrix provides a convenient means for calculating fault currents and voltages. The main advantage of this method is that once the bus impedance matrix is formed the elements of this matrix can be used directly to calculate the currents and voltages associated with various types of faults.

Bus and current voltages of a general n-port passive linear system can be related as follows:

$$\begin{aligned}
&\overline{v}_1 = \overline{z}_{11} \cdot \overline{i}_1 + \overline{z}_{12} \cdot \overline{i}_2 + \ldots\ldots\ldots \overline{z}_{1n} \cdot \overline{i}_n \\
&\vdots \\
&\overline{v}_k = \overline{z}_{k1} \cdot \overline{i}_1 + \overline{z}_{k2} \cdot \overline{i}_2 + \ldots\ldots\ldots \overline{z}_{kn} \cdot \overline{i}_n \\
&\vdots \\
&\overline{v}_n = \overline{z}_{n1} \cdot \overline{i}_1 + \overline{z}_{n2} \cdot \overline{i}_2 + \ldots\ldots\ldots \overline{z}_{nn} \cdot \overline{i}_n
\end{aligned} \tag{8}$$

This equation can be written in matrix notation

$$\mathbf{V} = \mathbf{Z} \cdot \mathbf{I} \tag{9}$$

where **Z** is the bus impedance matrix of the network.

The impedance matrix contains, in its diagonal, the driving point impedance of every bus with respect to the reference bus. The driving point impedance of a bus is the Thevenin's equivalent impedance seen into the network from that bus. The diagonal elements of the impedance matrix allow determining the short-circuit current of every potential fault at buses of the system. The off-diagonal elements of the impedance matrix are the transfer impedances between each bus of the system and every other bus with respect to the reference bus. The transfer impedance gives the voltage at bus *k* when a current (unitary) is injected at bus *j*. Hence the transfer impedance allows determining the during-fault voltages due to the fault currents.

7.2.2 Voltage dip magnitude calculation

Faults in power systems can be symmetrical and unsymmetrical leading to balanced and unbalanced dips, respectively. For symmetrical faults only the positive sequence network is required to analyse the during-fault voltage. However the majority of the faults are single-phase-to-ground faults requiring the use of symmetrical components in the analysis [77].

A. Balanced voltage dips

Consider a network with *N* buses plus a reference bus, which is named zero and is chosen to be the common generator bus. According to the superposition theorem, the voltage during a fault is the pre-fault voltage at that bus plus the change in the voltage due to the fault

$$v_{kf} = v_{pref(k)} + \Delta v_{kf} \tag{10}$$

where $v_{pref(k)}$ is the pre-fault voltage at bus *k* and Δv_{kf} is the voltage-change at bus *k* due to the fault at bus *f*. Expression (10) can be written as a matrix relation

$$\mathbf{V_{dfv}} = \mathbf{V_{pref}} + \mathbf{\Delta V} \tag{11}$$

where $\mathbf{V_{dfv}}$ is the dip matrix that contains the during fault voltages, $\mathbf{V_{pref}}$ is the pre-fault voltage matrix and because the pre-fault voltage at bus k is the same for a fault at any bus, the pre-fault voltage matrix is conformed by N equal columns. $\mathbf{\Delta V}$ is a matrix containing the changes in voltage due to faults everywhere. Row *k* of $\mathbf{V_{dfv}}$ contains the retained voltages at bus *k* when faults occur at buses 1, 2, ..k, ..N, while column *f* of $\mathbf{V_{dfv}}$ contains the retained voltage at buses 1, 2,...N for a fault at bus *f*.

During a three phase short-circuit at bus *f*, the current "injected" to this bus is given

$$i_f = \frac{-v_{pref(f)}}{z_{ff}} \tag{12}$$

where $v_{pref(f)}$ is the pre-fault voltage at the faulted bus *f*, z_{ff} is the impedance seen looking into the network at the faulted bus and the minus sign is due to the direction of the current. Only positive sequence values are needed to perform the calculations.

Once the "injected" current is known, the change in voltage at any bus *k* can be calculated using the transfer impedance z_{kf} between bus *k* and bus *f*. Then (12) gives the change in voltage due to the current expressed by

$$\Delta v_{kf} = -z_{kf} \cdot \frac{v_{pref(f)}}{z_{ff}} \tag{13}$$

The matrix version for this equation is given is the following one

$$\mathbf{\Delta V} = -\mathbf{Z} \cdot \mathbf{inv(diagZ)} \cdot \mathbf{V_{pref}^T} \tag{14}$$

where **inv(diagZ)** is the inverse of the matrix containing the diagonal elements of the impedance matrix and the *T* over $\mathbf{V_{pref}}$ indicates transposition of the pre-fault voltage matrix. It should be noted that $\Delta v_{kf} \neq \Delta v_{fk}$ because $z_{ff} \neq z_{kk}$.

Voltage dips caused by a three-phase fault are therefore obtained as follows

$$v_{kf} = v_{pref(k)} - z_{kf} \cdot \frac{v_{pref(f)}}{z_{ff}} \tag{15}$$

The voltage seen at a bus *k* due to a fault at bus *f* can be expressed by the following general equation

$$\mathbf{V_{dfv}} = \mathbf{V_{pref}} - \mathbf{Z} \cdot \mathbf{inv(diagZ)} \cdot \mathbf{V_{pref}^T} \tag{16}$$

If the pre-fault load can be neglected, then pre-fault voltages can be assumed 1 pu, and (16) can be written as follows

$$\mathbf{V_{dfv}} = \mathbf{ones} - \mathbf{Z} \cdot \mathbf{inv(diagZ)} \cdot \mathbf{ones} \tag{17}$$

The positive-sequence impedance matrix **Z** is a diagonal dominant full matrix for a connected network. This means that every bus in the network is exposed to dips due to faults everywhere in the network, however the magnitude of the voltage drop depends on the transfer impedance between the observation bus and the faulted point. In general, the transfer impedance decreases with the distance between the faulted point and load bus. Hence load points will not seriously be affected by faults located far away in the system. The voltage change also depends on the driving impedance at the faulted bus. The driving impedance determines the weakness of the bus, the stronger the faulted bus the larger the voltage drop at another bus and vice versa.

A radial distribution system is a particular case for which the above procedure can also be applied. The during-fault voltage at the point of common coupling (*pcc*) due to a fault at bus *f*, assuming that the pre-fault voltage is 1 pu, can be obtained as follows

$$v_{pre(k)} = 1 - \frac{z_{kf}}{z_{ff}} = 1 - \frac{z_S}{z_S + z_F} = \frac{z_F}{z_S + z_F} \tag{18}$$

where Z_S is the source impedance (impedance between the source and bus *k*) and Z_F is the impedance between the *pcc* and the fault point (bus *f*). Expression (18) is suitable to analyse radial systems and is the base of the method of critical distances [67].

B. Unbalanced voltage dips

Unbalanced voltage dips are caused by unsymmetrical faults requiring the use of symmetrical components for their analysis. Because of the independence of sequences in symmetrical systems, expression (16) can be obtained for each sequence network and used to determine the during-fault voltage for each of the sequence components. Before the fault, bus voltages only contain a positive-sequence component, thus pre-fault voltage matrices of zero and negative sequences are null.

$$\mathbf{V}^{\mathbf{z}}_{\mathbf{dfv}} = \mathbf{0} + \mathbf{\Delta V}^{\mathbf{z}} \tag{19a}$$

$$\mathbf{V}^{\mathbf{p}}_{\mathbf{dfv}} = \mathbf{V}^{\mathbf{p}}_{\mathbf{pref}} + \mathbf{\Delta V}^{\mathbf{p}} \tag{19b}$$

$$\mathbf{V}^{\mathbf{n}}_{\mathbf{dfv}} = \mathbf{0} + \mathbf{\Delta V}^{\mathbf{n}} \tag{19c}$$

Phase voltages can be calculated applying the symmetrical components transformation as follows

$$\mathbf{V}^{\mathbf{a}}_{\mathbf{dfv}} = \mathbf{V}^{\mathbf{z}}_{\mathbf{dfv}} + \mathbf{V}^{\mathbf{p}}_{\mathbf{dfv}} + \mathbf{V}^{\mathbf{n}}_{\mathbf{dfv}} \tag{20a}$$

$$\mathbf{V}^{\mathbf{b}}_{\mathbf{dfv}} = \mathbf{V}^{\mathbf{z}}_{\mathbf{dfv}} + a^2 \cdot \mathbf{V}^{\mathbf{p}}_{\mathbf{dfv}} + a \cdot \mathbf{V}^{\mathbf{n}}_{\mathbf{dfv}} \tag{20b}$$

$$\mathbf{V}^{\mathbf{c}}_{\mathbf{dfv}} = \mathbf{V}^{\mathbf{z}}_{\mathbf{dfv}} + a \cdot \mathbf{V}^{\mathbf{p}}_{\mathbf{dfv}} + a^2 \cdot \mathbf{V}^{\mathbf{n}}_{\mathbf{dfv}} \tag{20c}$$

Replacing (19) into (20) gives

$$\mathbf{V}^{\mathbf{a}}_{\mathbf{dfv}} = \mathbf{V}^{\mathbf{p}}_{\mathbf{pref}} + \mathbf{\Delta V}^{\mathbf{z}} + \mathbf{\Delta V}^{\mathbf{p}} + \mathbf{\Delta V}^{\mathbf{n}} \tag{21a}$$

$$\mathbf{V}^{\mathbf{b}}_{\mathbf{dfv}} = a^2 \cdot \mathbf{V}^{\mathbf{p}}_{\mathbf{pref}} + \mathbf{\Delta V}^{\mathbf{z}} + a^2 \cdot \mathbf{\Delta V}^{\mathbf{p}} + a \cdot \mathbf{\Delta V}^{\mathbf{n}} \tag{21b}$$

$$\mathbf{V}^{\mathbf{c}}_{\mathbf{dfv}} = a \cdot \mathbf{V}^{\mathbf{p}}_{\mathbf{pref}} + \mathbf{\Delta V}^{\mathbf{z}} + a \cdot \mathbf{\Delta V}^{\mathbf{p}} + a^2 \cdot \mathbf{\Delta V}^{\mathbf{n}} \tag{21c}$$

Equations (21) provide the retained phase voltages during the fault and are valid regardless of the fault type.

7.2.3 Propagation of voltage dips

The rms voltage depression caused by a fault propagates through the network and is seen as a voltage dip at remote observation buses. The square matrix $\mathbf{V_{dfv}}$ contains the dips at each bus of the network due to faults at each one of the buses. The during fault voltage at any bus when a fault occurs at that bus is contained in the diagonal of $\mathbf{V_{dfv}}$ and is zero for solid three-phase faults. Off-diagonal elements of $\mathbf{V_{dfv}}$ are the voltage dips at a general bus *k* due to a fault at a general position *f*. Hence, column *f* contains the during-fault voltages at buses 1, 2…*f*,…*N* during the fault at bus *f*. This means that the effect, in terms of dips, of a fault at a given bus of the system is contained in columns of the dip matrix. This information can be graphically presented on the one-line diagram of the power system and it is called *affected area*. The dip matrix can also be read by rows. A given row *k* identifies that bus in the system and the potential dips to which the load connected at this bus is exposed due to faults around the system. This information can also be presented in a graphical way on the one-line diagram and is called *exposed area* or *area of vulnerability*.

A. Affected area

The affected area contains the load buses that present a during fault voltage lower than a given value due to a fault at a given point. Consider the power system of Figure 25, it has 19 load buses. Its impedance matrix has the following form

$$\mathrm{V_{dfv}} = \begin{bmatrix} 0 & 1-\frac{z_{1,2}}{z_{2,2}} & .. & 1-\frac{z_{1,8}}{z_{8,8}} & 1-\frac{z_{1,11}}{z_{11,11}} & .. & 1-\frac{z_{1,19}}{z_{19,19}} \\ 1-\frac{z_{2,1}}{z_{1,1}} & 0 & .. & 1-\frac{z_{2,8}}{z_{8,8}} & 1-\frac{z_{2,11}}{z_{11,11}} & .. & 1-\frac{z_{2,19}}{z_{19,19}} \\ \vdots & \vdots & \vdots & \vdots & \vdots & \vdots & \vdots \\ 1-\frac{z_{8,1}}{z_{1,1}} & 1-\frac{z_{8,2}}{z_{2,2}} & .. & .. & 1-\frac{z_{8,11}}{z_{11,11}} & .. & 1-\frac{z_{8,19}}{z_{19,19}} \\ 1-\frac{z_{11,1}}{z_{1,1}} & 1-\frac{z_{11,2}}{z_{2,21}} & .. & 1-\frac{z_{11,8}}{z_{8,8}} & 0 & .. & 1-\frac{z_{11,19}}{z_{19,19}} \\ \vdots & \vdots & \vdots & \vdots & \vdots & \vdots & \vdots \\ 1-\frac{z_{19,1}}{z_{1,1}} & 1-\frac{z_{19,2}}{z_{2,21}} & .. & 1-\frac{z_{19,8}}{z_{8,8}} & 1-\frac{z_{19,11}}{z_{11,11}} & .. & 0 \end{bmatrix} \qquad (22)$$

The during-fault voltages for all buses due a fault can be obtained by applying (22). For instance, column 11 contains the during-fault voltages at each bus when a three-phase fault occurs at bus 11; that is, this column contains the information to draw the affected area of the system due to a fault at bus 11. In Figure 25 two affected areas are presented for a fault at bus 11. The larger one encloses the load buses presenting a dip more severe than a retained voltage of 0.9 pu. The smaller one contains the load buses that will see a depression in the voltage more severe than 0.3 pu or equivalently the retained voltage will be less than 0.7 pu. These affected areas have been built considering faults on buses of the system. Faults on lines are more frequent, however faults on buses cause more severe dips in terms of magnitude and therefore are considered for building the affected areas.

B. Exposed area

The exposed area or area of vulnerability encloses the buses and line segments where faults will cause a dip more severe than a given value. The exposed area is contained in

rows of the voltage-dip matrix and as in the case of the affected area can be graphically presented on the one-line diagram. Figure 26 presents the exposed area of bus 8; the 0.5 pu exposed area of bus 8 contains buses 8, 9 and 11 and lines connecting them indicating that faults at these buses and lines will cause a during-fault voltage lower than 0.5 pu. Similarly, the 0.9 pu exposed area for bus 8 contains all the buses and line segments where faults will cause a retained voltage lower than 0.9 pu. The exposed area does not enclose the whole length of lines connecting the surrounded buses, because some faults on the lines might cause dips less severe than the threshold that defines the exposed area; that is, part of a line may be actually outside the exposed area, meaning that faults in this part of the line will lead to dips less severe than the magnitude under consideration. To clarify, suppose that bus 6 is fed through a relatively long double circuit line from bus 9. In such a case, faults on any of the lines occurring far from the buses 6 or 9 will be seen as shallow voltage dips at bus 6. However, faults near bus 6 or bus 9 will be seen as more severe dips at bus 6. The exposed area for bus 6 (severe dips) would be formed by bus 6, segments of the lines connecting this bus, bus 9 and segments of the lines connecting bus 9. The central part of the lines between buses 9 and 6 might be outside of the exposed area.

The exposed area has been built using the original bus impedance matrix; however, a more precise description is needed when faults occur on lines. In order to simulate faults on lines additional fictitious buses are needed along the lines. Those fictitious buses are called fault positions. As more fault positions are used to calculate the exposed areas more precise is the description of these areas and more accurate the stochastic assessment of dips, but also bigger the computational effort needed to perform the calculation. Consider the 0.5 pu exposed area in Figure 26. The border of this area crosses the line between bus 9 and bus 4. In other words: for a fault at bus 4 the retained voltage at bus 8 is above 0.5 pu; for a fault at bus 9 the retained voltage at bus 8 is below 0.5 pu. To obtain a more accurate border, the retained voltage at bus 8 should be determined for faults at different locations on the line between bus 9 and bus 4. Also additional fault positions should be considered along the other lines connecting these buses. This results in a larger dip matrix $\mathbf{V}_{\mathbf{dfv}}$. The number of rows of this matrix equals the number of original (or physical) buses, but the number of columns increases with the number of fault locations.

The exposed area is also the area for which a monitor, installed at a particular bus k, is able to detect events. For example, if a monitor were installed at bus 8 and the boundary for dip recording were adjusted to 0.5 pu, then the monitor would be able to see events in the 0.5 pu exposed area of bus 8. When referring to power-quality monitors the exposed area is called *Monitor Reach Area*.

7.3 Stochastic assessment of voltage dips

The method of fault positions is probably the most suitable tool for stochastic prediction of voltage dips. Basically, short-circuit faults are simulated at a number of different positions along the lines and at different buses throughout the system. Voltage magnitudes and phase angles following the faults are calculated for each bus. The dip frequency at each location is calculated using the information about the fault rate. After taking into account the fault rate for each type of fault, the expected number of dips is calculated. In practise, faults are randomly distributed along the line, and they may occur at any location in the power system. The information about the location of the fault is very important as it will result in voltage dips of different characteristics. Therefore, the choice of the fault positions may significantly influence the accuracy of the prediction of the voltage dips.

Different approaches have been used for selection of fault positions [71], [78], [79]. In the majority of the studies, the faults were grouped into discrete types and applied at the middle of the line, or at each 25% of the line length. This however, may not yield high accuracy of the prediction result. Alternatively, if the lines are divided into several fault sections (e.g., every 2% of the line length) the time of calculation will increase significantly. Faults might not be distributed uniformly along the line. A particular bus or some part of the line may be exposed to adverse environmental or weather conditions resulting in greater fault occurrence. The fault rate at such location will be higher than the fault rate at other locations. In general, the actual distribution of faults might be uniform, normal, exponential or a combination of those. Different fault distributions will result in different prediction of voltage dips at different buses. The predicted number of dips at a given bus may be sufficiently different from the

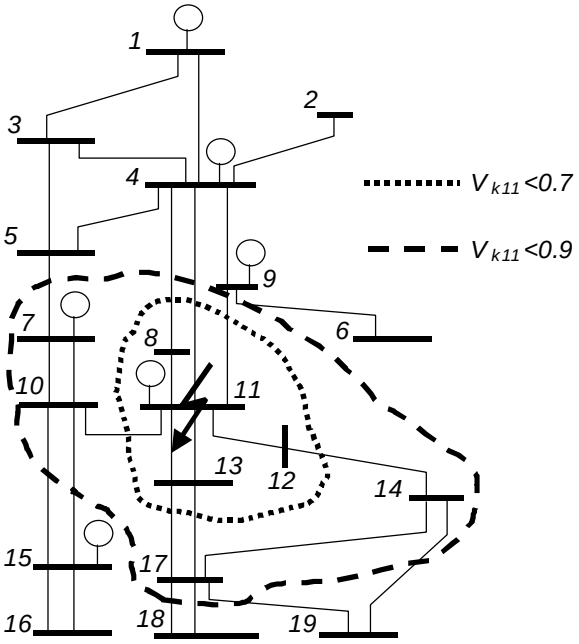

Figure 25. Affected area for a three-phase fault at bus 11 [77].

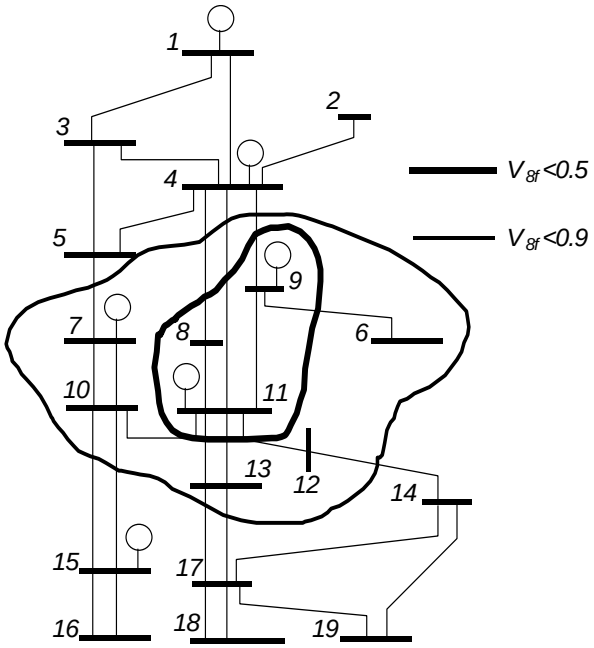

Figure 26. Exposed area of bus 8 for three-phase faults [77].

results obtained by using uniform fault distribution to warrant additional effort in modelling the actual fault distributions.

Two illustrative studies, based on the method of fault positions, are presented in this section:

1. The main objective of the first study is to illustrate how affected and exposed areas can be determined considering both balanced and unbalanced dips, and assuming an uniform distribution of faults in transmission lines.
2. The objectives of the second study are:
   - to determine compound areas of vulnerability and to assess the influence of modelling of different fault distributions along the area boundary crossing lines on prediction of the number and characteristics of voltage dips;
   - to assess the influence of the modelling of fault distribution along the line on prediction of the number and characteristics of voltage dips.

7.3.1 Example 1

A. Test system

The system used in this work is a simplified model of the National Interconnected System of Colombia (230 kV and 500 kV), see Figure 27. The system has 87 buses and 164 lines with a total length of 11651 km. It consists of two 230 kV grids connected by a double-circuit 500 kV line (buses 15, 16, 63 and 68). To calculate the impedance of generation buses, the maximum short-circuit level at some buses was used. Resistive component of the generator impedance was neglected. Power transformers interconnecting the 500 kV sector with the 230 kV sector were modelled as delta-wye solidly grounded.

B. Balanced dips

To obtain the stochastic assessment of balanced dips and their characteristics, the positive-sequence impedance matrix was used to model the system. Line capacitance was neglected. Three-phase faults were simulated around the system and dips due to them saved in the dip-matrix. The following cases were analysed:

i. Base case: This simulation considers 87 fault-positions each one coinciding with a bus position. Faults at lines were represented by the fault position at the nearest bus. The fault rate for each fault position was calculated taking the quotient between the expected total number of faults (buses and lines) and the number of fault positions -87 in this case-. This is a rough estimation but it helps to identify the boundaries of dip frequencies. No provision was made for different number of lines connected to a bus and for different line lengths.

ii. Case 1: This simulation considers 251 fault positions with 87 at buses and 164 at lines. Fault positions on lines were chosen in the middle of each line. Fault rates were assigned at each fault-position corresponding to the type of fault (bus or line). The fault rate for faults on lines was determined from the quotient between the expected annual number of faults on lines and the number of fault positions on lines. No provision was made for different line lengths.

iii. Case 2: This simulation considers 781 fault positions with 87 faults at buses and 694 faults at lines. Lines were divided so that each line segment was no longer than 15 km. Fault rates were assigned corresponding to the type of fault. Fault rate for line faults was

determined in the same form as in case 1. In this case the number of fault-positions per line was dependent on the line length.

- *During-fault voltages*

  The voltage magnitude at each bus and for each fault position was calculated. In Table VIII the during-fault voltages at a selected number of buses are presented for some fault positions at lines and buses. This table is part of the voltage-dip matrix, but it has been transposed to present the results in a more suitable manner. From the table it is easy to note that substations near to the fault experience severe dips. Consider substation 87, which is in the last column of the table; when a fault occurs at bus 6 (far away from 87), the voltage at 87 only drops 3%. However when the fault occurs at a nearer place as 37 the voltage drop is 39%. Also faults on the lines connecting substation 87 cause severe dips at this bus.

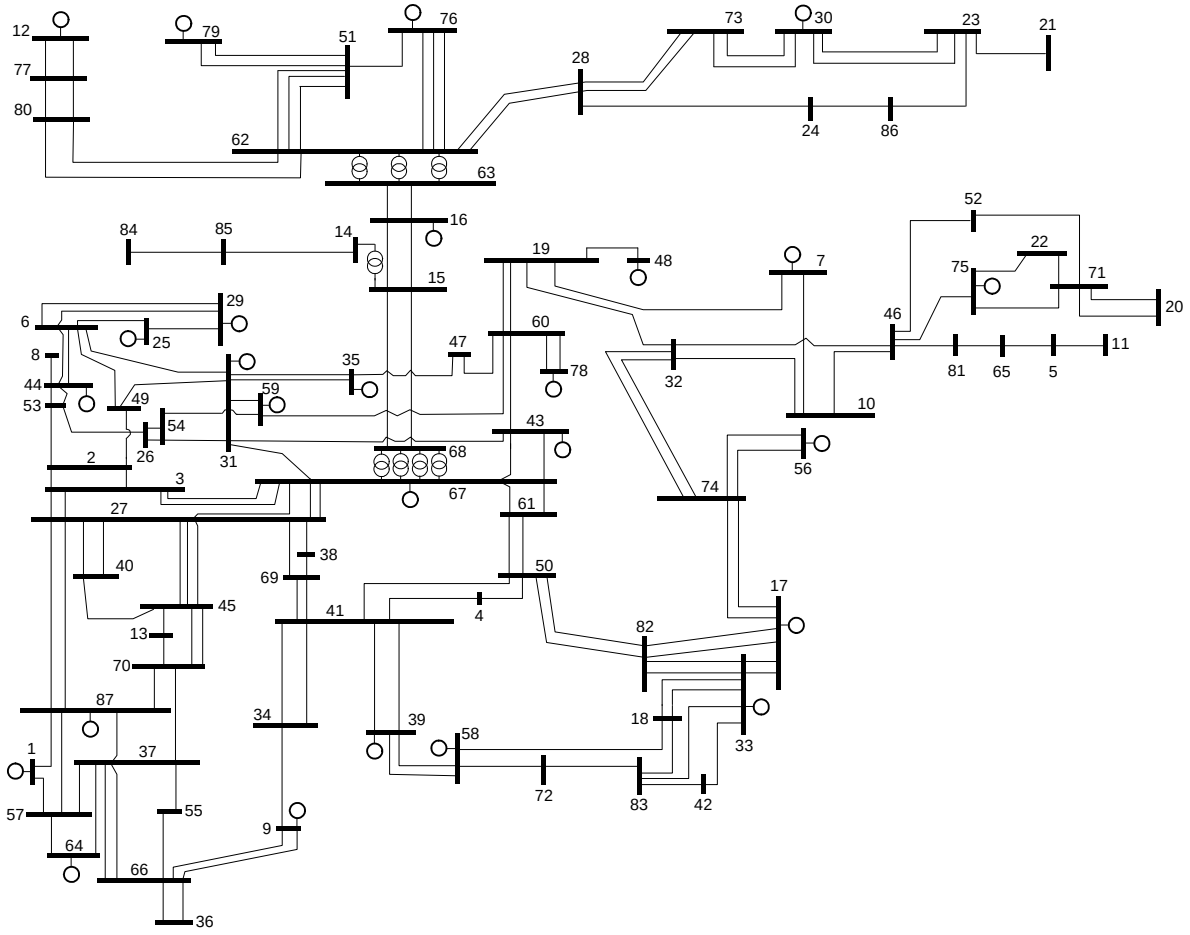

Figure 27. National Interconnected System of Colombia - Simplified model [77].

- *Affected areas*

  Figure 28 depicts the affected areas for a fault at bus 67. It is obvious that faults at this bus affect a larger area of the system. The figure shows that more than half of the buses experience dips more severe than 95% when a fault occurs at bus 67. Consequently, such a fault has the potential to cause dip-related equipment tripping for a large number of customers. In general, the size of these affected areas depends on the short-circuit level at the fault point, which depends on the generator scheduling. The stronger the bus (higher short-circuit level) the bigger the influence of a short-circuit fault on the system and the larger the affected area.

Table VIII – During-fault dip voltages due to three-phase faults [77].

SUBSTATIONS > ---------- FAULT POSITIONS	1	6	17	24	29	37	41	55	59	87
6	0.99	0.00	1.00	1.00	0.63	0.98	0.99	0.98	0.88	0.97
17	1.00	1.00	0.00	1.00	1.00	0.99	0.83	0.99	1.00	0.99
24	1.00	1.00	1.00	0.00	1.00	1.00	1.00	1.00	1.00	1.00
29	0.99	0.61	1.00	1.00	0.00	0.99	0.99	0.99	0.94	0.99
37	0.79	0.99	1.00	1.00	0.99	0.00	0.98	0.14	0.99	0.61
41	0.98	0.98	0.82	1.00	0.99	0.95	0.00	0.95	0.99	0.95
55	0.92	0.99	1.00	1.00	1.00	0.63	0.99	0.00	1.00	0.84
59	0.99	0.87	1.00	1.00	0.93	0.99	0.99	0.99	0.00	0.98
87	0.63	0.97	0.99	1.00	0.98	0.30	0.95	0.35	0.98	0.00
50% Line 27_87	0.95	0.99	1.00	1.00	0.99	0.90	0.98	0.91	0.99	0.87
50% Line 57_87	0.74	0.99	0.99	1.00	0.99	0.48	0.97	0.53	0.99	0.50
50% Line 39_41	0.98	0.98	0.83	1.00	0.99	0.96	0.10	0.96	0.99	0.95
50% Line 37_57	0.77	0.99	1.00	1.00	0.99	0.28	0.98	0.37	0.99	0.65
50% Line 37_55	0.88	0.99	1.00	1.00	1.00	0.46	0.99	0.08	1.00	0.78
50% Line 24_86	1.00	1.00	1.00	0.35	1.00	1.00	1.00	1.00	1.00	1.00

- *Exposed areas*

  The exposed area for substation 28 is shown in Figure 29. It should be noted that part of the transmission lines connecting buses inside the exposed area might be actually outside the area. In Figure 29 the 95% exposed area encloses all the buses and line segments where the occurrence of faults cause retained voltage lower than 95% in the load point 28.

- *Cumulative dip frequencies*

  The remaining voltage is used to classify the total number of dips experienced by a given load. In order to distinguish between severe dips and shallow ones a classification of these in terms of magnitude is useful. A suitable way to present this information is the cumulative histogram of voltage dips.

  The frequency of occurrence of a particular voltage dip at a given location depends on several factors, the number of faults occurring in the "electrical neighbourhood" being the most important one. This "electrical neighbourhood" has been already identified as the exposed area. Other factors, which do affect the magnitude of the dips and their distribution, can be identified as system configuration, generation scheduling, number of lines connecting the load bus, etc.

  How often one of those dips occurs at a given bus k depends on the reliability of the bus f, namely on the fault rate of the fault position f. If the fault rate of the fault position f is λ_f the particular dip caused by this fault will be seen λ_f times per year. The exposed area shows that bus k will see dips caused by faults inside this area. The expected number of faults inside the exposed area is given by the sum of the fault rates of the fault positions contained in the exposed area. Frequency of dips can be calculated from the dip matrix and the fault rate corresponding to the fault positions.

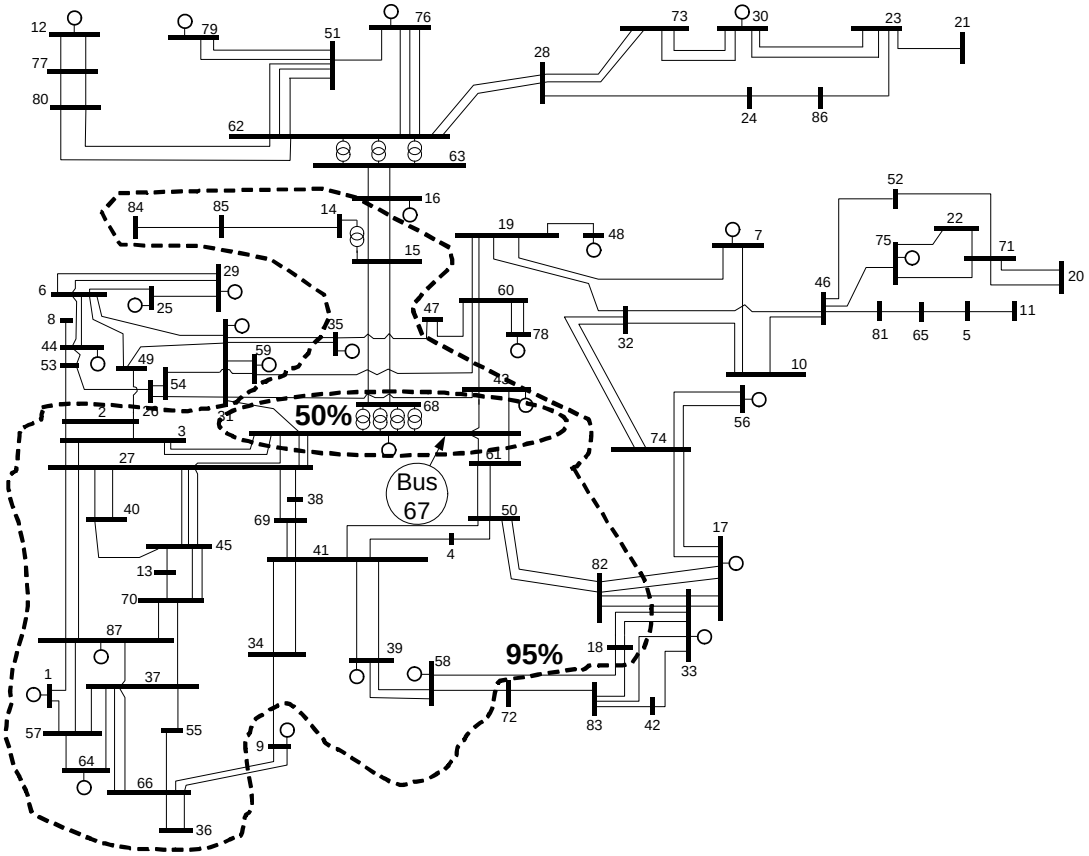

Figure 28. Affected area due to a three-phase fault at bus 67 [77].

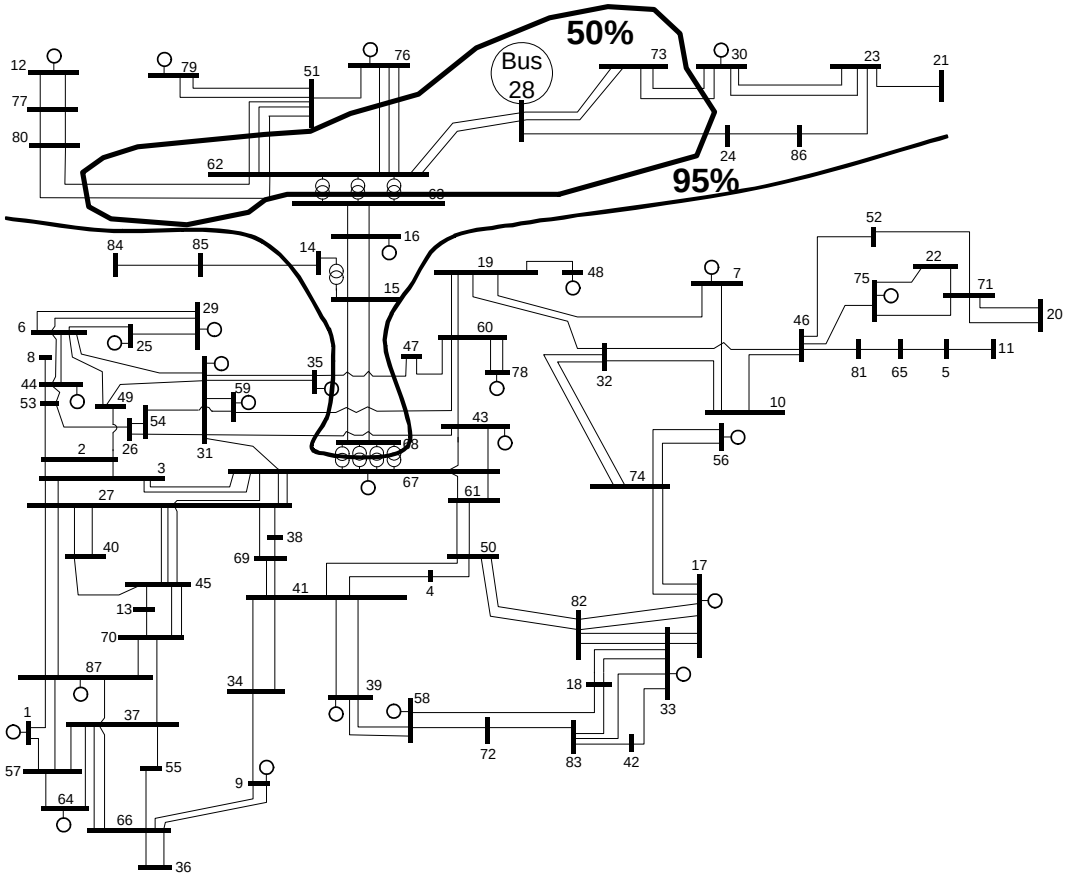

Figure 29. Exposed area (50% and 95%) for bus 28 [77].

The dip-matrices contain more buses than the physical buses because they include several fault positions on lines. Buses corresponding to physical buses of the system have a fault rate given by the actual fault rate of the bus. Fault positions on lines have a fault rate that is a fraction of the actual line fault rate. If more than one fault position is considered on the line the actual fault rate need to be divided by the number of fault positions in order to calculate the frequency of the resulting dips. If only one fault position is considered on a given line, then the actual fault rate is taken.

Once the fault rate for all fault positions is determined, the expected number of dips and their characteristics can be determined by combining the dip-matrices and the fault rates. Let $\boldsymbol{\lambda}$ be the vector containing the corresponding fault rate of each F_p fault position.

$$\boldsymbol{\lambda} = \left(\lambda_1 .... \quad \lambda_k \quad ... \quad \lambda_N .... \quad \lambda_f \quad .. \quad \lambda_{Fp}\right) \tag{23}$$

Each fault will cause a drop in voltage for all buses. However only part of these fault-caused events will be counted as dips at load buses ($v_{kf} < 0.9$ pu). A large part of these events will result in retained voltages above 0.9 pu. The number of total fault-caused events is the same for all buses, however the resulting during-fault voltages are different which result in different cumulative histograms. Hence, vector λ contains the yearly event rate (voltage drops) caused by faults.

For the system under study, the expected number of dips can be estimated by combining the information contained in Table VIII and the fault rate for each fault position. This analysis was performed for all cases. It is worth recalling that the base case only considers fault-positions on buses, Case 1 considers 251 fault positions, 87 faults at buses and 164 faults in the middle of each line, while Case 2 considers 781 fault positions, 87 faults at buses and 694 faults at lines.

Cumulative dip frequencies for substations 11 and 67 are presented in Figure 30 and 31, respectively. It can be seen that the result depends on the number of fault positions. As more fault positions are considered, the estimation of the expected number of dips becomes more accurate; in the limit an infinite number of fault positions would be necessary to get the probability density function for dips at each bus. The rough estimation obtained from the base case shows the same shape as the more elaborated cases 1 and 2. This confirms that the base case is a good starting point. However the base case cannot be seen as an overestimation or an underestimation of the real expected number of dips. Another conclusion is that the expected number of dips and their shape notably differs between buses with different short-circuit levels: while the weak bus 11 shows almost 20 dips, the strong bus 67 shows 8 dips per year deeper than 85%.

- *System statistics*

  To characterize the system as a whole, dip indices are needed. One approach is to characterize the system by using the average number of cumulative dip frequencies for a given magnitude. This average number takes into account the spatial variation around the network. It is the average of the cumulative expected number of dips -in a given bin- of the all network buses. It could be interpreted as the expected performance of the average bus. Another approach is to describe the system performance by means of the 95th percentile. Again the spatial variation of the performance is taken into account. In this case the index can be interpreted as the expected cumulative number of dips that is not exceeded by 95% of the system buses. Table IX shows system statistics for the four simulated cases. From

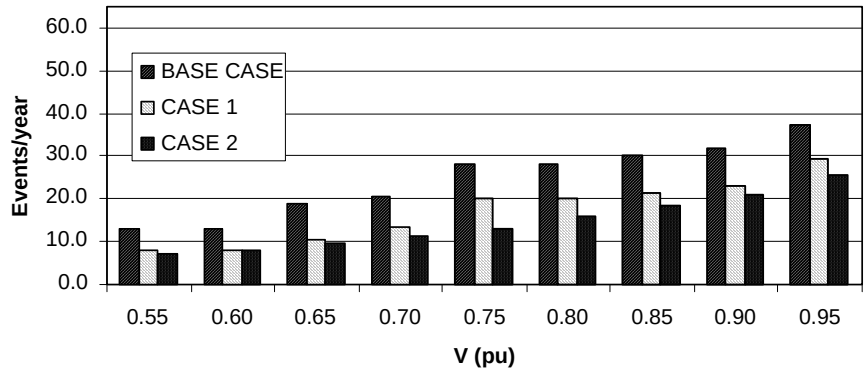

Figure 30. Cumulative dip frequency at bus 11 with maximum generation [77].

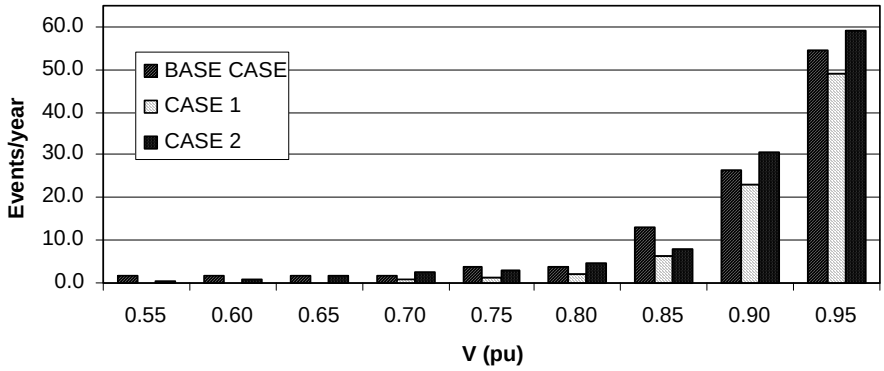

Figure 31. Cumulative dip frequency at bus 67 with maximum generation [77].

Table IX-A it can be seen that for dips more severe than 90%, the worse site is located in the area of bus 27. In Table IX-B there is no clarity about the worse site for dips deeper than 70%, however we should expect the worse site near bus 14, because Case 2 is the most elaborated simulation. This lack of clarity could be explained by the need of a non-homogeneous split of lines for fault position purpose. For some lines a 15 km long segmentation of the line implies a similar short-circuit level along the line, for others this same 15 km implies an important variation in short-circuit level. Hence some dips are over or under-classified in terms of severity.

Table IX – System statistics based on balanced dips [77].

A.- Number of dips more severe than 0.9 pu						
Case Base	#Fault positions	# Events	Worst site		95^{th} %	Average
	87	2068	46.86	Bus 69	41.24	23.77
1	251	1787	40.87	Bus 27	38.10	20.53
2	781	1556	44.65	Bus 40	40.55	17.88
B.- Number of dips more severe than 0.7 pu						
Case base	#Fault positions	# Events	Worst site		95^{th} %	Average
	87	913	20.62	Bus 5	20.06	10.49
1	251	623	15.87	Bus 28	13.21	7.16
2	781	540	18.86	Bus 14	15.70	6.21

C. Unbalanced dips

The system was modelled by means of the positive and zero sequence impedance matrices. Negative sequence impedance matrix was taken equal to the positive one. Lines were modelled as medium-length lines perfectly transposed and their shunt parameters were considered. Independence of sequence components is assumed, meaning that the different sequences do not react upon each other. Transformers were modelled as delta-wye solidly grounded. The simulations are based on Case 2. They consider 781 fault positions with 87 faults at buses and 694 faults at lines. In order to count the number of dips occurring at the load positions, the following criterion was adopted: each fault-originated event, balanced or unbalanced, was counted as one single dip. The minimum phase-to-neutral voltage was used to characterize the resulting dip. During fault voltages were registered for all buses and for each simulated fault.

Three simulation cases were developed as explained below.

i. Case A. This simulation only considers three phase faults. The fault rate for lines is 0.0134 faults per year-km and is the same for the 164 lines. The fault rate for buses is 0.08 faults per bus-year and is the same for the 87 buses.

ii. Case B. Only single phase to ground faults were simulated. Fault rates as in case A.

iii. Case C. Four types of faults were simulated: single-phase to ground, phase to phase, two phases to ground and three-phase fault. The probabilities of these faults were assumed to be 80% single phase, 5% two phases, 10% two phases ground and 5% three phases. Fault rates were as in Case A.

- *Exposed areas*

  Figure 32 presents the 85% exposed areas for buses 5, 15 and 87 deduced from simulations corresponding to cases A and B. The lowest phase to ground voltage is used to characterize the magnitude of the event. Faults on buses or lines inside the areas would cause a remaining voltage in the worst phase lower than 85% at the indicated buses. The single-phase fault exposed areas for buses 5 and 87 are almost coincident with the three-phase fault exposed area, however a bit smaller. The three-phase fault exposed area is bigger than the single-phase fault exposed area but they do not differ too much when there is no power transformer inside the area. When the exposed area contains power transformers its shape changes drastically. This can be explained by the blocking of the zero-sequence component and the changing in the dip type due to the transformer winding connections. For an impedance-grounded system the single-phase fault exposed area would be significantly smaller than for three-phase faults.

  The exposed areas have been drawn as closed sets to simplify the drawing, however they might be isolated sets enclosing the part of the system in which a fault would cause a dip more severe than a given value. To illustrate this, consider the lines connecting bus 87 and 27. Figure 33 shows the during fault voltage at bus 87 when a moving fault is applied on the line connecting these buses. Single-phase fault and three-phase faults are shown. It can be seen that, for both fault types, part of the line does not pertain to the 85% exposed area of bus 87. The term critical distance is used to describe the length of the line exposed to faults that might lead to critical dips. Hence, for this line and three-phase faults, the critical 85%-distance would be approximately the first 40% of line plus the last 10% of it. Figure 33 corresponds to a line connecting the load bus. The data contained in the voltage-dip matrix also allows the description of the during fault voltage due to faults on lines not connecting the load bus. Consider now the line connecting buses 62 and 76.

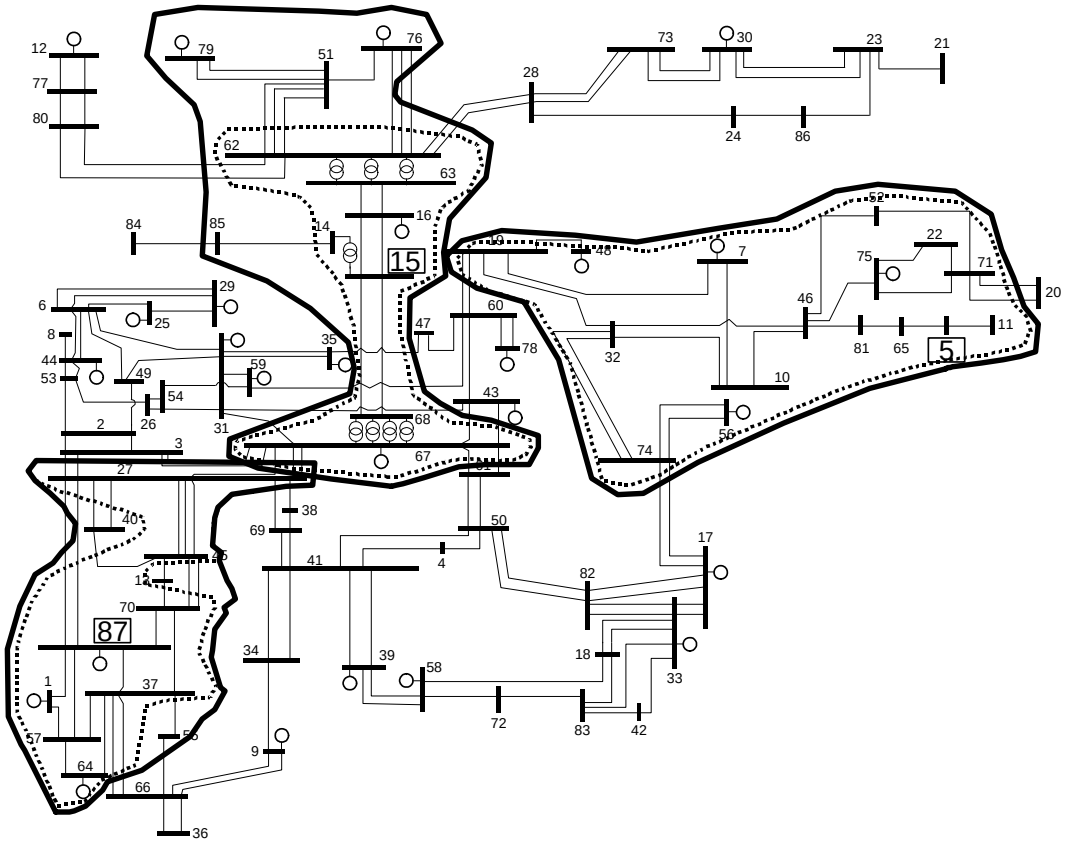

Figure 32. 85% exposed areas for buses 5, 15 and 87.
Dashed line for single-phase fault caused dips; solid line for balanced dips [77].

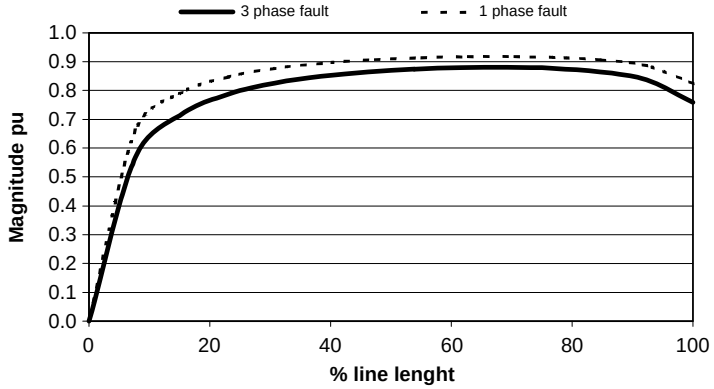

Figure 33. During-fault voltage at bus 87 due to faults on line 87-27 [77].

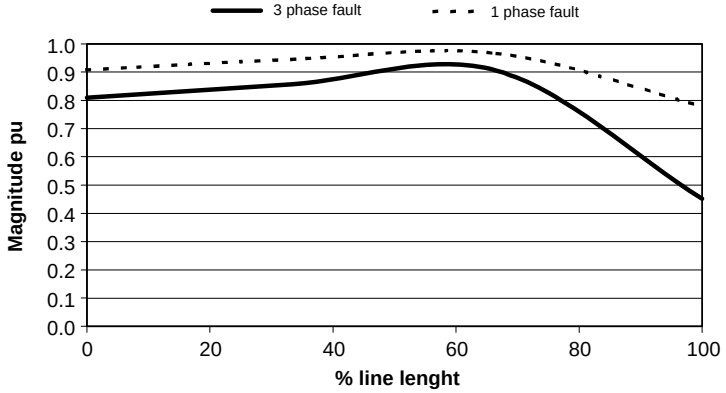

Figure 34. During-fault voltage at bus15 due to faults on line 76-62 [77].

According to the exposed areas shown in Figure 32, only part of this line is inside the 85% exposed area of bus 15 for single-phase fault. This is confirmed by Figure 34, which shows the resulting remaining voltage caused by faults along line 76-62. The figure also shows the effect of the zero-sequence blocking by the transformers; the voltage drop due to single-phase faults are only about half of the drops due to three-phase faults. These results confirm that single-phase faults are less severe than three-phases faults, in the sense that the worst phase shows a higher remaining voltage than the dip due to a three-phase fault at the same position.

- *Dip frequencies*

  Figure 35 shows the cumulative number of dips at bus 87 due to balanced and unbalanced faults. As it would be expected the contribution of single-phase faults is dominant. However the contribution of the different type of faults does not exactly follow the distribution probability of faults. The exposed area can explain this. As the exposed area for three phase faults is larger than for any other fault the resulting contribution of this faults to the total frequency is more than the 5% that could be expected.

  Table X shows that the three-phase faults contribute with more than 29% of the total dips more severe than 0.6 pu at bus 87. It should be noted that this bus has several lines converging to that bus. For buses at the end of a line (radial source) the distribution probability of the faults is a reasonable indicator of the contribution of unbalanced dips to the total number of dips.

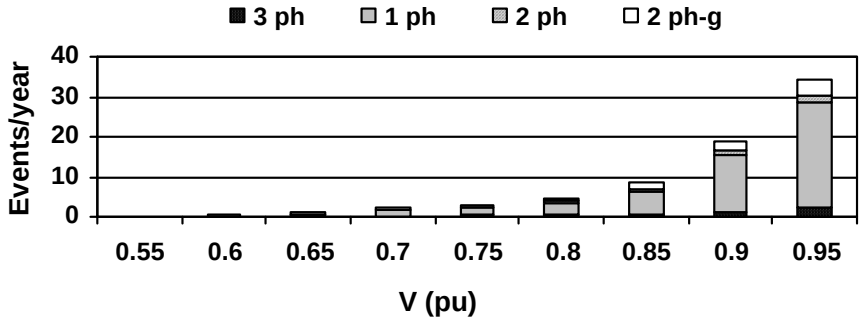

Figure 35. Cumulative balanced and unbalanced dip frequency at bus 87 [77].

Table X – Cumulative dip frequency at Bus 87 [77].

Remaining voltage v_{kf} pu	Cumulative dip frequency at Bus 87				
	3 ph	1 ph	2 ph	2 ph-g	Total
0.55	0.04	0.13	0.00	0.04	0.21
0.60	0.10	0.13	0.01	0.11	0.34
0.65	0.12	0.67	0.02	0.21	1.02
0.70	0.16	1.70	0.10	0.26	2.22
0.75	0.28	2.06	0.12	0.39	2.85
0.80	0.45	3.20	0.23	0.62	4.50
0.85	0.82	5.55	0.46	1.44	8.26
0.90	1.28	14.02	0.99	2.33	18.62

- *System statistics*

  System statistics have been also calculated using asymmetrical faults and different number of faults positions. Table XI presents some results. An interesting conclusion can be derived from this table: when only symmetrical faults are considered; the stochastic assessment of dips overestimates event frequencies. The error is more important for severe dips. An explanation for this overestimation is, again, the fact that three-phase fault are more severe, which causes bigger exposed areas.

Table XI – System statistics based on balanced and unbalanced dips [77].

A.- Number of dips more severe than 0.9 pu						
Case	#Fault positions	# Events	Worst site		95^{th} %	Average
C	781	1333	43.30	Bus 27	37.50	15.33
2	781	1556	44.65	Bus 40	40.55	17.88
B.- Number of dips more severe than 0.7 pu						
Case	#Fault positions	# Events	Worst site		95^{th} %	Average
C	781	415	14.11	Bus 36	11.94	4.83
2	781	540	18.86	Bus 14	15.70	6.21

7.3.2 Example 2

A. Test system

The studies were carried out using the power system shown in Figure 36 [80]. The network consists of four 230-kV transmission system infeeds, a 33-kV (predominantly meshed) sub-transmission network, and an 11-kV radial distribution network. The network comprised 295 buses and 296 overhead lines and underground cables. It is fed from four substations: two 400/132 kV and two 275/132 kV.

B. The area of vulnerability and associated boundary crossing lines

i. Introduction

Faults in a power system have a random nature and they can occur at any location in the system. The fault distribution might be uniform, normal, exponential or a combination of those. By changing distribution parameters, virtually any fault distribution pattern can be modelled. Different fault distribution patterns will yield different dip prediction results. Once the area of vulnerability is identified for a particular plant, its boundary may cross some lines. This results in only a part of such line being inside the area while the other lines in the system may be completely inside or outside the area, as shown in Figure 37. The lines that are only partially inside the area of vulnerability are called the boundary crossing lines. The fault distribution pattern along these lines will cause changes in the expected number of dips at a bus of interest. The fault distribution along the lines that are completely inside the area of vulnerability will not alter the predicted results because the whole length of those lines is considered as a single fault position.

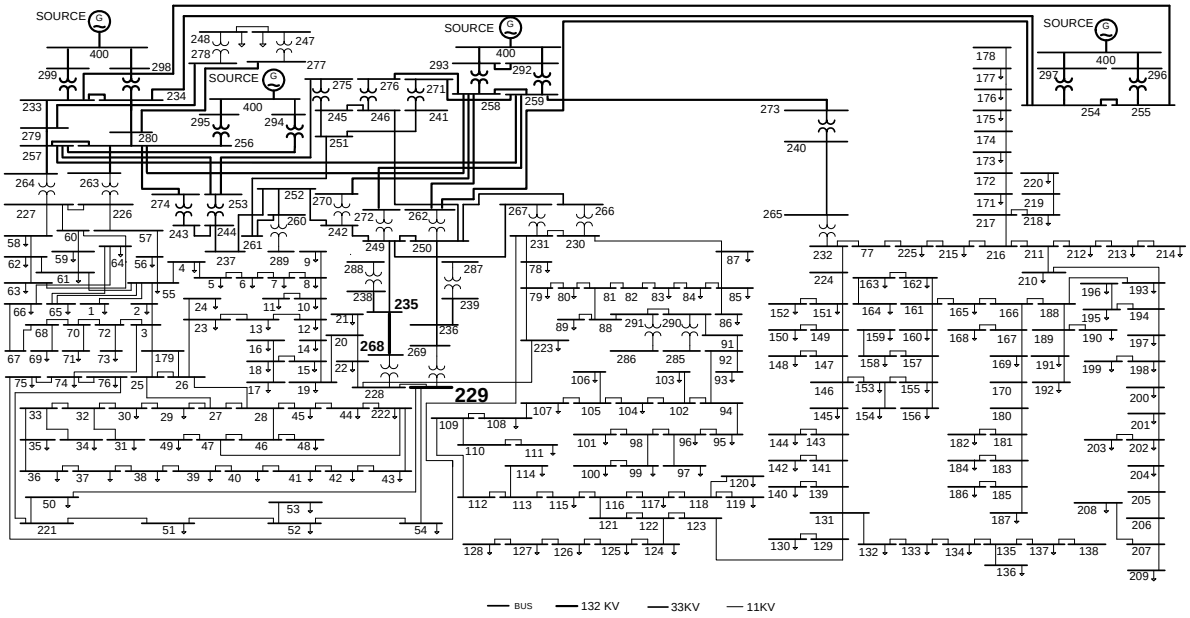

Figure 36. Single line diagram of the test system with marked bus 229 and line 235-268 [82].

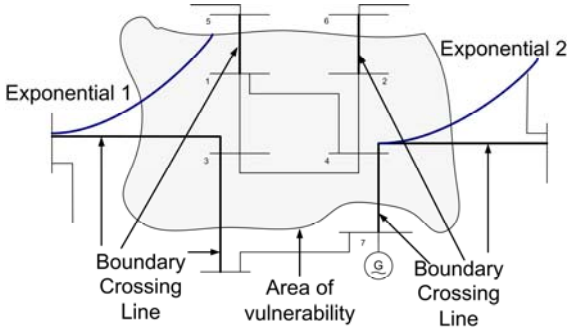

Figure 37. Example of the area of vulnerability and the associated boundary crossing lines [80].

ii. Methodology

The methodology applied in this study is based on the guidelines recommended by the IEEE Std 493-1997 (Gold Book) [81]. Two different approaches are used to calculate the total expected number of dips due to the faults inside the area of vulnerability and due to the faults along the boundary crossing lines. Dip performance within the area is assessed by using equations (26) to (28). A combination of the method of fault positions and exponential fault distribution pattern along the boundary crossing lines is used in determining the number of voltage dips. The fault rates at each location along the boundary crossing lines are calculated using the exponential distribution pattern and then applied to the corresponding fault positions. After taking into account calculated fault rates, the expected number of dips due to the faults along the boundary crossing lines is calculated.

$$NSBF = \sum_{i=1}^{4} \sum_{j=1}^{n} B \times BFR \tag{24}$$

$$NSLF = \sum_{i=1}^{4} \sum_{j=1}^{n} L \times LL \times LFR \tag{25}$$

After including fault occurrence probability, equations (24) and (25) become:

$$NSBF = \sum_{i=1}^{4} \sum_{j=1}^{n} \sum_{k=1}^{3} B \times PO \times BFR \tag{26}$$

$$NSLF = \sum_{i=1}^{4} \sum_{j=1}^{n} \sum_{k=1}^{3} L \times LL \times PO \times LFR \quad (27)$$

$$CNS = NSBF + NSLF \quad (28)$$

where B = Bus inside the area of vulnerability
L = Line inside the area of vulnerability
LL = Length of the line inside the area of vulnerability
PO = Fault occurrence probability (1 for symmetrical fault; 1/3 for asymmetrical faults)
BFR = Bus fault rate
LFR = Line fault rate
CNS = Cumulative number of dips
NSBF = Number of dips due to the bus faults
NSLF = Number of dips due to the line faults
i = Type of fault
n = Total number of buses or lines inside the area of vulnerability
j = Bus or line inside the area of vulnerability
k = Number of phases.

iii. System modelling and stochastic analysis

The fault clearing times used in the study are listed in Table XII. Each fault position represents a single fault at the system bus or at the particular fault location along each line. Each line is divided into five equal sections as illustrated in Figure 38. The fault rates of 0.08 events per bus per year and 2.98 events per kilometre of the line per year are applied to buses and lines respectively. Detailed system fault statistics are given in Table XIII and Table XIV. The realistic pre-fault voltages and phase angles obtained from the load flow study are used in all calculations. System fault analysis is performed using SIMPOW software. A dedicated voltage-dip database is created in Microsoft Access 2000. All statistical calculations are performed in the Visual Basic environment using specially developed software.

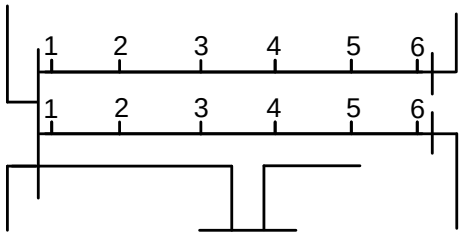

Figure 38. Fault positions along the lines.

Table XII – Typical fault clearing time.

Voltage level (kV)	Typical fault clearing time (ms)
132	80
33	150
11	300

Table XIII – System fault statistics for buses.

Type of fault	Bus fault rate (Event per year)	Distribution of type of fault	Fault rate per bus
Single line to ground fault	0.08	0.73	0.0584
Double line to ground fault	0.08	0.17	0.0136
Line to line fault	0.08	0.06	0.0048
Three phase fault	0.08	0.04	0.0032

Table XIV – System fault statistics for lines.

Type of fault	Line fault rate (Event/100 km/year)	Distribution of type of fault	Fault rate per line	Fault rate per line-fault position
Single line to ground fault	2.98	0.73	2.175	0.3626
Double line to ground fault	2.98	0.17	0.507	0.0844
Line to line fault	2.98	0.06	0.179	0.0298
Three phase fault	2.98	0.04	0.119	0.0199

iv. Study procedure

In order to investigate the influence of different fault distribution patterns along the boundary crossing lines on prediction of number of dips, the following procedure was used:

1. Symmetrical and asymmetrical faults were simulated in each phase separately for every fault position throughout the system.
2. Voltage dip magnitudes at each system bus and corresponding fault locations were recorded.
3. A voltage dip database containing system fault analysis data, the associated fault locations and typical fault clearing times was created.
4. Two customer sites, bus 229 and bus 100, from the 11-kV network were arbitrarily selected as buses of interest.
5. Area of vulnerability and the associated boundary crossing lines for each type of fault were determined using the equipment sensitivity level (voltage threshold) as a filtering criterion in database. Voltage magnitude thresholds of 0.7 p.u., 0.5 p.u. and 0.3 p.u. were applied to each phase of the bus of interest.
6. Number of dips at buses 229 and 100 due to the faults inside the area of vulnerability was calculated using equations (26) to (28).
7. Fault rates for each fault position along the boundary crossing lines were determined using exponential distribution and the number of dips due to these faults was calculated again.
8. Finally, the influence of modelling of different fault distribution patterns along the boundary crossing lines was investigated.

v. Case studies

Four different case studies were considered:

a) Minimum case: All faults along the boundary crossing lines occurred outside the area of vulnerability, resulting in minimum expected number of dips at buses 229 and 100.

b) Maximum case: All faults along the boundary crossing lines occurred inside the area of vulnerability, resulting in maximum expected number of dips at buses 229 and 100.

c) Exponential 1: The exponential fault distribution was used ($f(x) = \lambda e^{-\lambda x}$, λ=2) along the length of the boundary crossing lines. (exponential increase from the outside of the vulnerability area, as shown in Figure 39).

d) Exponential 2: The exponential fault distribution was used ($f(x) = \lambda e^{-\lambda x}$, λ=2) along the length of the boundary crossing lines. (exponential increase from the inside of the vulnerability area, as shown in Figure 39).

vi. Results

a) Area of vulnerability due to three-phase faults

Typically, symmetrical fault results in the same degree of severity of voltage dips in each phase of a three-phase system. Hence, identifying the area of vulnerability for each phase can be done easily, and each of them will be identical. Area of vulnerability determined using voltage threshold of 0.7 p.u. for bus 100 is illustrated in Figure 39.

b) Area of vulnerability due to single line-to-ground faults

The area for bus 229 is illustrated in Figure 40. Since the SLGFs are applied to each phase of a three-phase system, the dip magnitude in each phase will be different from the dip magnitudes in the other phases depending on the phase at which the fault occurs and the transformer winding connections. Therefore, the identified areas of vulnerability by taking into account effect of faults on each phase separately are likely to be different. Table XV, however, shows that only faults on two phases affect the number of voltage dips on the study phase. This means that only two different areas for the sensitive load at the study phase exist. In some cases only one area of vulnerability exists for a single-phase connected load. This case, however, is rare.

Table XV shows that higher number of buses and lines fall into the area of vulnerability when the faulted phase and the study phase coincide. Otherwise, the area due to the faults on other phases is relatively small. 47 buses and 255 line-fault positions are inside the area when the study phase coincides with the faulted phase. 255 line-fault positions correspond to 40 lines being completely within the area of vulnerability and 9 boundary-crossing lines. The other area of vulnerability due to the faults on other phases includes 2 buses and 17 line-fault positions corresponding to 1 line completely inside the area of vulnerability and 6 boundary-crossing lines. The resulting area of vulnerability for the sensitive load on the study phase is obtained by merging the corresponding areas. For example, the area of vulnerability for the sensitive load with 0.7 p.u. voltage threshold connected to phase A of Bus 229, as shown in Figure 40, is the result of combination of the area of vulnerability due to the faults on the study phase (grey shaded area in Figure 40) and due to the faults on non-study phases (dark grey shaded area in Figure 40). There are 15 boundary- crossing lines in total associated with that area. Since the power system is balanced, identified area of vulnerability and associated boundary crossing lines for phase A are the same for phases B and C.

Table XV – Single line-to-ground faults - Area determined by 0.7 p.u. voltage threshold [80].

Study phase of Bus 229	Number of buses inside the area			Total number of line-fault positions inside the area		
	Faulted phase			Faulted phase		
	A	B	C	A	B	C
A	47	2	0	255	17	0
B	0	47	2	0	255	17
C	2	0	47	17	0	155

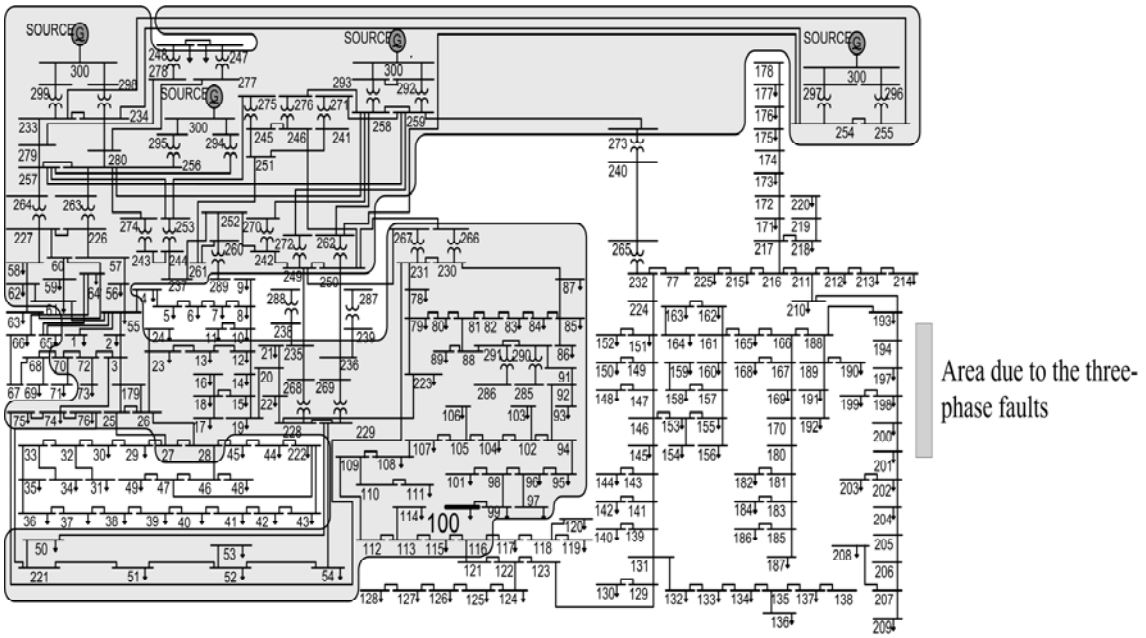

Figure 39. Area of vulnerability due to three-phase faults for bus 100 [80].

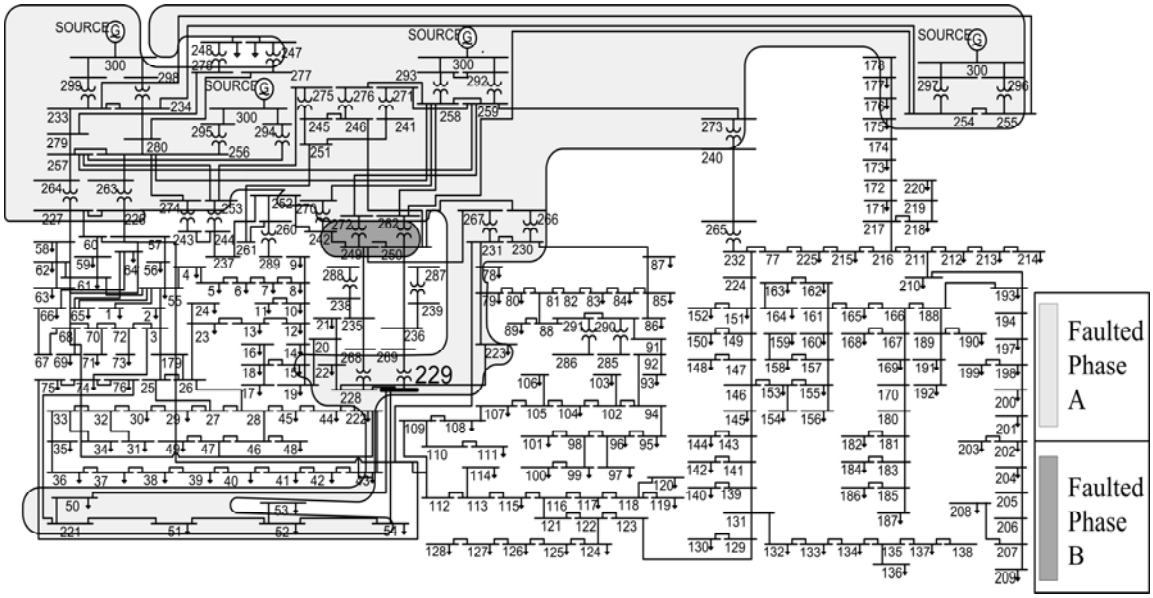

Figure 40. Area of vulnerability due to single line-to-ground faults for bus 229 [80].

c) Area of vulnerability due to double line-to-ground faults

The same as before, sensitive equipment is connected to phase A of bus 229. Consider the area of vulnerability due to the faults on any two phases of a three-phase system. As shown in Table XVI, all the 20 buses are within the area if the fault happens on phases B and C. The number of buses inside the area increases to 112 when the faults occur on phases A and C. Similarly, 95 and 740 fault positions along the lines fall into the area when the faults occur on phases B and C and phases A and C, respectively. This means that the number of voltage dips experienced by a single phase connected load at the bus of interest highly depends on faulted phases even when the faults occur at the same fault positions. Unlike the area of vulnerability due to a SLGF, three different areas are identified depending on the faulted phases. Resultant boundary crossing lines are the result of summation of crossing lines from these areas.

Table XVI – Double line-to-ground faults - Area determined by 0.7 p.u. voltage threshold [80].

Study phase of Bus 229	Number of buses inside the area			Total number of line-fault positions inside the area		
	Faulted phases			Faulted phases		
	AB	BC	CA	AB	BC	CA
A	51	20	12	290	95	740
B	112	51	20	740	290	95
C	20	112	51	95	740	290

d) Area of vulnerability due to line-to-line faults

The area of vulnerability caused by the line-to-line faults can be identified using the same approach. Two different areas appear in this case, as shown in Table XVII.

Table XVII – Line-to-line faults - Area determined by 0.7 p.u. voltage threshold [80].

Study phase of Bus 229	Number of buses inside the area			Total number of line-fault positions inside the area		
	Faulted phases			Faulted phases		
	AB	BC	CA	AB	BC	CA
A	37	0	117	201	0	774
B	117	37	0	774	201	0
C	0	117	37	0	774	201

e) The influence of fault distribution along the boundary crossing lines

The influence of different fault distributions along the boundary crossing lines is illustrated in Figure 41. The figure clearly shows that the number of voltage dips in each range (selected for the illustration of the effect) is affected by the fault distributions along the boundary crossing lines. The number of voltage dips with magnitude lower than 0.7 p.u., for example, can vary between 82.69 and 101.49 (i.e., approx. 23%), and between 112.81 and 129.77 (i.e., approx. 15%), at bus 229 and bus 100 respectively. The major difference in cumulative dip frequency appears in the case of voltage dips with lower magnitudes. At bus 229, the difference between the maximum and minimum number of voltage dips with magnitudes lower than 0.7 p.u is 18.8 dips. The difference however, increases to 22.47 dips in the case of voltage dips with magnitudes lower than 0.3 p.u.

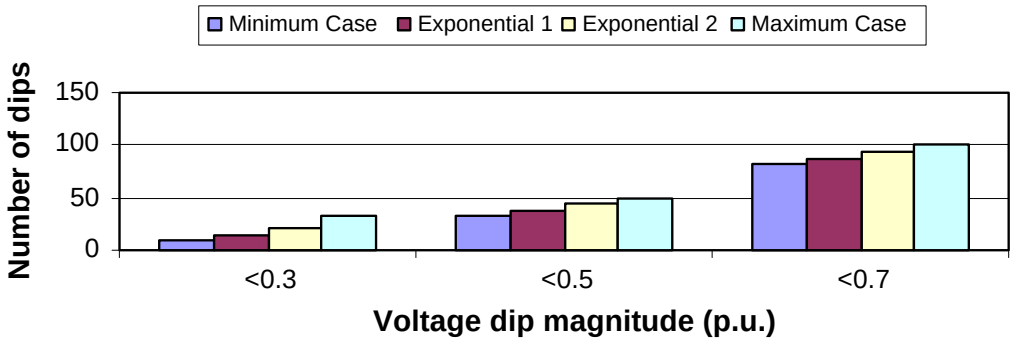

Figure 41. Cumulative voltage dip frequency for bus 229 (Adapted from [80]).

C. The influence of fault distribution on stochastic prediction of voltage dips

i. System modelling

Symmetrical and asymmetrical faults were simulated at various, randomly chosen locations and at different voltage levels [82]. Realistic pre-fault voltages, obtained from the load flow study were used in all calculations. The IPSA software package was used for fault calculations and MATLAB for calculating different fault distribution rates and the expected number of voltage dips.

ii. Study procedure

In order to assess the influence of different fault distributions on voltage dips the following procedure was used:

1. Firstly, all types of faults at all buses in the test network were simulated and the area of vulnerability (voltage drop below 95%) was determined for one particular bus (bus number 229 at 11 kV level). The selected bus and the single line diagram of the test network are presented in Figure 36.
2. Secondly, the line (between sending end bus 235 and receiving end bus 268, at 33 kV voltage level), within the identified area of vulnerability, was selected for the study of the influence of different fault distributions on voltage dips at bus 229.
3. Thirdly, the line was divided into 50 equal sections, and the voltage magnitude and phase shift at bus number 229 following the fault lasting 100ms at each position were calculated for all types of faults (three-phase fault, phase A-to-ground fault, phase A-to-B fault, phase A-to-B-to-ground fault). Fifty fault positions (one per sections) were used for all types of faults except for the three-phase faults. For the three-phase faults only 25 fault positions were used, as the total number of the three-phase faults along the line was only 25 according to the assumption made. The fault rates at each location were calculated using different fault distributions (uniform, normal, exponential) along the line.
4. Finally, after taking into account the fault rates, the expected number of voltage dips (having different characteristics, i.e., magnitude and phase shift) at bus 229 was calculated.

iii. Case studies

It was assumed that the total of 1250 faults occur along the line. The number of different types of faults is given in Table XVIII.

Table XVIII – Number of different faults simulated along the line [82].

Fault type	Percentage of different type of fault (%)	Total number of faults for specific fault type
Three-phase fault	2	25
Single line-to-ground	85	1063
Line-to-line	8	100
Double line-to-ground	5	62

The following case studies were considered:

1. Uniform distribution of faults along the line.
2. Normal distribution of faults with the same mean value and different standard deviations (three sub-cases).
3. Normal distribution of faults with different mean values and the same standard deviation (three sub-cases).
4. Exponential distribution of faults with different mean values - exponential decay from the sending end (bus 235) of the line to the receiving end (bus 268) of the line (three sub-cases).
5. Exponential distribution of faults with different mean values - exponential decay from the receiving end (bus 268) of the line to the sending end (bus 235) of the line (three sub-cases).

The fault distributions used in simulations are illustrated in Figures 42 to 45.

(*Note:* For case 3 when the mean value of normal distribution was varied, the edges of normal distribution curve went out of the line length range causing an error (i.e., the fault rate for each type of fault given by normal distribution was not the same as the total expected number of faults.) Hence, the fault rate was normalised to get the same total expected number of faults. The shape of the distribution curve remained the same but related fault rate at each point became higher.)

iv. Results

a) The influence of different fault distributions

The influence of modelling of different fault distributions along the line on the expected dip frequency at bus 229 is illustrated in Figures 46. It can be seen that the major difference in dip frequency appears in all phases for different fault distributions along the line. The majority of dips will have magnitudes above 0.8 p.u. The number of dips having different magnitudes in different phases is different. The differences in dip frequency in different voltage ranges and different phases obtained as a consequence of modelling different fault distributions along the line varies between a few dips and several hundred dips (e.g. dips in phase B in the range between 0.7 and 0.9 p.u.). Equipment connected to the phase C will experience the largest number of dips with magnitudes lower than 0.5 p.u. From the cumulative frequency plots it has been found that the major difference in cumulative dip frequency appears in phases A and B for the different fault distributions along the line. This is to be expected as these two phases were involved in the majority of the faults simulated. Similar differences in phase angle jumps were observed. The frequency of phase angle jumps in different ranges for the phase A is illustrated in Figure 47. It can be seen from this figure that the phase angle jump for the majority of dips is positive, i.e., the voltage during the fault lags the voltage before the fault.

b) The influence of different distribution parameters

The influence of the fault distribution parameters on dip prediction is illustrated in Figures 48 and 49. Figure 48 shows the frequency of voltage dips with different magnitudes obtained using normal distribution with different parameters. It has been found that the variation in distribution mean has bigger effect on dip frequency in different voltage ranges than the variation in standard deviation.

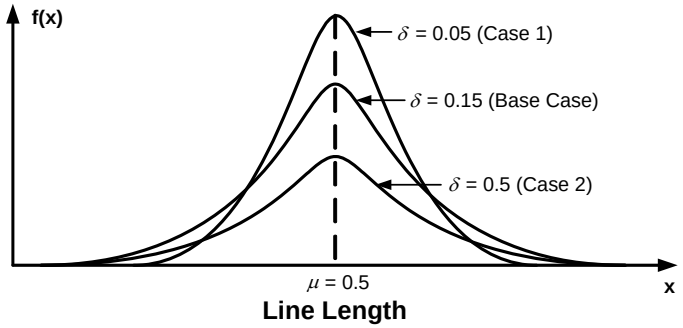

Figure 42. Normal distribution with the same mean value and different standard deviation [82].

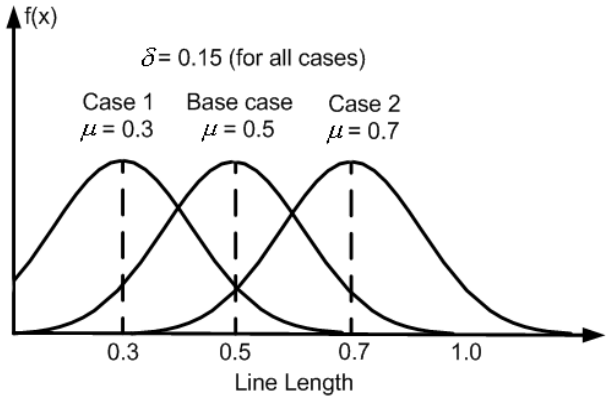

Figure 43. Normal distribution with different mean value and the same standard deviation [82].

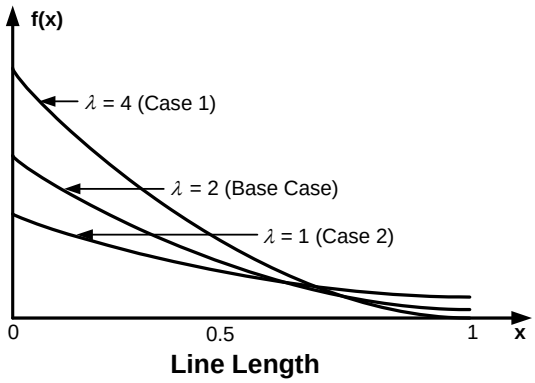

Figure 44. Exponential distribution with different mean value (exponential decay from sending end to receiving end) [82].

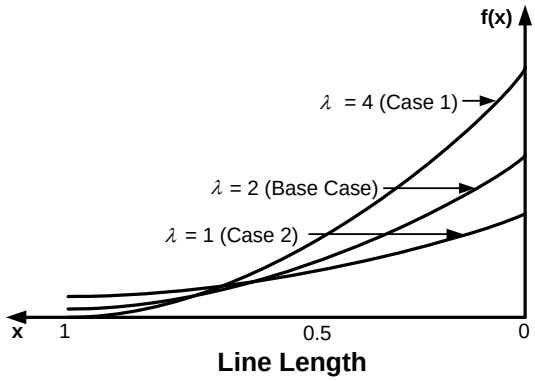

Figure 45. Exponential distribution with different mean value (exponential decay from receiving end to sending end) [82].

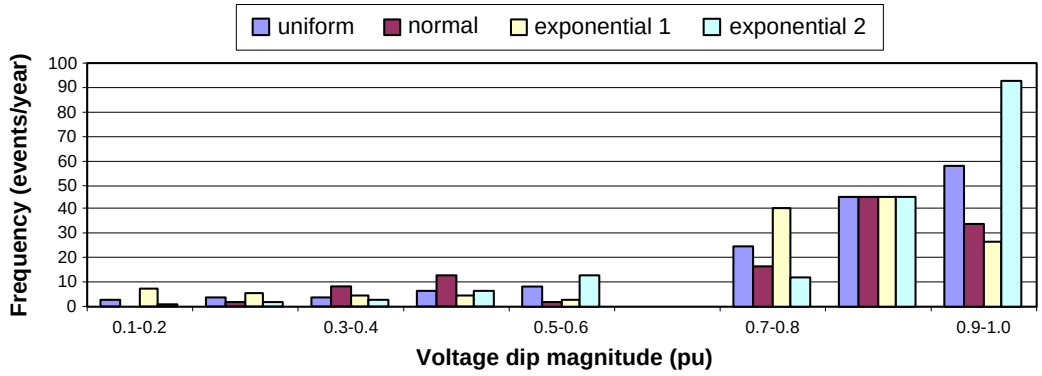

a) Phase A

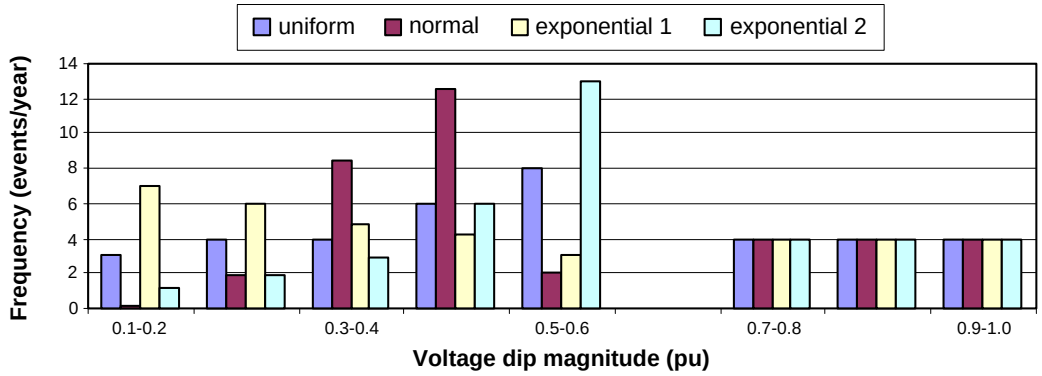

b) Phase B

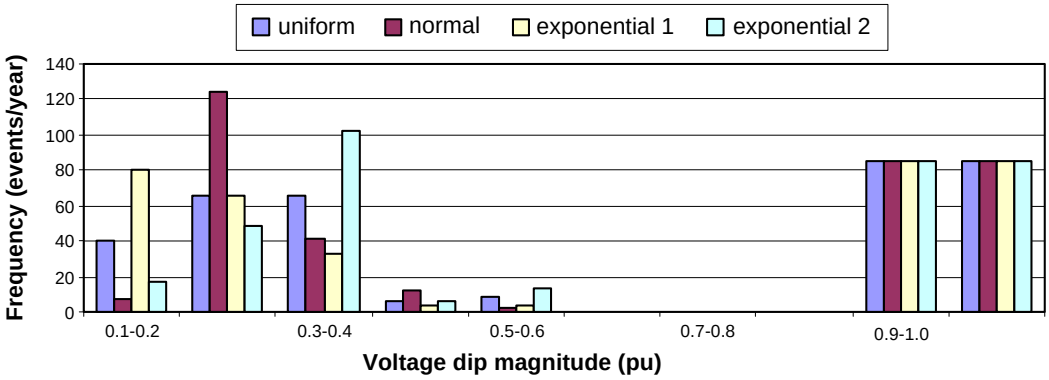

c) Phase C

Figure 46. Voltage dip frequency at bus 229 for different fault distributions along the line 235-268 (Adapted from [82]).

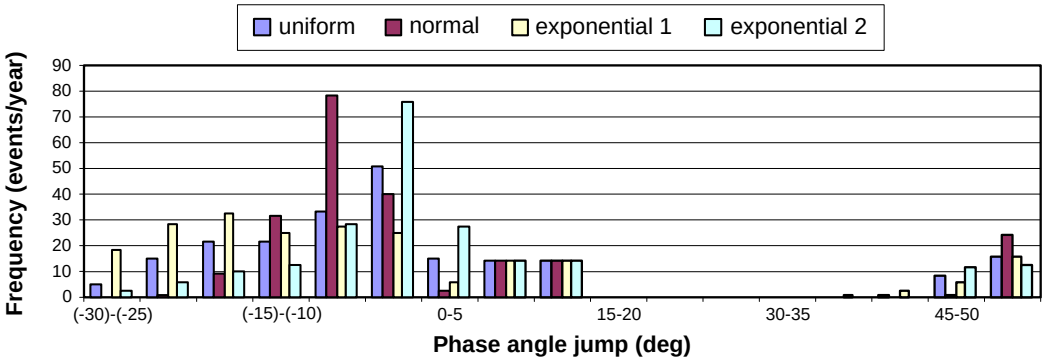

Figure 47. Phase angle jump frequency in phase A at bus 229 for different fault distributions along the line 235-268 (Adapted from [82]).

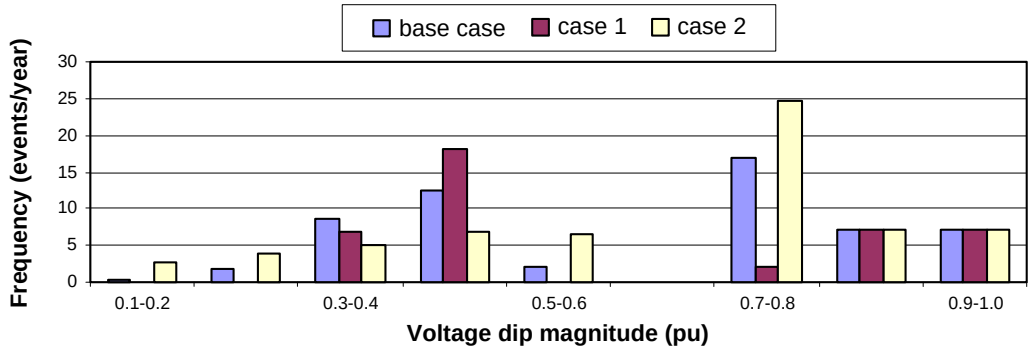

a) Different standard deviations

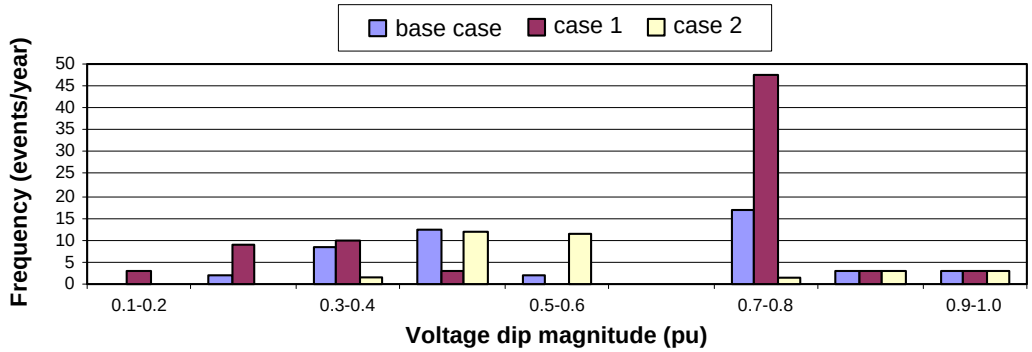

b) Different distribution means

Figure 48. Voltage dip frequency in phase A at bus 229 for normal distribution of faults along the line 235-268 (Adapted from [82]).

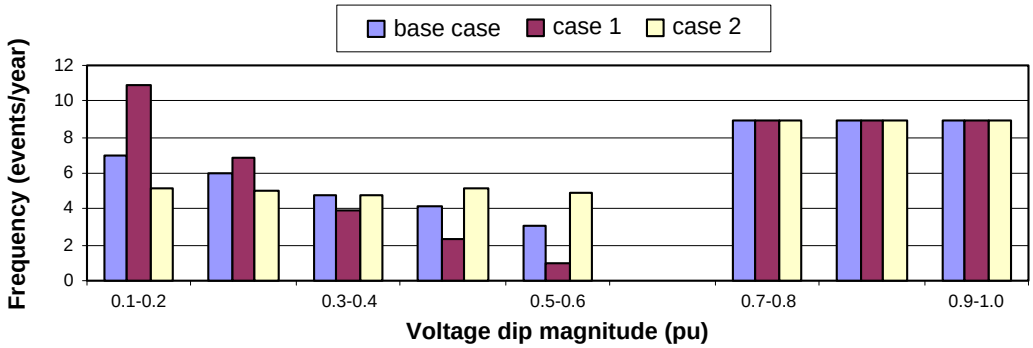

a) Decay from sending end to receiving end of the line

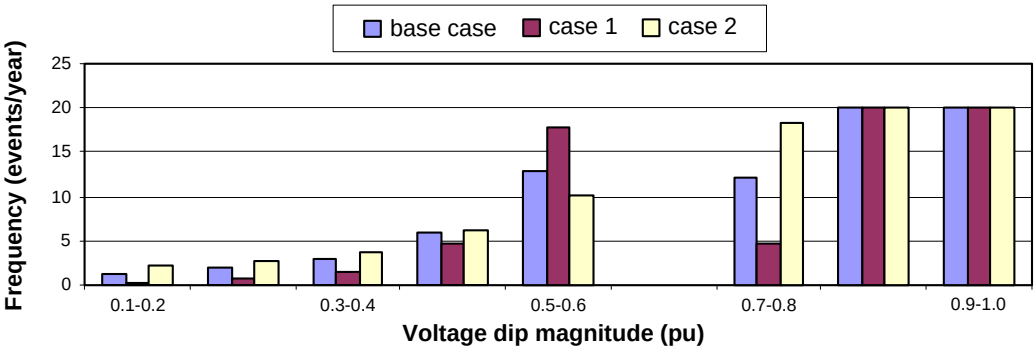

b) Decay from receiving end to sending end of the line

Figure 49. Voltage dip frequency in phase A at bus 229 for exponential distribution of faults along the line 235-268 – different distribution means (Adapted from [82]).

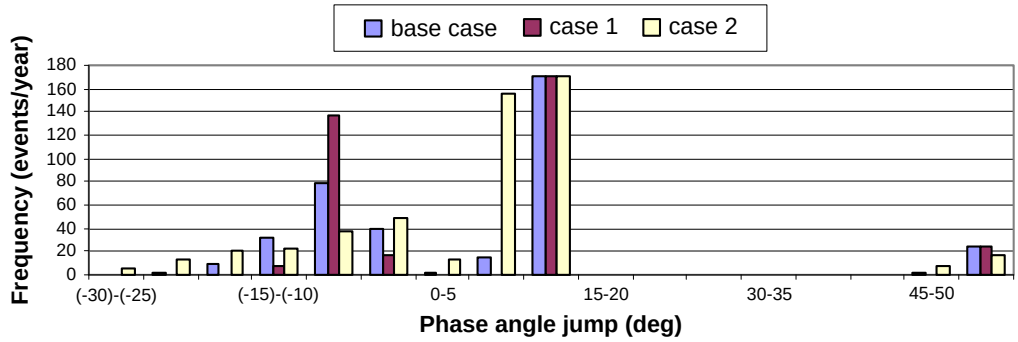

a) Different standard deviations

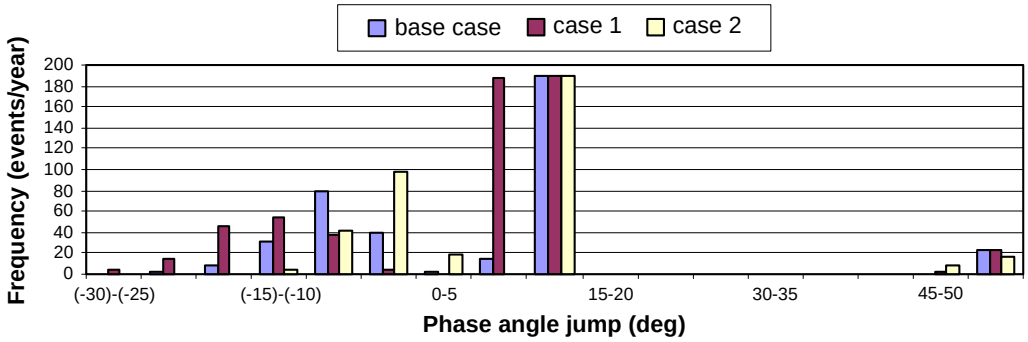

b) Different distribution means

Figure 50. Frequency of phase angle jump in phase A at bus 229 for normal distribution of faults along the line 235-268 (Adapted from [82]).

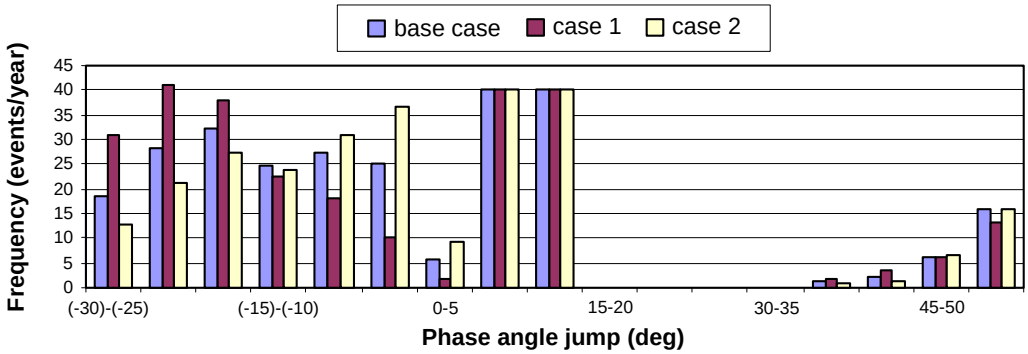

a) Decay from sending end to receiving end of the line

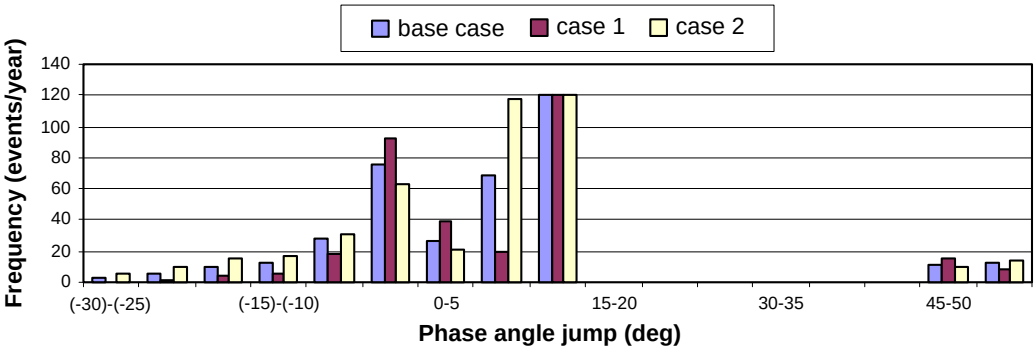

b) Decay from receiving end to sending end of the line

Figure 51. Frequency of phase angle jump in phase A at bus 229 for exponential distribution of faults along the line 235-268 – different distribution means (Adapted from [82]).

The influence of the parameters of the exponential distribution is illustrated in Figure 49. It can be seen from these figures that different distribution parameters result in different dip frequencies in different voltage ranges. The dependence of dip frequency on distribution parameters though still very pronounced, is smaller than the dependence on the type of distribution used. Dependence of dip frequency on the parameters of normal distribution is bigger than the dependence on the parameters of exponential distribution (for the ranges of distribution parameters used in simulations). As far as the influence of different distribution parameters on the phase angle jump is concerned it was found that the phase angle jump in phase A is the most affected. (This was expected having in mind the types of faults modelled.) The effect of different distribution parameters on phase angle jump in phase A is illustrated in Figures 50 and 51.

v. Conclusions

The study has shown that different fault distributions along the line lead to different number and characteristics of voltage dips even though the total number of faults along the boundary lines is the same. The difference in the expected number of dips is bigger for the dips with lower magnitudes. It is however, still very significant even for the dips with higher magnitudes. The size and the shape of the area of vulnerability are not only dependent on the sensitivity level of the equipment but also on the relationship between the faulted phase and the study phase. The change in the size and the shape of the area of vulnerability results in different number of associated boundary crossing lines and such leads to different estimate of the number of voltage dips at the bus of interest. In order to achieve higher accuracy of prediction of number and characteristics of voltage dips at the bus of interest it is important to take into account the effect of faults on non-study phases when the area of vulnerability is identified, and to properly model the fault distribution along the boundary crossing lines.

The influence of different fault distributions on frequency of voltage dips within different voltage ranges can be very high. The influence of parameters of different fault distributions on number and characteristics of voltage dips is also illustrated. It was found that different distribution parameters have different effects depending on the type of distribution used. The sensitivity of the number of dips and dip characteristics to distribution parameter variation is smaller than to the type of the distributions used. The variation in the results however, is still very significant. The results emphasise the importance of a proper modelling of fault distribution along the lines within relevant area of vulnerability. This is particularly important in the case of the lines in close electrical proximity to the customer bus if the correct information about the number and characteristics of voltage dips is needed.

The variation in expected number of dips and their characteristics indicates that the proper modelling of fault distribution along the line is particularly important in cases when the border of the area of vulnerability is crossing the line. In such cases the method used for modelling of fault distribution along the line may significantly alter the number and characteristics of voltage dips expected at the customer bus. Depending on the fault distribution along the transmission line (in an electrical proximity to the bus of interest) a single phase equipment connected to different phases will experience different number of voltage dips having different characteristics. Depending on the sensitivity threshold of the equipment connected to a particular phase and dip characteristics in that phase, there will be different number of equipment failures or misoperations in the plant. The cumulative loss in the revenue that might result due to the voltage dips therefore, should be assessed based on the information about the voltage dip performance of each phase (A, B or C) separately.

8. Voltage Dip Indices

8.1 Introduction

Voltage dip indices can be used to quantify a site or a system performance. The characteristic exposure that a typical distribution system encounters needs to be quantified in order to guide manufacturers in the appropriate design of ride-through alternatives for user load equipment. For many years, the only indices defined to quantify rms variation service quality were the sustained interruption indices (SAIFI, CAIDI, etc.), which quantify momentary interruption performance as defined in the IEEE Standard 1366 [83]. On the other hand IEEE Standard 1159*, Recommended Practice on Monitoring Electric Power Quality* [10], defines magnitude ranges for dips, swells and interruptions and suggests that the terms dip, swell, and interruption be preceded by a modifier describing the duration of the event (instantaneous, momentary, temporary, or sustained). Rms variations are therefore classified by the magnitude and duration of the disturbances.

The present draft of IEEE Std. P1564 identifies voltage dip indices for customers, vendors and electric utilities and the method of calculating such indices [5]. The draft proposes a five-step procedure to give a value to the performance of a power system:

1. Obtain sampled voltages with a certain sampling rate and resolution.
2. Calculate event characteristics from the sampled voltages.
3. Calculate single-event indices from the event characteristics
4. Calculate site indices from single-event indices of all events measured over a period of time.
5. Calculate system indices from the site indices for all sites within the system.

The first two steps have been introduced in the second chapter of this document. A short summary is included below. A more detailed description of the other steps is presented in the subsequent sections.

The following section presents new concepts related to the characterization of a single event. Indices proposed to characterize a site and a system, respectively, are described in the subsequent sections. The last section of this chapter includes some test cases on calculations of voltage dip indices.

Readers interested in this subject will find a good survey on voltage dip indices and other power quality indices in the report published by the Joint WG CIGREC4.05/CIRED, *Power Quality Indices and Objectives* [84].

8.2 Indices for event characterization

8.2.1 Magnitude and duration

According to IEC 61000-4-30, a voltage dip or voltage swell should be characterized by its *duration* (the time the rms voltage stays below the threshold) and its *retained voltage* (the lowest rms voltage during the event). Instead of retained voltage the *depth* (the difference between the retained voltage and a reference voltage) may be used.

The choice of a dip threshold is essential for determining the duration of the event. This choice of threshold is also important for counting events, as events are only counted as voltage dips when the rms voltage drops below the threshold. Dip threshold can be a percentage of either nominal or declared voltage, or a percentage of the sliding voltage reference, which takes into account the actual voltage level prior to the occurrence of a dip. The user shall declare the reference voltage in use.

Voltage dip envelopes may not be rectangular. As a consequence, for a given voltage dip, the measured duration is dependent on the selected dip threshold value. The shape of the envelope may be assessed using several dip thresholds set within the range of voltage dip and voltage interruption threshold detection. The latter concept also called "*Time Below Specified Voltage Threshold*" is presented in more details in reference [85]. Another method for treating non-rectangular dips is part of IEEE Std 493 [81] and discussed in detail in [69]. In the latter method, characteristics are no longer determined for each individual event, but the rms voltage versus time curves are directly used to obtain a so-called "voltage-dip co-ordination chart".

An annex to IEC 61000-4-30 mentions other characteristics for voltage dips: phase angle shift, point-on-wave, three-phase unbalance, missing voltage and distortion during the dip. The use of additional characteristics and indices may give additional information on the origin of the event, on the system and on the effect of the dip on equipment. Even though several of these terms are used in the power-quality literature there is no consistent set of definitions.

IEC 61000-2-8 document also refers to IEC 61000-4-30 for measurement, but introduces a number of additional recommendations for calculating voltage-dip indices. Recommended values are 90% and 91% for dip-start threshold and dip-end threshold, respectively, and 10% for the interruption threshold. Dips involving more than one phase should be designated as a single event if they overlap in time. Voltage dips with a retained voltage below the interruption threshold can be classified as momentary interruptions. The duration of the event would be the amount of time the rms voltage is below the dip threshold. Alternatively the duration of a momentary interruption can be defined as the amount of time the rms voltage is below the interruption threshold. The difference between these two definitions is normally small compared to the duration of momentary interruptions.

Voltage swells can be characterized in the same way as voltage dips. The rms voltage is again used as a characteristic versus time. The single-event indices are the "duration" and the "retained voltage". The duration equals the amount of time the rms voltage is above the swell threshold. The retained voltage is the highest value of the rms voltage. The recommended value for the swell threshold is 110% of the declared voltage or of the sliding-reference voltage.

For multi-channel measurements the rms voltage versus time is calculated for each channel separately. For single-phase measurements only the voltage magnitude versus time is needed for further processing. The voltage phase angle versus time is needed with some methods to calculate characteristics for three-phase measurements.

IEC 61000-4-30 distinguishes between single-channel and multi-channel measurements. For multi-channel measurements,

- the retained voltage is the lowest of the retained voltage for the individual phases.

- the starting instant of the dip is the moment the rms voltage in one of the phases drops below the dip-starting threshold.
- the ending instant of the dip is the moment all rms voltage have recovered above the dip-ending threshold.
- the duration is obtained as the time difference between the ending instant and the starting instance.

The event may end in a different channel as the one in which it started. The same result is obtained by defining the multi-channel rms voltage at any instant as the lowest of the rms voltages in the different channels. The duration of the multi-channel event is defined as the time during which the multi-channel rms voltage is below the threshold. In case only retained voltage and duration in the different channels are available, the lowest retained voltage and the longest duration are used to characterize the multi-channel event.

8.2.2 Other voltage dip indices

The IEEE P1564 draft introduces two other single-event indices:

A. The voltage dip energy is defined as:

$$E_{VS} = \int_0^T \left[1 - \left\{ \frac{V(t)}{V_{nom}} \right\}^2 \right] dt \qquad (29)$$

where $V(t)$ is the rms voltage during the event and V_{nom} the nominal voltage. The integration is taken over the duration of the event; i.e. for all values of the rms voltage below the threshold. The rms voltage can be expressed in any unit (Volt, kV, per unit) as long as the nominal voltage is expressed in the same unit. The voltage-dip energy has the unit of time; it may be expressed in cycles, milliseconds or seconds.

B. The voltage-dip severity is calculated from the retained voltage (in pu) and the duration of a voltage dip in combination with a reference curve. It is recommended to use the SEMI curve as a reference, but the method works equally well with other methods.

From the retained voltage V and the event duration d the event voltage-dip severity is calculated as follows:

$$S_e = \frac{1 - V}{1 - V_{curve}(d)} \qquad (37)$$

where $V_{curve}(d)$ is the retained voltage of the reference curve for the same duration. For an event on the reference curve the voltage-dip severity equals one; for an event above the curve the index is less than one; for an event below the curve the index is greater than one. For events with the retained voltage above the voltage-dip threshold (with 90% being the recommended value) the voltage-dip severity is equal to zero.

A voltage-swell severity can be defined for voltage swells in a similar way, by choosing a reference curve. It is however recommended treating voltage dips and swells as separate events. A voltage dip and a voltage swell with the same “severity” will not have a similar effect on equipment.

For other voltage dip indices see references [86] and [87].

8.2.3 Aggregation [5]

The definition of "event" is an important aspect because the total count of "events" would be very different if three-phase measurements were counted as three single-phase measurements. An approach would consist on collecting small elemental components of measurements (i.e., measurement components) and aggregate them at analysis time. The word "aggregate" literally refers to the collection of units or parts into a mass or whole. Aggregation refers to the data reduction technique of collecting many distinct measurement components into a single *aggregate event* for the purpose of computing system performance indices. How the measurements are combined depends on the specific needs.

A. *Measurement aggregation*: Many monitoring instruments will record one or more phases during an rms variation. For example, a three-phase voltage dip may result in a meter recording one measurement for each phase. In conducting measurement aggregation, we choose to represent the multiple phase measurements as only one measurement. A common practice is to choose the phase measurement that exhibits the greatest deviation from nominal voltage.

B. *Time aggregation*: The time aggregation is counting a single event if there is succession of events within a short time, generally caused by a single power system event. This is generally accepted practice in indexing voltage dip events. If the customer equipment is impacted by a voltage dip event, it is unlikely that the equipment will be up and running and impacted by a succeeding event during the aggregation time period. The EPRI DPQ project's results published in IEEE journals used 60-second aggregation time, but also explored using 120 seconds and 300 seconds. An example of a longer aggregation time is seen in the Detroit Edison special manufacturing contracts (SMC) with its automotive manufacturers. The contracts require bookkeeping of the worst voltage dip in fifteen-minute aggregation intervals.

C. *Spatial aggregation*: Spatial aggregation refers to finding the worst voltage dips from more than one monitoring point. An example where this is necessary is with the Detroit Edison SMC computations, which need only to determine the lowest voltage dip measured by all of the meters monitoring the various service entrances of a facility. Spatial aggregation has also been employed when meters are configured to monitor only a single phase. In this case, three meters, each monitoring one phase of a feeder, can be combined to give the voltage dip performance of the bus supplying the feeder. In using *spatial aggregation* to reduce the number of rms variation measurements, the measurements from multiple monitoring instruments are combined into a single measurement. An example on when this has an application is if one is interested in computing rms variation indices at a single substation that is monitored at multiple buses. Another example is if one if computing rms variation indices for a single industrial facility that is monitored at each service entrance of its supplying feeders.

8.3 Indices for site characterization

Single-event characteristics are used as obtained from events recorded at a given site over a given period, typically one month or one year, as input to the site indices. When publishing site indices it is important to indicate which method has been used to obtain the single-event characteristics: e.g. lowest of the three phase-to-ground voltages; lowest of the three phase-to-phase voltages; characteristic voltage obtained from three-phase measurements.

8.3.1 SARFI indices

SARFI is an acronym that stands for *System Average RMS Variation Frequency Index*. It is a power quality index that provides a count or rate of voltage dips, swells, and/or interruptions for a system. The size of the system is scalable: it can be defined as a single monitoring location, a single customer service, a feeder, a substation, groups of substations, or for an entire power delivery system. There are two types of SARFI indices: *SARFI-X* and *SARFI-Curve*.

1) SARFI-X corresponds to a count or rate of voltage dips, swell and/or interruptions below a voltage threshold. For example, SARFI-90 considers voltage dips and interruptions that are below 0.90 per unit, or 90% of the reference voltage. SARFI-70 considers voltage dips and interruptions that are below 0.70 per unit, or 70% of the reference voltage. And SARFI-110 considers voltage swells that are above 1.1 per unit, or 110% of the reference voltage. These indices are meant to assess short-duration rms variation events only, meaning that only those events with durations less than the minimum duration of a sustained interruption (5 minutes) are included in its computation. For voltage swells SARFI-X is defined as the number of events per year with a retained voltage exceeding X percent (for X greater than 100).
2) SARFI-Curve corresponds to a rate of voltage dips below an equipment compatibility curve. For example SARFI-CBEMA considers voltage dips and interruptions that are below the lower CBEMA curve. SARFI-ITIC considers voltage dips and interruptions that are below the lower ITIC curve.

8.3.2 Voltage dip tables

A commonly used method of presenting the performance of a site is by means of a voltage dip table. The columns of the tables represent ranges of voltage-dip duration, the columns represent ranges of retained voltage. Each cell in the table gives the number of events with the corresponding range of retained voltage and duration. Strictly speaking a voltage-dip table is not an index but a way of presenting a set of indices. Each element in the table can be used as an index, just like there are multiple choices for the SARFI indices.

In the two examples shown below the retained voltage is expressed in percent, but it may also be expressed in Volts. The duration should be expressed in milliseconds, seconds or minutes, with the exception of the first row in case the maximum duration is one cycle.

IEC 61000-4-11 prescribes a number of retained voltage and duration values for testing equipment against voltage dips and short interruptions. Table XIX shows the recommended tabulation in which each cell is intended to contain the number of dips of the corresponding magnitude and duration within a specified period, usually one year.

Table XIX – Voltage dip table based on the values in IEC 61000-4-11 [17].

Retained voltage	<1 cycle	1 cycle-200 ms	0.2-0.5s	0.5-5 s	5s-1 min
70-80%					
40-70%					
10-40%					
≤10%					

IEC 61000-2-8 table: The voltage-dip table as proposed in draft IEC 61000-2-8 is shown in Table XX. The main difference with the UNIPEDE table is in the higher resolution in the remaining voltage ranges. Also is an additional duration range added with 250 milliseconds as a limit.

Table XX – Voltage dip table according to IEC 61000-2-8 [3].

Retained voltage	<0.1 s	0.1-0.25 s	0.25-0.5 s	0.5-1 s	1-3 s	3-20 s	20-60 s	1-5 min
80-90%								
70-80%								
60-70%								
50-60%								
40-50%								
30-40%								
20-30%								
10-20%								
≤10%								

8.4 Indices for system characterization

System indices are used by the network operator to assess the performance of a whole system; e.g. they can be used to compare year-to-year performance. The results of such a performance assessment or comparison can be used as a basis for improvements in the system.

System indices are calculated from the site indices obtained for a number of sites. Two principally different methods can be distinguished for calculating system indices.

- The system index is defined as a weighted average of the site indices. To determine weighting factors, system and load information is needed, but often a unity weighting factor is used for all monitored sites.
- The system index is defined as the value not exceeded for 95% of the sites (the 95 percentile of the site indices). To be able to determine a 95 percentile a reasonable number of sites has to be monitored, at least 20. When between 10 and 20 sites are available, the 90 percentile may be used instead. For less than 10 sites, the weighted average and the maximum value should be reported.

SARFI indices are obtained as the average of the indices for the different sites. They thus give the "average voltage quality" over the whole system. When using SARFI indices to describe individual sites, it is possible to give a 95 percentile to characterize the quality of the whole system. This is however not common practice.

When voltage-dip tables are used, both average values over all sites and 95 percentile values can be used. When average values are used, weighting of the values may be considered. Weighing is also possible when using the 95 percentile but less useful unless a very large number of sites is being monitored. The voltage-dip table for the whole system may contain a smaller number of cells than for individual sites. For individual sites a certain level of detail is needed to determine the compatibility of sensitive equipment with the supply. For system indices a lesser level of detail may be more appropriate as that makes e.g. the study of year-to-year variations easier.

8.5 Voltage dip index evaluation

The calculation of voltage dip indices is straightforward from the results derived with a stochastic prediction. Not much experience is presently available on the application of indices to analyze the voltage dip performance of transmission and distribution systems. In addition, most publications deal only with the count of event frequency (i.e. SARFI indices). The following subsections present three examples of SARFI calculations. In the first one several SARFI indices are derived and analyzed for a distribution network from the stochastic prediction of voltage dips using a time-domain simulation tool. The last two examples use the calculation of SARFI indices to analyze the impact of distributed generation at transmission and distribution levels.

8.5.1 Example 1: Calculation of indices for a distribution network

A. Introduction

The aim of this study is to predict the voltage dip performance of a distribution network by estimating voltage dip indices and using a time-domain simulation tool. The work is based on the application of a Monte Carlo procedure developed using capabilities of the ATP package [34], [88], a well known EMTP-like tool.

The tasks needed to obtain voltage dip indices can be summarized as follows: internal capabilities of the transients program are used for the development of power components and load models; capabilities of the program are linked to external routines for assessment of voltage dips using a Monte Carlo method; the output results are post-processed to obtain voltage dip indices.

The study will be performed by assuming that voltage dips are caused only by faults, there is no distributed generation in the system, and mitigation devices are not installed.

B. Modelling guidelines

Guidelines used in this case are those presented in Chapter 6. Simulations have been based on a constant impedance representation of loads, which are only installed at LV buses. A constant resistance model is used for representing the fault impedance.

C. Test system

Figure 52 shows the diagram of the test system and the characteristic of the protective devices [89]. The lower voltage side of the substation transformer is grounded by means of a zig-zag reactor of 75 Ω per phase. This grounding system limits overcurrents caused by single-line-to-ground faults to 600 A.

D. Stochastic prediction of voltage dips

The procedure for voltage dip assessment is based on the Monte Carlo method and assumes that dips are due only to faults caused within the distribution network. The test system is simulated as many times as required to achieve the convergence of the Monte Carlo method. Every time the system is run, fault characteristics are randomly generated using the following distributions [34]:

- The fault location is selected by generating a uniformly distributed random number, since it is assumed that the probability is the same for any point of the distribution system.
- The fault resistance has a normal distribution.
- The initial time of the fault is uniformly distributed within a power frequency period.
- The duration of the fault has also a normal distribution.
- Different probabilities are assumed for each type of fault.

Given the topology, the location of protective devices and the parameters of the test system, it is worth mentioning the following consequences:

- The retained voltage during a three-phase fault at the secondary of the substation can be approximated by means of the following expression

$$V_{(sag)} \approx \frac{R_F}{Z_S + Z_{Tr} + R_F} \cdot V_{(pre-sag)} \tag{31}$$

  where Z_s and Z_{tr} are respectively the impedances of the high voltage (HV) equivalent and the substation transformer, R_F is the fault resistance, while $V_{(pre\text{-}dip)}$ and $V_{(dip)}$ are the voltages prior and during the fault, respectively.

  The impedance of the substation transformer seen from the medium voltage (MV) side is 2.5 Ω. If the mean value of the fault resistance is greater than 5 Ω, which is a realistic value, the retained voltage will be above 90% of the pre-fault voltage. If the threshold voltage for dip severity is 90% of the rated voltage, then not many equipment trips should be caused by three-phase faults.

- It is well known that the severity of a voltage dip caused at the MV side of a Delta-wye transformer is not the same at the low voltage (LV) side [1]. Figure 53 shows the voltage dips caused by a single-phase-to-ground fault at the MV and LV sides of a distribution transformer. Therefore, if customer equipment is installed only at the lower voltage side, as assumed in this work, the percentage of trips due to single-phase-to-ground faults will significantly decrease.
- The probability density charts of voltage dips corresponding to both terminals of the same transformer will be very different. Consequently, the number of severe dips at the customer installation (LV side) will be significantly reduced, since most equipment trips will be caused by three-phase and two-phase faults located within a certain distance from the substation.
- A consequence of protective device operation is that voltage dips will not be always rectangular, as those shown in Figure 53. The coordination between protective devices can produce multiple events with different retained voltages. An important aspect is then the characterization of these events. Figure 54 shows different cases.

  According to IEEE P1564 [5], multiple events should be merged in a single event since the effect on end-user equipment will be the same. Consider the case depicted in Figure 54(a); the retained voltage for the three phases would be zero, while the dip duration would be the time interval between the instant at which the voltage drops below the threshold value and the instant at which this value is recovered. Although, the profiles are different, a similar reasoning would be used with the case depicted in Figure 54(b). The case shown in Figure 54(c) is different, since the retained voltage is the same for each

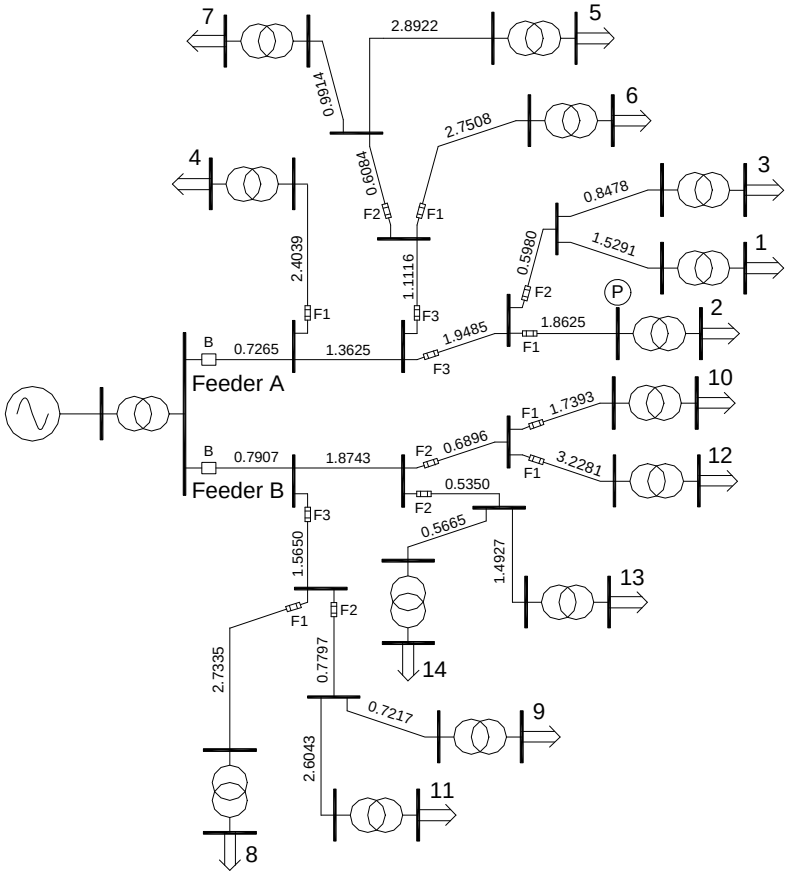

HV equivalent: 110 kV, 1500 MVA, X/R = 10
Substation transformer: 110/25 kV, 20 MVA, 8%, Yd
Distribution transformers: 25/0.4 kV, 1 MVA, 6%, Dy
Lines: $Z_{1/2} = 0.61 + j0.39$, $Z_0 = 0.76 + j1.56$ Ω/km

a) Diagram of the test system. (Non integer quantities indicate the length of line sections, in km), (B ≡ Breakers, F1, F2, F3 ≡ Fuses)

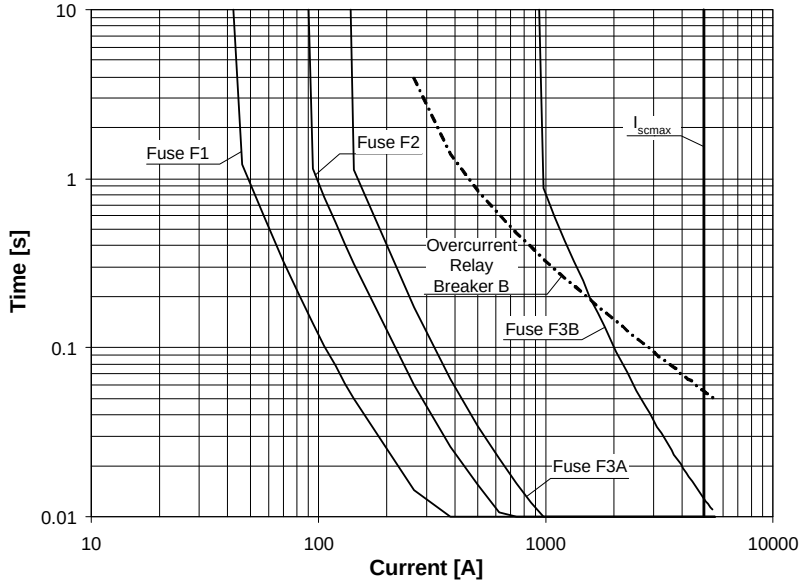

b) Time-current characteristics of protective devices.

Figure 52. Test system [89].

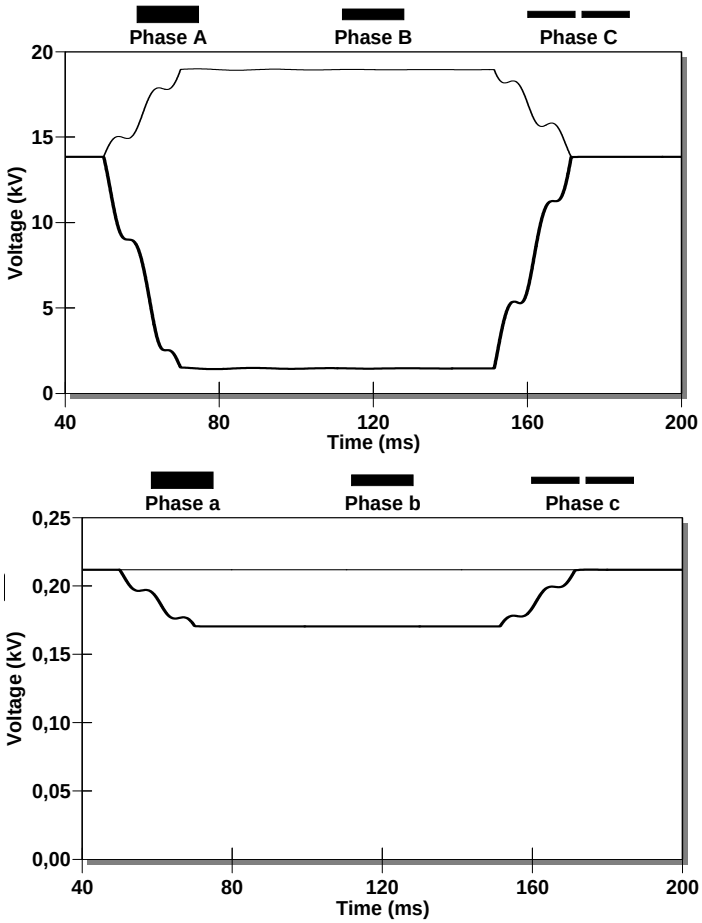

a) Voltage dip – MV side (Dy transformer)

b) Voltage dip – LV side (Dy transformer)

Figure 53. Voltage dips at both sides of a distribution transformer.

phase during both events; only the dip duration would be affected now, being its value that which results from the addition of the duration of each event.

E. Voltage dip assessment

The following studies, considering a different coordination between protective devices, were performed [89]:

i. Protective devices do not operate; that is, the fault condition disappears before any device could open.

ii. Circuit breakers operate faster than fuses and their relays have one reclose operation, being the reclosing time 200 ms. The simulations are performed without including fuse models.

iii. The coordination between overcurrent relays and fuses allows fuses to operate. Curve labelled F3A in Figure 52(b) is selected for fuses F3. Relays will have one 200 ms reclose operation.

iv. The same as for the previous study, but allowing feeder relays to have two 200 ms reclose operations, and selecting fuse curve F3B.

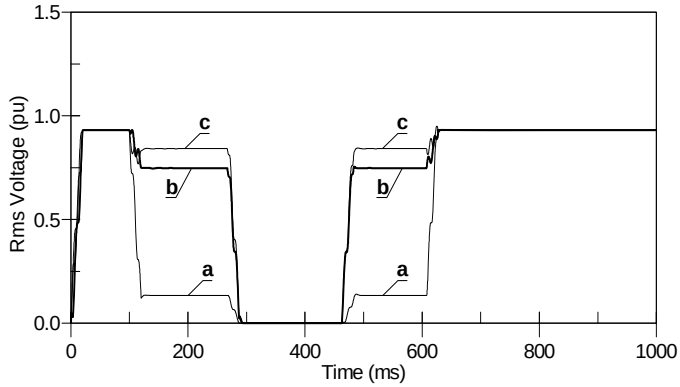

a) Voltage dip caused by a two-phase-to-ground fault

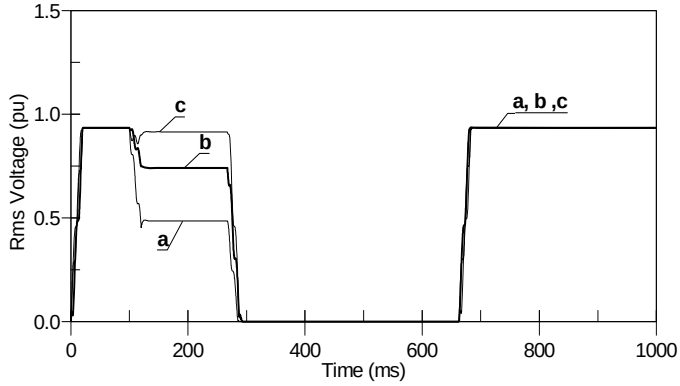

b) Voltage dip caused by a two-phase-to-ground fault

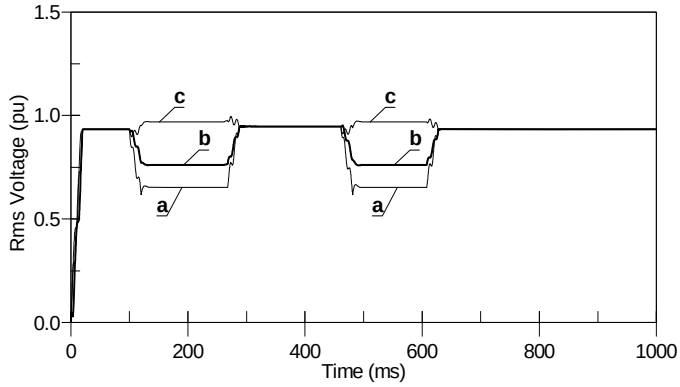

c) Voltage dip caused by a two-phase fault

Figure 54. Different clusters of voltage dips, measured at the LV side (Adapted from [89]).

The fault characteristics were randomly generated according to the following distributions:

- The fault location was selected by generating a uniformly distributed random number.
- The fault resistance had a normal distribution, with a mean value of 5 Ω and a standard deviation of 1 Ω, for each faulted phase.
- The initial time of the fault was uniformly distributed between 0.05 and 0.07 s.
- The mean value of the fault duration was varied, and by default the standard deviation was 10% of the mean value.
- The probabilities of each type of fault were LG = 75%, 2LG = 17%, 3LG = 3%, 2L = 3%, 3L = 2%.

In all studies the test system is run 1000 times and the following information is recorded during every run:

- fault characteristics (location, initiation time, duration, resistance, faulted phases, type of fault)
- voltage dip characteristics (retained voltage, duration) on every phase of all load buses.

If it is assumed a probability of occurrence of 12 faults per year and 100 km of overhead lines, 1000 runs are equivalent to analyze the performance of the test system during 214 years. Figure 55 shows respectively the number of dips per year caused at a MV bus and the severity of these dips as compared to the ITIC curve. These results were deduced by assuming that the average fault duration was 600 ms and the standard deviation was 60 ms. Only dips caused at one phase are shown; since the probability of occurrence of faults is assumed to be the same at each phase in all lines, the charts will be very similar for each phase of the same bus.

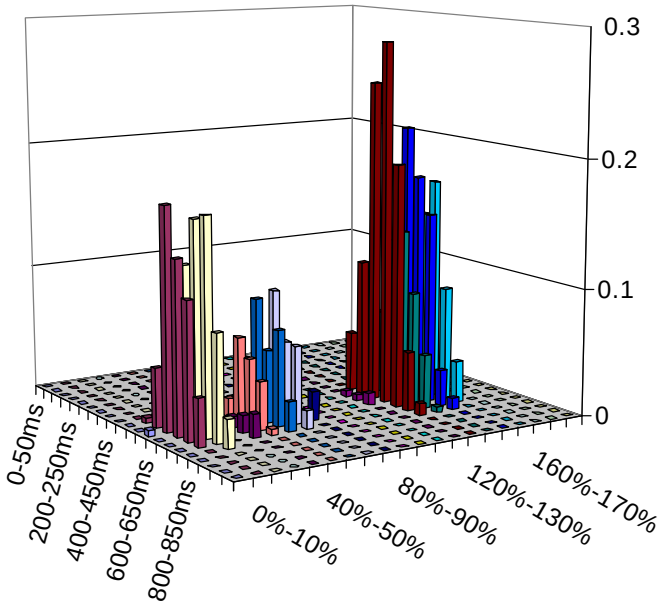

a) Number of dips per year

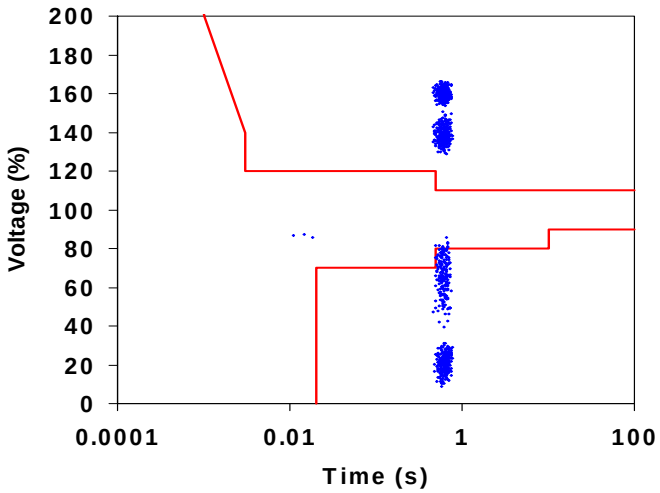

b) Voltage dip characteristics – ITIC curve

Figure 55. Simulation results – 1000 runs (Bus 6, MV side, phase A – Mean fault duration = 600 ms) (Adapted from [89]).

Voltage tolerance (acceptability) curves can be used to predict equipment maloperation. Although not much information is available in the literature about equipment performance in front of three-phase unbalanced dips, acceptability curves for single-phase equipment are widely used. Voltage dip indices can be easily calculated when only single-phase equipment is installed. It is important to emphasize that the dips caused at the LV side of a transformer can be very different from those caused at the MV side. Since it is assumed that only LV single-phase equipment is installed, only dips caused at the LV side of load transformers will be analyzed.

Figure 56 shows some simulation results that were derived from the four studies mentioned above. All these results correspond to the voltage dips caused at the LV side of the load bus 6 and were deduced by assuming that the mean fault duration was 600 ms. The plots show the number of trips per phase (i.e. the number of voltage dips below the lower ITIC curve) caused to sensitive equipment, and were obtained after removing events with a retained voltage between 90 and 110% of the rated voltage.

From these results one can deduce that the number of trips shows an evident dependence with respect to the design of the protection system and that the quantity of dangerous dips is very different at each side of a distribution transformer, see Figure 53. The performance can be improved by including recloser and fuse operations, but the optimal design should also consider the characteristic curves of protective devices.

Table XXI shows a summary of the main results obtained in this work. The results were derived after 1000 runs, and using the same random generation of fault characteristics for all cases. Equipment sensitivity was represented by the ITIC curve and only single-phase equipment was installed at the LV level. The quantities within parenthesis indicate the number of trips per year of sensitive equipment, and were calculated by assuming that the test system is analyzed during 214 years, see above. Note that the quantities shown in the table do not match those depicted in Figure 56; the quantities shown in figures correspond to one phase only, while the quantities in the table are the average of the three phases.

One can see that the number of trips can decrease by increasing the fault-clearing time and by introducing reclose operations. The improvement achieved by increasing the fault-clearing time is evident after comparing results derived with a mean fault duration of 200 ms: the lowest number of trips is obtained when protective devices do not operate (i.e. its operation is delayed), but a significant improvement can be also achieved if they operate and the fault-clearing time is increased for small fault currents, i.e. for single-phase-to-ground faults. The second conclusion is deduced after comparing the results obtained with a mean fault duration of 600 ms: the lowest number of trips is achieved when reclose operations are allowed. Both results are simultaneously confirmed with the last study, when reclosing is allowed and a fuse operation is delayed (see curve F3B in Figure 52(b)).

F. Calculation of voltage dip indices

Voltage dip indices can provide a count of event frequency and duration, the undelivered energy during events, or the cost and severity of the disturbances. Only the first type of index, i.e. count of events, is analyzed in this test case. The information obtained with the above procedure is manipulated to obtain the number of trips per year in combination with an acceptability curve [87].

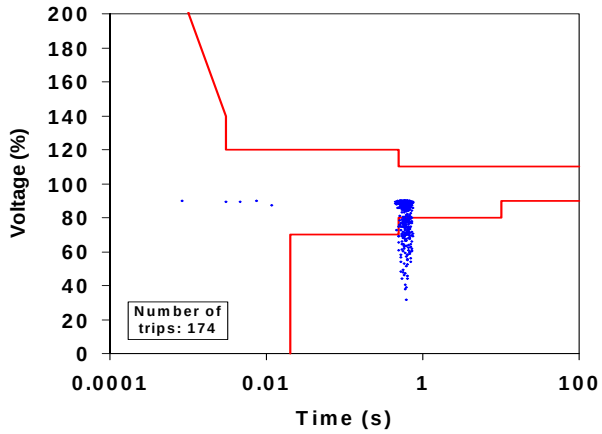

a) Protective devices do not operate

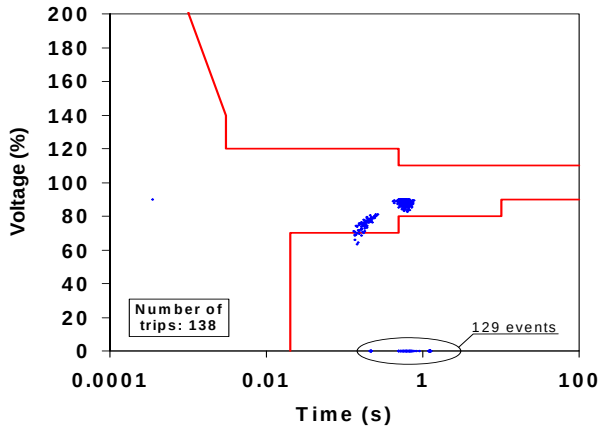

b) Breaker operation (Reclosing interval = 200 ms)

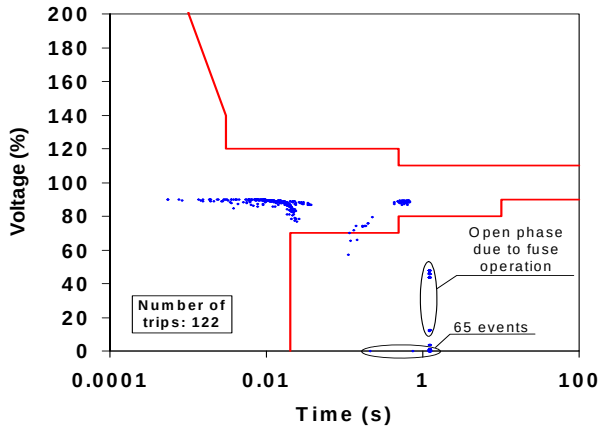

c) Fuse operation (Reclosing interval = 200 ms)

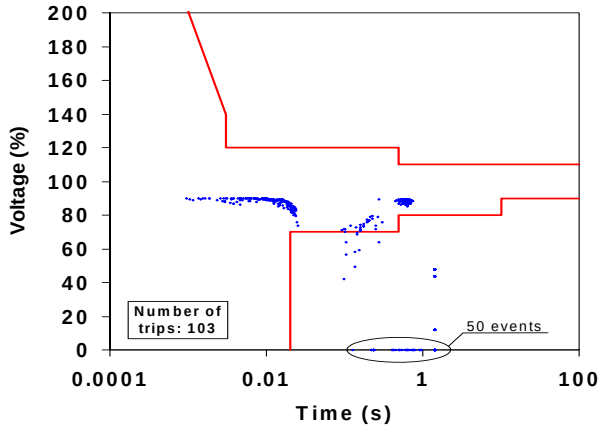

d) Breaker and fuse operation (Two reclosing intervals)

Figure 56. Simulation results (Bus 6, LV side, phase A – Mean fault duration = 600 ms) (Adapted from [89]).

Table XXI – Average number of equipment trips per phase and year (Bus 6 - LV level) [89].

Protection system	Fault duration		
	200 ms	600 ms	1 s
No operation	64 (0.30)	169 (0.79)	176 (0.82)
Breaker operation (t_R = 200 ms)	111 (0.52)	133 (0.62)	500 (2.34)
Breaker and fuse operation (t_R = 200 ms)	121 (0.56)	122 (0.57)	159 (0.74)
Breaker and fuse operation (change fuse F3) (t_R = 200 + 200 ms)	82 (0.38)	85 (0.40)	194 (0.91)

As detailed above, *SARFI* gives the average number of events (dips, swells, short interruptions) over the assessment period, usually one year, per customer served. A *SARFI* value is obtained by means of the following expression

$$SARFI = \frac{\sum_{i=1}^{n_s} N_i}{N_T} \tag{32}$$

where n_s is the number of events, N_i is the number of customers experiencing an event and N_T is the number of customers served from the section to be assessed.

Since only events caused at the MV distribution level are analyzed, the number of costumers that will experience an event at a LV load bus is the number of costumers served from that bus. Therefore, for a single site the *SARFI* value is the number of dips over the assessment period. The index for an entire system can be obtained as follows

$$SARFI = \frac{\sum_{j=1}^{n_n} N_j \cdot SARFI_{(j)}}{N_T} \tag{33}$$

where n_n is the number of load buses, N_j is the number of costumers served from bus j, and $SARFI_{(j)}$ is the value for bus j.

SARFI indices are based on the number of customers served from every load bus; it will be assumed that this number is the same at every load bus; therefore, expression (33) becomes

$$SARFI = \frac{\sum_{j=1}^{n_n} SARFI_{(j)}}{n_n} \tag{34}$$

Figure 57 shows the index values deduced for the entire test system [87]. The main conclusions derived from the simulation results can be summarized as follows:

- The performance obtained with each protection scenario is not the same for every $SARFI_x$ index and some differences can be easily noted when comparing indices derived for different sites. *SARFI* values corresponding to different thresholds can show different behaviour; for instance, at load bus 6, the best $SARFI_{90}$ performance is achieved when all protective devices can operate, while the best $SARFI_{60}$ performance corresponds to a different scenario, i.e. when fuses are saved.
- SARFI values as a function of the mean fault duration do not show very significant

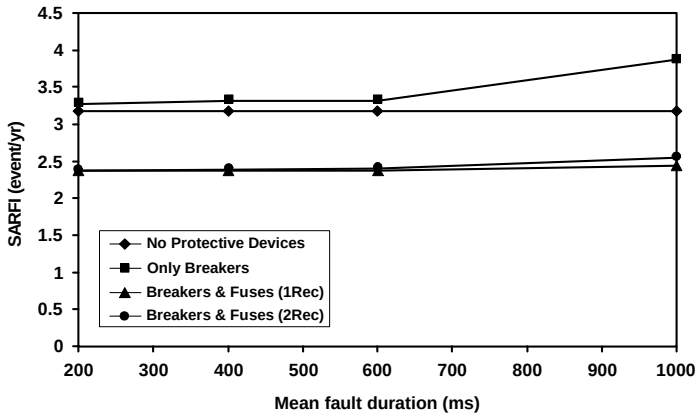

a) $SARFI_{90}$

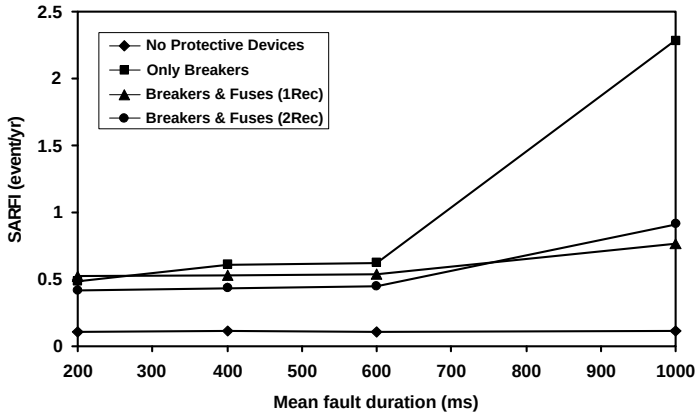

b) $SARFI_{60}$

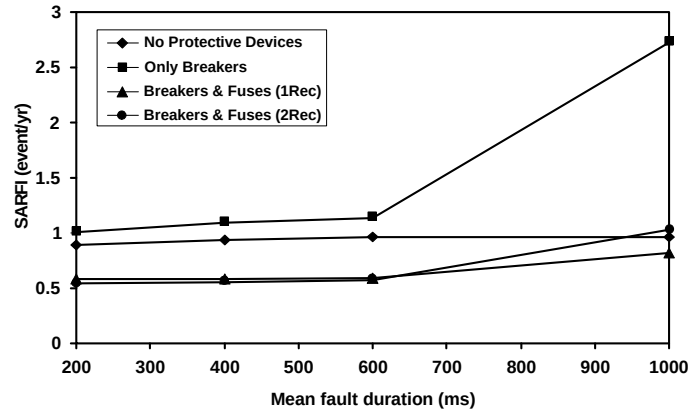

c) *SARFI-CBEMA*

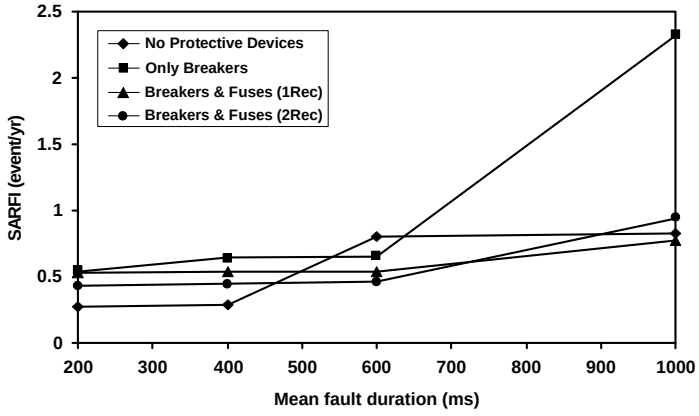

d) *SARFI-ITIC*

Figure 57. *SARFI* calculations for the whole system – LV buses (Adapted from [87]).

changes for a given protection system, except when the fault duration is about 1 second or longer.

- ITIC equipment has a better performance that CBEMA equipment; however, when fuses operate the performance is very similar. Results deduced when loads are represented by means of ITIC and SEMI curves were the same.

G. Conclusions

This study has presented the application of a procedure for stochastic prediction of voltage dips to the calculation of voltage dip indices in distribution networks. The results deduced from the procedure are used to obtain the average number of events experienced by each customer served over the assessment period. The results presented in these test cases have shown the influence that the design of the protection system and the equipment vulnerability can have on these indices.

8.5.2 Example 2: Impact of distributed generation

A. Introduction

The replacement of conventional generation by distributed energy resources (DER), like wind turbines, leads to a reduction of the fault level, and this reduction will in general lead to an increased number of dips at the interface between transmission and distribution. For instance, if wind turbines are sensitive to voltage dips, one single fault may lead to loss of several thousands of MW of generation. This in turn may trigger stability problems in the grid. A study presented in [77] compares the dip frequency in a transmission system for a high generation scheduling and a low generation scheduling. The low generation scheduling had only half the generation capacity connected to each bus. The result was a significant increase in the dip frequency, especially for locations close to generator stations.

The impact of DER penetration in both transmission and distribution levels when voltage dips are caused by faults located at the transmission system is discussed below.

B. Impact at transmission levels

Part of the UK transmission system was modelled to study the impact of a reduction in large generation connected to the transmission system. The system data was obtained from the 2004 Seven Year Statement [90]. The case study has been based on the 400 kV grid in the North of England and Wales and the 275 kV grids around Sheffield, around Manchester and around Newcastle. The remaining part of the 400 kV system was modelled as a number of Thevenin equivalents. The load was taken equal to the one during “NGC peak” according to the 2004 Seven Year Statement.

A DER increase, equally spread over the system, was assumed, being the reduction in reactive power was the same as the reduction in active power. This was modelled as a reduction in the load as seen from the transmission system, which results in a reduction of the amount of generator units in operation. It was assumed that the oldest units are the most expensive ones and the first to be taken out of operation. No voltage control problems were observed when taking generator units out of operation. In fact, the voltage profile of the transmission system improved due to the reduction in load. The increase in distributed generation was studied in a five-stage scenario as summarized in Table XXII.

Table XXII – Five-stage scenario of increase in distributed generation.

Stage	Total load reduction	Load remaining	Generation reduction compared to previous stage
0	None	100%	n.a.
1	490 MW	97.24%	1 unit commissioned in 1966
2	2959 MW	83.33%	5 units commissioned in 1967
3	5399 MW	69.59%	6 units commissioned in 1968
4	7888 MW	55.57%	5 units commissioned in 1969
5	10356 MW	41.67%	5 units commissioned in 1970

The impact of faults at 400 kV level was studied for each of the stages. Only three-phase faults were assumed. For a given short-circuit position, the during-fault voltage was calculated for each 275-kV and 400-kV bus in the system. The impact of the fault was quantified as the sum of all active-power loads that experienced a dip below a certain threshold.

An example is shown in Table XXIII. The stage-0 loads have been used to calculate the impact of the fault. This fault is located in the south-eastern part of the network. As expected, the impact of the fault increases with an increase in DER (i.e. with a decrease in large central generation). From a customer viewpoint, the threshold values should be translated into immunity (voltage tolerance, sensitivity) of end-user equipment against voltage dips. For high DER penetration, end-user equipment also includes generation. When the total amount of generation tripping due to a fault is large, the system stability may be endangered. Such dynamic effects have not been considered in this study.

These calculations have been repeated for 17 different fault locations equally distributed over the 400-kV grid studied. It has been assumed that all faults have an equal probability of occurrence. The sum (or average) of the impacts of each individual fault is in that case a measure for the number of dips experienced by the load. This "total impact" is obtained as the sum of the values as in Table XXIII for each of the 17 fault positions. The results are shown in Tables XXIV and XXV; the former one gives the absolute value (in MW) whereas the latter one gives the relative increase compared to the base case [91].

Table XXIII – Example of the impact of a fault.

Stage	70%	75%	80%
0	917 MW	1166 MW	3436 MW
1	917 MW	1166 MW	3436 MW
2	917 MW	2071 MW	3732 MW
3	920 MW	2637 MW	3871 MW
4	1166 MW	3436 MW	5920 MW
5	1166 MW	4128 MW	6344 MW

Table XXIV – Average impacts of all fault positions.

Stage	70%	75%	80%
0	2371 MW	3164 MW	4197 MW
1	2458 MW	3196 MW	4254 MW
2	2728 MW	3416 MW	4581 MW
3	2966 MW	3754 MW	4918 MW
4	3104 MW	4054 MW	5162 MW
5	3283 MW	4389 MW	5574 MW

Table XXV – Relative voltage-dip frequency.

Stage	% DER	70%	75%	80%
0	0%	100%	100%	100%
1	2.7%	103%	101%	101%
2	16.7%	115%	108%	109%
3	30.4%	125%	119%	117%
4	44.4%	131%	128%	123%
5	58.3%	138%	139%	133%

The relative increase in dip frequency is shown graphically in Figure 58, where the three curves correspond to three values of end-user equipment's immunity against voltage dips. In more standardized terms, the three curves give the relative increase in SARFI-70, SARFI-75 and SARFI-80.

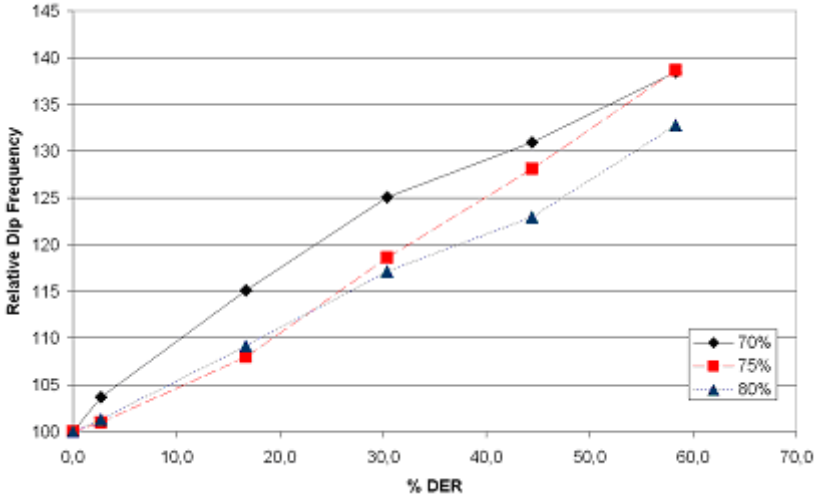

Figure 58. Relative increase in dip frequency with increasing percentage of distributed energy resources, for three values of the end-user immunity: 70%; 75% and 80% residual voltage.

The values in Tables XXIV and XXV can be used as voltage-dip indices to quantify the performance of the system. These indices can be used to apply the hosting-capacity approach when a limit value is defined for what is an acceptable behaviour [92], [93]. There is however no limit set in any standard on what is an acceptable voltage-dip frequency. An alternative approach is to use the increase in voltage-dip frequency as an index. This has been done in Table XXV. An acceptable limit is set as a maximum-permissible increase in average voltage-dip frequency. If an increase of 25% is allowed, the hosting capacity is around 30%. If an increase of 50% is allowed, the hosting capacity is at least 60%. Again, the hosting capacity depends strongly on what are perceived to be acceptable limits. This is a subject that is part of all system design and operational issues, not just related to distributed energy resources.

Strictly speaking the index in Table XXIV is not a voltage-dip frequency. A voltage-dip frequency is expressed in events per year, whereas the quantities shown in the table are expressed in MW. A weighted voltage-dip frequency (SARFI), as defined in [5], is obtained by multiplying the value in Table XXIV by the total number of faults per year and dividing it by the total load connected to the system. As the multiplication factors are independent of the amount of distributed energy resources, the relative increase in Table XXV and Figure 58 also holds for the weighted voltage-dip frequency.

In the system under study, 12 large industrial customers were directly supplied from 14 transmission buses (at 275 and at 400 kV). The increase in dip frequency experienced by these large industrial customers has been assessed separately. The resulting voltage-dip indices are given in Table XXVI, which provides the average number of dips per fault location below the threshold, experienced by the large industrial customers. To obtain a weighted dip frequency (SARFI) the values should be multiplied by the number of faults per year (for the total 400-kV grid) and divided by the number of industrial customers (12 in this case). The relative voltage-dip frequency (compared to the stage-0 value) is plotted in Figure 59. As the multiplication factors are independent of the percentage DER, the same figure holds for the weighted voltage-dip frequency.

Table XXVI – Average impacts of all faults on large industrial customers.

Stage	70%	75%	80%
0	0.9	1.2	1.7
1	0.9	1.2	1.7
2	0.9	1.2	1.8
3	1.0	1.3	2.1
4	1.0	1.5	2.3
5	1.1	1.6	2.6

Note the difference in weighting factors. In the first case, weighting was based on the total active power load supplied from the bus during the system peak. In the second case the weighting was based on the number of large industrial customers supplied from the bus. The resulting weighted dip frequencies (SARFI values) are obviously different, but their general trend with increasing penetration of DER is very similar.

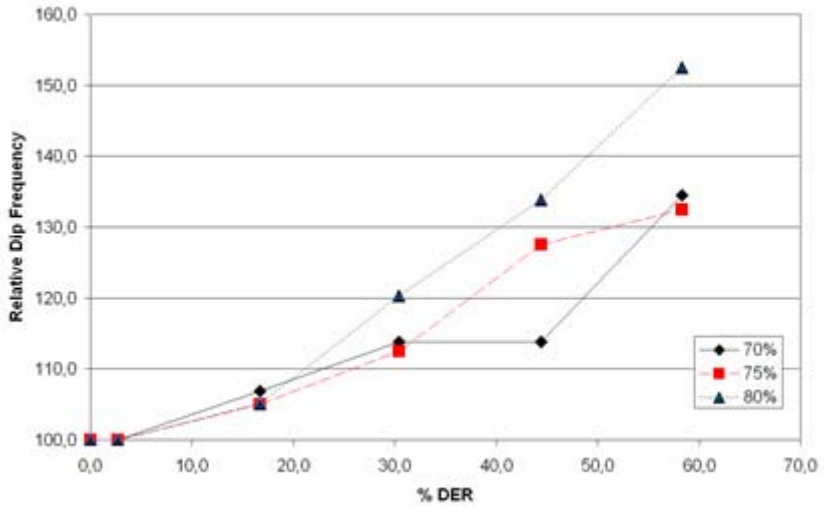

Figure 59. Relative voltage-dip frequency for large industrial customers with increasing penetration of distributed energy resources.

From the comparison of Figures 58 and 59, one can deduce that the increase in SARFI-80 is larger for the industrial customers than for the average load. The curves in Figure 59 are less smooth due to the limited number of sites involved (12 versus 26). It can be stated, however, that the increase in voltage-dip frequency is very similar for the average large industrial customer as for the average load.

Other aspects may also impact the voltage-dip frequency. In parts of the transmission system with a high concentration of large power stations, fault-current reduction techniques are often used (e.g. busbar splitting or series reactors); shutdown of those stations will make that these techniques are no longer needed so that the reduction in fault level will be less dramatic. The resulting increase in connectivity may, however, lead to an increase in the dip frequency, despite the fault level remaining the same.

C. Impact at distribution levels

The presence of generator units at distribution level will affect the dip frequency experienced by the end customers. The effect will depend to a large extend on the kind of interface with the grid. Units with synchronous machines have the ability to mitigate voltage dips due to three-phase faults. Induction generators only contribute to a symmetrical fault during the first one or two cycles. Both synchronous and induction generators have a small negative-sequence impedance (0.15 - 0.2 per-unit) so that they lead to a reduction of the negative-sequence voltage during a non-symmetrical fault. Voltage dips become thus more balanced. During a non-symmetrical fault the decay in the positive-sequence current contribution of an induction generator is much slower than during a symmetrical fault, so that it can consider this as a sustained contribution for all but the longest dips. The induction generators behave in this sense similar to the rest of the load, as discussed in [93].

Power-electronic interfaces can be designed to somewhat mitigate unbalanced voltage dips as well, but for mitigating balanced dips overrating of the converters is needed. However most power-electronic interfaces will trip rather quickly during a voltage dip as the currents and/or voltages will exceed their design ratings. For most voltage-dip studies it may thus be assumed that power-electronic converters do not contribute anything to the current during the fault.

Consider the simplified system model in Figure 60. During a fault at transmission level, the synchronous machine can be modelled as a voltage source behind impedance. If the load influence on the voltage and the influence of the synchronous machine on the voltage at transmission level are neglected, the model to calculate the voltage as experienced by the end-customers becomes that on the right.

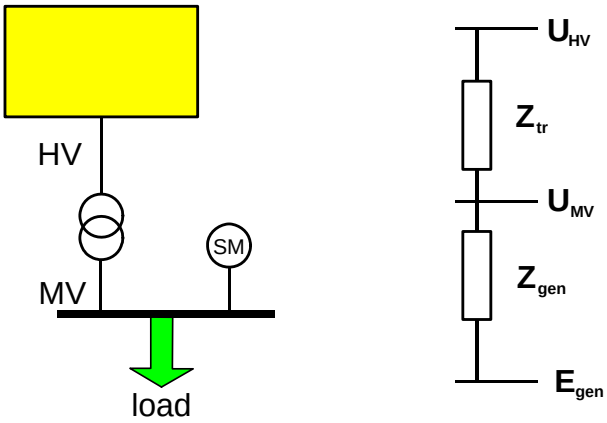

Figure 60. Distribution network with synchronous generator at MV level.

The residual voltage is found from the voltage-divider model. If the back-emf of the synchronous machine E_{gen} is equal to 1 pu, the following expression for the drop in voltage during the fault is deduced [91]:

$$(1-U_{MV}) = \frac{Z_{gen}}{Z_{gen}+Z_{tr}}(1-U_{HV}) \tag{35}$$

The voltage experienced by end-customers in case there is no generator connected at MV, is equal to U_{HV}, so that the reduction in voltage drop is related to the impedance ratio between the transformer and the synchronous generator.

To estimate the impact on the number of dips experienced by the end-customers, a simplified relationship between the number of dips and the residual voltage can be used:

$$N_{dips} = N_{50}\frac{V}{1-V} \tag{36}$$

where N_{50} is the number of voltage dips below residual voltage; it depends on the system configuration and the fault frequency.

The above expression was derived from theoretical models and has been confirmed from both simulations and measurements [1].

Combining (35) and (36) gives the following expression for the number of dips at the MV bus (thus as experienced by the end-customer):

$$N_{MV}(V) = N_{50}\frac{V'}{1-V'} \tag{37}$$

with

$$V' = V - \frac{z_{tr}}{z_{gen}}(1-V)\Pi_{DER} \tag{38}$$

$$\Pi_{DER} = \frac{S_{gen}}{S_{tr}} \tag{39}$$

where Π_{DER} is the fraction of distributed energy resources, z_{tr} is the transformer impedance in per-unit on a base equal to the transformer rating S_{tr} and z_{gen} is the per-unit generator impedance on a base equal to the generator rating S_{gen}.

An example is given in Figure 61, where a transformer impedance of 0.20 pu and a generator impedance of 0.25 pu have been used [91]. The increase in DER penetration can result in a significant reduction in the dip frequency. If the local penetration is higher than the average for the whole system, the local dip frequency reduces significantly.

The dip frequency for end-customers is however not only determined by dips originating at distribution level, but also by dips originating at transmission level. For some locations the later may dominate and the overall power quality will only show a limited influence of the level of DER penetration. An important conclusion from this discussion is that there is no general rule on how the dip frequency is impacted. It depends strongly on the transmission system, on the type of distributed generation and on the immunity of the end-customers against voltage dips. For customers at a location far away from large power stations, e.g. many customers in large urban areas, the dip frequency may actually reduce with an increasing level of local small generation.

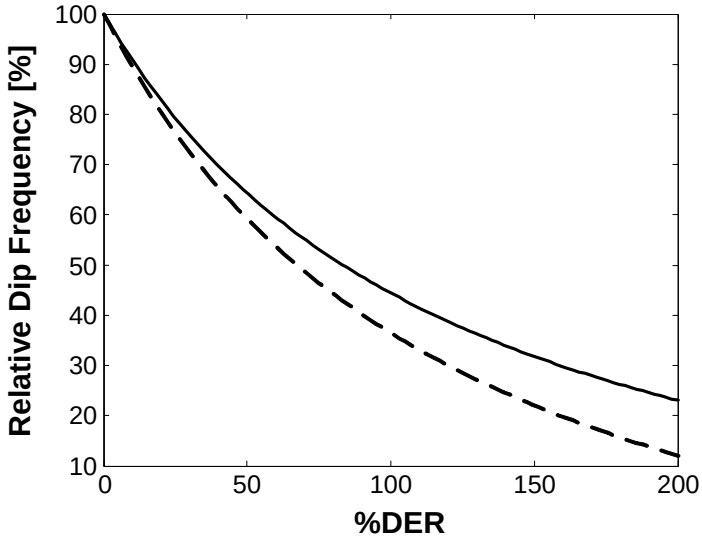

Figure 61. Relative voltage-dip frequency as a function of the DER penetration: SARFI-80 (solid line) and SARFI-70 (dashed).

9. Conclusions

Present software packages for power system analysis are powerful tools that can be used to perform any type of voltage dip study. Users can take advantage of capabilities implemented in general purpose simulation tools, e.g. EMTP-like tools, apply capabilities of equation-oriented tools, e.g. MATLAB, or just use a high level language compiler, e.g. C++, to develop custom-made models of power equipment, test the performance of mitigation devices, analyze the effect of new distributed generation technologies, embed new signal processing algorithms for voltage dip characterisation into simulation tools or calculate voltage dip indices.

Computer simulations provide an efficient mean to analyze the effect of disturbances and the behaviour of sensitive equipment, but results are as accurate and reliable as models and data used in calculations. Since the knowledge on the behaviour of sensitive equipment during unbalanced dips is rather limited, computer models cannot represent all factors that have some influence on the equipment response.

In addition, standards are only concerned about rectangular voltage dips, which are characterised by the magnitude and the duration. Characterisation of non-rectangular dips, assessment of their effects on equipment operation or the possible influence of non-ideal voltage supply characteristics are aspects not covered by present standards. Recommendations for testing of sensitive electrical equipment should be, therefore, extended and reformulated in order to include all characteristics, parameters and conditions of influence.

Disturbances that can lead to voltage dips, i.e. faults, are random in nature. Fault characteristics are based on reliability data. Although utilities have records of failures and their causes, many uncertainties still exist in this field. For example, the probability of occurrence associated to each type of fault can be specified with certain accuracy, but accurate statistics about fault durations are very rare or do not exist at all.

The selection of the simulation tool and the solution technique can be made once the goals of the voltage dip study have been fixed. A study aimed at estimating voltage dip indices based on the calculation of during-fault voltages only could be performed by a frequency-domain tool, since the calculations will be faster than those derived from the application of a time-domain tool. However, the use of phasors restricts models to the context of linear systems running under AC steady state and to the calculation of single-stage events. More realistic and accurate results can be derived only from the application of a time-domain simulation tool.

Two methods have been developed and applied for stochastic prediction of voltage dips; the method of fault positions and the method of critical distances. The first one is generally accepted as the most suitable because the method of critical distances has been usually applied by considering analytical expressions that are correct for radial systems only.

Strictly speaking the method of fault positions can be seen as a Monte Carlo method. Although fault positions are in many studies distributed uniformly along lines, the distribution can follow different probabilities density functions. Obviously, different fault distributions will result in different prediction of voltage dips at different buses. The differences can justify additional effort in modelling the actual fault distributions.

The main drawback of a Monte Carlo simulation is the number of iterations (i.e. the sample size or population) that are needed to obtain accurate enough results. The accuracy increases with the increase of the sample size. However, this can also be achieved by decreasing the variance of the sample estimates, without increasing the sample size. Several procedures, known as variance reduction techniques, have been proposed for that purpose: antithetic variables, importance sampling, stratification, control variates [94]. For example, when using stratification or stratified sampling the sample size is first divided into mutually exclusive sub-populations or strata; then units are selected for each stratum. Several strategies may be used: proportionate allocation (the number of samples per stratum is proportional to the full sample size ratio; if 80% of all faults are single-line-to-ground, 80% of the samples are taken for the corresponding stratum), optimum allocation (each stratum is proportional to the standard deviation of the sub-population), or equal allocation (equal number of samples per stratum and results are weighted according to the full population ratio).

A computer-based estimation of a power quality index may be the ultimate goal of a voltage dip study. As for other simulation results, the estimated index will be as accurate and reliable as the models and data used in calculations. Not much experience is still available on the application of voltage dip indices, and it is difficult to predict the usefulness of the indices discussed in this report. Since these indices are based on values related to voltage dip characteristics and to the comparison of those values to voltage-tolerance curves, see SARFI definitions in Section 8.3.1, their limitations are evident. For example, readers can review the discussions about voltage dip characterisation included in Sections 2.2, 2.3 and 8.2, the discussion about aggregation included in subsection 8.2.3, or the discussions about testing and behaviour of sensitive equipment included in Section 3.6. To overcome other limitations, e.g. those related to costs, other indices have been proposed.

10. References

[1] M.H.J. Bollen, *Understanding Power Quality Problems. Voltage Dips and Interruptions*, IEEE Press, 2000, New York.

[2] M.H.J. Bollen, "What is power quality," *Electric Power Systems Research*, vol.66, Issue 1, pp. 6-14, July 2003.

[3] IEC 61000-2-8, "Electromagnetic Compatibility (EMC) – Part 2-8: Environment - Voltage Dips and Short Interruptions on Public Electric Power Supply Systems with Statistical Measurement Results", 2002.

[4] IEC 61000-4-30, "Electromagnetic Compatibility (EMC) – Part 4-30: Testing and Measurement Techniques - Power Quality Measurement Methods" 2003.

[5] IEEE P1564, "Recommended Practice for the Establishment of Voltage dip Indices", Draft, June 2004.

[6] DISDIP Group, "Voltage Dips and Short Interruptions in Medium Voltage Public Electricity Supply Systems," Report from the International Union of Producers and Distributors of Electrical Energy (UNIPEDE), 1990.

[7] ANSI/IEEE Std. 493-1980, IEEE Recommended Practice For Design of Reliable Industrial and Commercial Power Systems, 6th Printing, 1989.

[8] IEEE Std. 1346-1998, IEEE Recommended Practice for Evaluating Electric Power System Compatibility with Electronic Process Equipment.

[9] D.L. Brooks, R.C. Dugan, M. Waclawiak and A. Sundaram, "Indices for assessing utility distribution system RMS variation performance", *IEEE Trans. on Power Delivery*, vol. 13, no. 1, pp. 254-259, January 1998.

[10] IEEE Std. 1159-2001, IEEE Recommended Practice for Monitoring Electric Power Quality.

[11] M.H.J. Bollen, "Characterisation of voltage sags experienced by three-phase adjustable-speed drives", *IEEE Trans. on Power Delivery*, vol. 12, no. 4, pp. 1666-1671, October 1997.

[12] M.H.J. Bollen and L.D. Zhang, "Different methods for classification of three-phase unbalanced voltage dips due to faults", *Electric Power Systems Research*, vol.66, Issue 1, pp. 59-69, July 2003.

[13] M.H.J. Bollen, "Algorithms for characterizing measured three-phase unbalanced voltage dips", *IEEE Trans. on Power Delivery*, vol. 18, no.3, pp. 937-944, July 2003.

[14] M.H.J. Bollen, Ph. Goossens and A. Robert, "Assessment of voltage dips in HV-networks: deduction of complex voltages from the measured rms voltages", *IEEE Trans. on Power Delivery*, vol. 19, no. 2, pp. 783-790, April 2004.

[15] T.S. Key, "Diagnosing power-quality related computer problems", *IEEE Trans. on Industry Applications*, vol.15, pp. 381-393, 1979.

[16] ITIC (Information Technology Industry Council), "ITIC Curve Application Note", available at http://www.itic.org/archives/iticurv.pdf.

[17] IEC 61000-4-11, "Electromagnetic Compatibility (EMC) – Part 4-11: Voltage Dips, Short Interruptions and Voltage Variations Immunity Tests", 1994.

[18] J.V. Milanović and S. Ž. Djokić, "Equipment sensitivity to disturbances in voltage supply", *Proc. Int. Electrical Equipment Conf. JIEEC 2003: The Electric Network of the Future and Distributed Generation*, pp. 3.7/1-3.7/14, Bilbao, Spain, 28-29 October 2003.

[19] S. Ž. Djokić, J. V. Milanović and D.S. Kirschen, "Sensitivity of ac coil contactors to voltage sags, short interruptions and undervoltage transients", *IEEE Trans. on Power Delivery*, vol. 19, no. 3, pp. 1299-1307, July 2004.

[20] S. Ž. Djokić, K. Stockman, J.V. Milanović, J.J.M. Desmet and R. Belmans, "Sensitivity of ac adjustable speed drives to voltage sags and short interruptions", *IEEE Trans. on Power Delivery*, vol. 20, no. 1, pp. 494-505, January 2005.

[21] S. Ž. Djokić, J.J.M. Desmet, G. Vanalme, J.V. Milanović and K. Stockman, "Sensitivity of personal computers to voltage sags and short interruptions", *IEEE Trans. on Power Delivery*, vol. 20, no. 1, pp. 375-383, January 2005.

[22] A. Sannino, J. Svensson and T. Larsson, "Power-electronic solutions to power-quality problems", *Electric Power Systems Research*, vol.66, Issue 1, pp. 71-82, July 2003.

[23] N. Woodley, L. Morgan, and A. Sundaram, "Experience with an inverter based dynamic voltage restorer", *IEEE Trans. on Power Delivery*, vol. 14, no. 3, pp. 1181-1186, July 1999.

[24] J.W. Schwartzenberg and R.W. De Doncker, "15 kV medium voltage static transfer switch", *IEEE IAS Annual Meeting 1995*, vol. 3, pp.2515–2520.

[25] IEEE P1409 Distribution Custom Power Task Force, "Trial Use Guide for Application of Power Electronics for Power Quality Improvement on Distribution Systems Rated 1 kV Through 38 kV", Draft 4, July 14, 2000.

[26] H.W. Dommel, "Digital computer solution of electromagnetic transients in single- and multi-phase networks", *IEEE Trans. on Power Apparatus and Systems*, vol. 88, no. 2, pp. 734-741, April 1969.
[27] H.W. Dommel, *ElectroMagnetic Transients Program. Reference Manual (EMTP Theory Book)*, Bonneville Power Administration, Portland, 1986.
[28] CIGRE Working Group 02 (SC 33), "Guidelines for Representation of Network Elements when Calculating Transients", 1990.
[29] A.M. Gole, J.A. Martinez-Velasco, and A.J.F. Keri (Ed.), "Modeling and Analysis of System Transients Using Digital Programs", IEEE PES Special Publication, TP-133-0, 1999.
[30] J.A. Martinez and J. Martin-Arnedo, "Voltage sag analysis using an electromagnetic transients program", *IEEE PES Winter Meeting 2002*, January 27-31, New York.
[31] J.A. Martinez and B.A. Mork, "Transformer modeling for low- and mid-frequency transients – A review", *IEEE Trans. on Power Delivery*, vol. 20, no. 2, pp. 1625-1632, April 2005.
[32] J.A. Martinez, R. Walling, B. Mork, J. Martin-Arnedo and D. Durbak, "Parameter determination for modeling systems transients. Part III: Transformers", *IEEE Trans. on Power Delivery*, vol. 20, no. 3, pp. 2051-2062, July 2005.
[33] J.A. Martinez and J. Martin-Arnedo, "Voltage sag stochastic prediction using an electromagnetic transients program", *IEEE Trans. on Power Delivery*, vol. 19, no. 4, pp. 1975-1982, October 2004.
[34] J.A. Martinez and J. Martin-Arnedo, "Voltage sag studies in distribution networks. Part I: system modeling", *IEEE Trans. on Power Delivery*, vol. 21, no. 3, pp. 1670-1678, July 2006.
[35] J.J. Burke, *Power Distribution Engineering. Fundamentals and Applications*, Marcel Dekker, 1994.
[36] K.L. Leix, Lj.A. Kojovic, M. Marz and G.C. Lampley, "Applying current-limiting fuses to improve power quality and safety", *IEEE T&D Conf*., pp. 636-641, April 1999.
[37] Lj.A. Kojovic, S.P. Hassler, K.L. Leix, C.W. Williams and E:E. Baker, "Comparative analysis of expulsion and current-limiting fuse operation in distribution systems for improved power quality and protection", *IEEE Trans. on Power Delivery*, vol. 13, no. 3, pp. 863-869, July 1998.
[38] Lj.A. Kojovic and S.P. Hassler, "Application of current-limiting fuses in distribution systems for improved power quality and protection", *IEEE Trans. on Power Delivery*, vol. 12, no. 2, pp. 791-800, April 1997.
[39] A. Petit, G. St-Jean and G. Fecteau, "Empirical model of a current-limiting fuse using EMTP", *IEEE Trans. on Power Delivery*, vol. 4, no. 1, pp. 335-341, January 1989.
[40] "IEEE Standard Inverse-Time Characteristic Equations for Overcurrent Relays", IEEE Std C37.112-1996.
[41] IEEE Computer Representation of Overcurrent Relays Characteristics WG, "Computer representation of overcurrent relay characteristics", *IEEE Trans. on Power Delivery*, vol. 4, no. 3, pp. 1659-1667, July 1989.
[42] N. Mohan, T.M. Undeland and W.P. Robbins, *Power Electronics: Converters, Applications, and Design*, Second Edition, John Wiley & Sons, 1995, New York.
[43] N.G. Hingorani and L. Gyugyi, *Understanding FACTS: Concepts and Technology of Flexible AC Transmission Systems*, IEEE Press, 2000, New York.
[44] IEEE TF on Power Electronics (L. Tang, Chairman), "Guidelines for modeling power electronics in electric power engineering applications", *IEEE Trans. on Power Delivery*, vol. 12, no.1, pp. 505-514, January 1997.
[45] B. Johnson, H. Hess and J.A. Martínez, "Parameter determination for modeling systems transients. Part VII: Semiconductors", *IEEE Trans. on Power Delivery*, vol. 20, no. 3, pp. 2086-2094, July 2005.
[46] IEEE Task Force on Load Representation for Dynamic Performance, "Load representation for dynamic performance analysis", *IEEE Trans. on Power Systems*, vol. 8, no. 2, pp. 472-482, May 1993.
[47] IEEE Task Force on Load Representation for Dynamic Performance, "Bibliography on load models for power flow and dynamic performance simulation", *IEEE Trans. on Power Systems*, vol. 10, no. 1, pp. 523-538, February 1995.
[48] IEEE Task Force on Load Representation for Dynamic Performance, "Standard load models for power flow and dynamic performance simulation", *IEEE Trans. on Power Systems*, vol. 10, no. 3, pp. 1302-1313, August 1995.
[49] Ch. J. Lin et al., "Dynamic load models in power systems using the measurement approach", *IEEE Trans. on Power Systems*, vol. 8, no. 1, pp. 309-315, February 1993.
[50] D. Karlsson and D.J. Hill, "Modelling and identification of nonlinear dynamic loads in power systems", *IEEE Trans. on Power Systems*, vol. 9, no. 1, pp. 157-166, February 1994.
[51] K. Morison, H. Hamadani and L. Wang, "Practical issues in load modelling for voltage stability studies", *IEEE PES General Meeting*, July 2003, Toronto.
[52] S. Ihara, K. Tomiyama and M. Tani, "Residential load characteristics observed at KEPCO power system", *IEEE Trans. on Power Systems*, vol. 9, no. 2, pp. 1092-1101, May 1994.

[53] K. Tomiyama, J.P. Daniel and S. Ihara, "Modeling air conditioner load for power system studies", *IEEE Trans. on Power Systems*, vol. 13, no. 2, pp. 414-421, May 1998.
[54] K. Tomiyama, S. Ueoka and T. Takano, "Modeling of load during and after system faults based on actual field data", *IEEE PES General Meeting*, July 2003, Toronto.
[55] P.A. Gnadt and J.S. Lawler (Eds.), *Automatic Electric Utility Distribu-tion Systems*, Prentice Hall, 1990.
[56] J. Key et al., "The design of power acceptability curves", *IEEE Trans. on Power Delivery*, vol. 17, no. 3, pp. 828-833, July 2002.
[57] J.A. Martinez, J. Martin-Arnedo and J.V. Milanović, "Load modeling for voltage dip studies", *IEEE PES General Meeting*, July 2003, Toronto.
[58] B. Khodabackhchian and G.T. Vuong, "Modeling a mixed residential-commercial load for simulation involving large disturbances", *IEEE Trans. on Power Systems*, vol. 12, no. 2, pp. 791-796, May 1997.
[59] M. Reformat, D. Woodford, R. Wachal and N.J. Tarko, "Nonlinear load modelling for simulation in time domain", *8th ICHQP*, vol. 1, October 1998.
[60] J.V. Milanović, R. Gnativ and K.W.M. Chow, "The influence of loading conditions and network topology on voltage sags", *9th ICHQP*, October 2000.
[61] J. Arrillaga, C.P. Arnold and B.J. Harker, *Computer Modelling of Electrical Power Systems*, John Wiley & Sons, 1983.
[62] P.M. Anderson and A.A. Fouad, *Power System Control and Stability*, IEEE Press, 1994.
[63] IEEE Std. 1110, "IEEE Guide for Synchronous Generator Modeling Practices in Stability Studies," 1991.
[64] IEEE Committee Report, "Excitation systems dynamic characteristics," *IEEE Trans. on PAS*, vol. 92, pp. 64-75, January-February 1973.
[65] "CIGRE TF 38.01.10 (Convener N. Hatziargyriou), "Modeling New Forms of Generation and Storage", Technical Brochure 2002.
[66] L. Conrad, K. Little and C. Grigg, "Predicting and preventing problems associated with remote fault-clearing voltage dips", *IEEE Trans. on Industry Applications*, vol. 27, no.1, pp.167-172, January 1991.
[67] M.H.J. Bollen, "Fast assessment methods for voltage sags in distribution systems", *30th IEEE IAS Annual Meeting*, vol. 3, pp. 2282 -2289, 1995.
[68] M.H.J. Bollen, "Fast assessment methods for voltage sags in distribution systems", *IEEE Trans. on Industry Applications*, vol. 32, no. 6, pp. 1414-1423, November/December 1996.
[69] L.E. Conrad and M.H.J. Bollen, "Voltage dip co-ordination for reliable plant operation", *IEEE Trans. on Industry Applications*, vol.33, no.6, November 1997, pp.1459-1464.
[70] M.H.J. Bollen, "Method of critical distances for stochastic assessment of voltage sags". IEE Proc. Generation, Transmission and Distribution, vol. 145, no. 1, pp. 70-76, January 1998.
[71] M.H. Qader, M.H.J. Bollen, and R.N. Allan, "Stochastic prediction of voltage sags in a large transmission system," *IEEE Trans. on Industry Applications*, vol. 35, no. 1, pp. 152-162, January/February 1999.
[72] S. Omar Faried and S. Aboreshaid, "Stochastic evaluation of voltage sags in series capacitor compensated radial distribution systems," *IEEE Trans. on Power Delivery*, vol. 18, no. 3, pp. 744-750, July 2003.
[73] P. Heine and M. Lehtonen, "Voltage dip distributions caused by power system faults", *IEEE Trans. on Power Systems*, vol. 18, no. 4, pp. 1367-1373, November 2003.
[74] J. Wang, S. Chen, and T.T. Lie, "System voltage sag performance estimation", *IEEE Trans. on Power Delivery*, vol. 20, no. 2, pp. 1738-1747, April 2005.
[75] S. Omar Faried, R. Billington and S. Aboreshaid, "Stochastic evaluation of voltage sag and unbalance in transmission systems", *IEEE Trans. on Power Delivery*, vol. 20, no. 4, pp. 2631-2637, October 2005.
[76] E. Styvaktakis, "Automating Power Quality Analysis", PhD thesis, Chalmers University of Technology, Gothenburg (Sweden), 2002.
[77] G. Olguin, "Voltage dip (sag) estimation in power systems based on stochastic assessment and optimal monitoring", PhD Thesis, Chalmers University of Technology, Gothenburg, Sweden, 2005.
[78] G. Olguin and M.H.J. Bollen, "Method of fault positions for stochastic prediction of voltage sags: A case study", *PMAPS Conference 2002*, September 22-26, Naples, Italy, pp. 557-562.
[79] P. Heine, P. Pohjanheimo, E. Lakervi and P. Rissanen, "Methods and tools for voltage sag evaluation implemented in a network information system", *35th UPEC*, Belfast, September 6-8, 2000.
[80] M.T. Aung, J.V.Milanović and C.P. Gupta, "Propagation of asymmetrical sags and the influence of boundary crossing lines on voltage dip prediction", *IEEE Trans. on Power Delivery*, vol.19, no. 4, pp. 1819-1827, October 2004.
[81] IEEE Std. 493-1997, IEEE Recommended Practice for Design of Reliable Industrial and Commercial Power Systems.
[82] J.V. Milanović, M.T. Aung and C.P. Gupta, "The influence of fault distribution on stochastic prediction of voltage sags", *IEEE Trans. on Power Delivery*, vol.20, no. 1, pp. 278-285, January 2005.
[83] IEEE Std. 1366-2001, Trial Use Guide for Electric Power Distribution Reliability Indices.

[84] Joint WG CIGRE C4.07/CIRED, "Power Quality Indices and Objectives", Technical Brochure 261, October 2004.
[85] Brooks et al, and Joint WG CC02 CIGRE-CIRED, Recommendations for Tabulating RMS Voltage Variations Disturbances with Specific Reference to Utility Power Contracts.
[86] G-J. Lee, M.M. Albu and G.T. Heydt, "A power quality index based on equipment sensitivity, cost, and network vulnerability", *IEEE Trans. on Power Delivery*, vol. 19, no. 3, pp. 1504-1510, July 2004.
[87] J.A. Martinez and J. Martin-Arnedo, "Voltage sag studies in distribution networks. Part III: Voltage sag index calculation", *IEEE Trans. on Power Delivery*, vol. 21, no. 3, pp. 1689-1697, July 2006.
[88] J.A. Martinez and J. Martin-Arnedo, "Expanding capabilities of EMTP-like tools: From analysis to design", *IEEE Trans. on Power Delivery*, vol. 18, no. 4, pp. 1569-1571, October 2003.
[89] J.A. Martinez and J. Martin-Arnedo, "Voltage sag studies in distribution networks. Part II: Voltage sag assessment", *IEEE Trans. on Power Delivery*, vol. 21, no. 3, pp. 1679-1688, July 2006.
[90] National Grid Transco, 2004, Seven Year Statement, available at http://www.nationalgrid.com.
[91] M.H.J. Bollen and M. Häger, "Impact of increasing penetration of distributed generation on the number of voltage dips experienced by end-customers", *18th CIRED*, 6-9 June, Turin, 2005.
[92] C. Schwaegerl, M.H.J. Bollen, K. Karoui and A. Yagmur, "Voltage control in distribution systems as a limitation of the hosting capacity for distributed energy resources", *18th CIRED*, 6-9 June, Turin, 2005.
[93] M.H.J. Bollen and M. Häger, "Power quality: interactions between distributed energy resources, the grid and other customers", *1st Int. Conf on Renewable Energy Sources and Distributed Energy Resources*, 2004.
[94] G.J. Anders, *Probability Concepts in Electric Power Systems*, John Wiley, 1990.